Viscoelastic Effects on Structure and Dynamics of Liposomes in Polymeric Matrices

by

Selcan Karaz

A Dissertation Submitted to the
Graduate School of Sciences and Engineering
in Partial Fulfillment of the Requirements for
the Degree of

Master of Science

in

Chemical and Biological Engineering

KOÇ
ÜNİVERSİTESİ

January 5, 2023

Viscoelastic Effects on Structure and Dynamics of Liposomes in Polymeric Matrices

Koç University

Graduate School of Sciences and Engineering

This is to certify that I have examined this copy of a master's thesis by

Selcan Karaz

and have found that it is complete and satisfactory in all respects,
and that any and all revisions required by the final
examining committee have been made.

Committee Members:

Asst. Prof. Erkan Şenses (Advisor)

Prof. Seda Kızılel (Co-Advisor)

Prof. Özlem Keskin

Prof. Kutlu Ülgen

Date: 05.01.2023

To my supportive parents and dear sisters Cansel and Era…

ABSTRACT

Viscoelastic Effects on Structure and Dynamics of Liposomes in Polymeric Matrices

Selcan Karaz

Master of Science in Chemical and Biological Engineering

January 5, 2023

Recent decades have seen significant advancements in the pharmaceutical industry and nanotechnology, which have led to the development of clinical research and the discovery of modern drug delivery methods. As one of the widely used nanoparticles, liposomes are employed in pharmaceutics, tissue engineering, cell membrane modelling, cosmetics, and agriculture with their high biocompatibility, biodegradability, low toxicity, and resemblance to biological membranes. Although liposomes offer serious advantages, they have drawbacks such as their thermodynamically unstable structure, quick elimination in the bloodstream, and a desire to targeted and dosage-controlled delivery. To overcome these issues, the combination of liposomes with polymer solutions, and hydrogels have been utilized since polymers provide mechanical support, stimuli-responsive release, and increased stability towards chemicals, enzymes, and immune systems. Besides, polymeric scaffolds can be designed to mimic the topology and mechanical characteristics of the native extracellular microenvironment. Although there is a great deal of interest in liposome-polymer complexes from the application point of view, the effects of viscoelasticity of polymers on liposome structure, permeability, and mobility need detailed understanding.

This thesis contains two different studies on liposomes and Polyethylene glycol (PEG) mixtures. In the first one, we used 100 nm unilamellar DMPC/DMPG liposomes, and aqueous solutions of poly (ethylene glycol) (PEG) with various molecular weights from 1.5 kDa to 400 kDa to simulate the viscous media of cells. The structural phase map and multiscale dynamics of liposomes in their neat form and in the presence of PEG solutions were investigated. The findings point to a dynamical coupling at various length/time scales between polymer chains and phospholipid bilayers. The relaxation of the entire chain directly affects the microviscosity of the lipid bilayers, which causes faster dynamics of the lipids within the bilayers when compared to the polymer-free liposome case. We observed a thermal-thickening behaviour of polymer-liposome solutions at the transition temperature of the lipids from gel to fluid, which is tuneable by

the concentration of liposomes and the length of the polymer chain. In the second study, we used unilamellar 100 nm DMPC/DMPG liposomes and PEG hydrogels having different elasticities, from 1 Pa to 180 Pa, and created a composite hydrogel. We studied the release of liposomes from the ECM-mimetic gel matrices under quiescent and shear deformation. The presence of liposomes provides composite hydrogels with temperature-controlled swelling capacity that is sensitive to membrane microviscosity. By systematically varying shear deformation from linear to nonlinear regimes, we studied the effect of shear deformation on the release of liposomes from the hydrogels of different stiffness.

ÖZETÇE

Polimerik Matrislerde Lipozomların Yapısı ve Dinamikleri Üzerindeki Viskoelastik Etkiler

Selcan Karaz

Kimya ve Biyoloji Mühendisliği, Yüksek Lisans

5 Ocak 2023

Son yıllarda, ilaç endüstrisinde ve nanoteknolojide, klinik araştırmaların gelişmesine ve modern ilaç dağıtım yöntemlerinin keşfedilmesine yol açan önemli gelişmeler görüldü. Yaygın olarak kullanılan nanoparçacıklardan biri olan lipozomlar, yüksek biyouyumluluk, biyobozunurluk, düşük toksisite ve biyolojik zarlara benzerlik özellikleri ile eczacılık, doku mühendisliği, hücre zarı modellemesi, kozmetik ve tarımda kullanılmaktadır. Lipozomların birçok avantajları olmasına rağmen termodinamik olarak kararsız yapıları, kan dolaşımında hızlı eliminasyon ve hedefli ve dozaj kontrollü dağıtım isteği gibi dezavantajları vardır. Bu sorunların üstesinden gelmek için, lipozomların polimer solüsyonları ve hidrojellerle kombinasyonu kullanılmıştır. Polimerler lipozomlara mekanik destek, uyaranlara duyarlı salınım ve kimyasallara, enzimlere ve bağışıklık sistemlerine karşı artan stabilite sağlar. Ayrıca, polimerik iskeleler, hücre dışı mikro ortamın topolojisini ve mekanik özelliklerini taklit edecek şekilde tasarlanabilir. Uygulama açısından lipozom-polimer komplekslerine büyük ilgi olmasına rağmen, polimerlerin viskoelastikliğinin lipozom yapısı, hücre zarı geçirgenliği ve hareketliliği üzerindeki etkilerinin ayrıntılı olarak anlaşılması gerekir.

Bu tez, lipozomlar ve Polietilen glikol (PEG) karışımları üzerine iki çalışma içermektedir. İlk çalışmada, hücrelerin viskoz ortamını simüle etmek için 100 nm tek lamelli DMPC/DMPG lipozomları ve 1.5 kDa ile 400 kDa arasında çeşitli moleküler ağırlıklara sahip polietilen glikol (PEG) solüsyonları kullanıldı. PEG varlığında lipozomların yapısal faz haritası ve çok ölçekli dinamikleri araştırıldı. Polimer zincirleri ve fosfolipid çift katmanları arasında çeşitli uzunluk/zaman ölçeklerinde dinamik bir bağlantı vardır. Tüm zincirin gevşemesi, lipit çift tabakalarının mikro viskozitesini doğrudan etkiler ve bu da, polimer içermeyen lipozom durumuyla karşılaştırıldığında çift tabakalar içindeki lipitlerin daha hızlı dinamik hareketlerine neden olur. Lipitlerin jelden sıvıya geçiş sıcaklığında, lipozomların konsantrasyonu ve polimer zincirinin uzunluğu ile ayarlanabilen, polimer-lipozom çözeltilerinin termal kalınlaşma davranışı gözlemlendi. İkinci çalışmada tek lamelli 100 nm DMPC/DMPG lipozomları ve 1 Pa'dan 180 Pa'ya kadar farklı elastikiyetlere sahip PEG hidrojelleri kullanıldı ve kompozit bir hidrojel oluşturuldu. Zamana bağlı ve kayma deformasyonu altında ECM-mimetik jel

matrislerinden lipozom salınımını incelendi. Lipozomların varlığı, membran mikro viskozitesine duyarlı, sıcaklık kontrollü şişme kapasitesine sahip kompozit hidrojeller sağlamıştır. Kayma deformasyonunu doğrusaldan doğrusal olmayan rejimlere sistematik olarak değiştirerek, farklı sertlikteki hidrojellerden lipozomların salınması üzerindeki etkisi incelendi.

ACKNOWLEDGEMENTS

I would like to express my sincere thankfulness to my advisor, Asst. Prof. Erkan Şenses for his guidance, patience, and supportive attitude throughout these two years. It was a great pleasure for me to work with such a successful, and great scientist in this field. He always welcomed me when I had a question or a new idea, and he encouraged me when I felt unmotivated. Most importantly, I learned how to ask necessary questions to start and conduct research from the discussions we had. His creative thinking, passion for science, and ambition will always be with me throughout my career.

I would like to thank my co-advisor, Prof. Seda Kızılel for her helpful suggestions, and guidance. She has been a role model for me as a successful scientist woman.

I would like to thank my undergraduate supervisor at Boğaziçi University, Prof. Kutlu Ülgen. My first research experience was with her in my bachelor thesis. Thanks to her encouraging and supportive attitude, I discovered my passion and interest towards science and research.

Special thanks to my committee member Prof. Özlem Keskin.

I would like to thank my lab mates Ebru, Emine, İlayda, Nazlı, Recep, and Saeid for sharing their experiences, and knowledge with me. I will miss our coffee breaks.

I would like to thank my best friends Ayşenur, and Sinem for the unforgettable memories we had. They have been my second family in İstanbul since we started sharing a room in the dorm.

I would like to thank my mom Hamiyet, my dad Tamer, and my sister Cansel. I wouldn't be able to complete this journey without your unconditional support, and love.

and to Mertcan, I am so grateful you are a part of my life. You have always been standing by our side during all the happy and difficult times we had. Thank you for the warmth of your love, I am looking forward to the memories there are to come.

TABLE OF CONTENTS

LIST OF TABLES

LIST OF FIGURES

ABBREVIATIONS

PC	Phosphatidylcholine
PE	Phosphatidylethanolamine
PS	Phosphatidylserine
PG	Phosphatidylglycerol
SM	Sphingomyelin
DPPC	Dipalmitoyl phosphatidylcholine
DMPC	Dimyristoyl phosphatidylcholine
DSPC	Distearoyl phosphatidylcholine
HSPC	Hydrogenated soy phosphatidylcholine
POPC	1-palmitoyl-2-oleoyl-sn-glycero-3-phosphocholine
D_T	Translational Diffusion Constant
R_H	Hydrodynamic radius
k_B	Boltzmann constant
η_s	Viscosity of the solution
F-MMM	Fluid-Mosaic Membrane Model
ECM	Extracellular matrix
PEG	Polyethylene glycol
FDA	Food and Drug Administration
PL	Pay load
EE	Encapsulation efficiency
HA	Hyaluronic acid
CHEMS	Cholesteryl hemisuccinate
DLS	Dynamic Light Scattering
DSC	Differential Scanning Calorimetry
SAXS	Small Angle X-Ray Scattering
FLS	Fluorescence Lifetime Spectroscopy
LVER	Linear Viscoelastic Region

Chapter 1:
INTRODUCTION

The self-assembly of molecules is one of the vital processes and as a prerequisite to life. The structure of the biological membranes is governed by the self-assembling process, as well as the folding of DNA and proteins.[1] In 1964, liposomes were first introduced to the pharmaceutical industry by Alec Bangham and coworkers while testing a new electron microscope by adding a negative stain to dry phospholipids.[2] The name of the liposomes is derived from *"lipo"* meaning fat, and "*soma"* meaning body. The self-assembling of phospholipid molecules forms liposomes in a vesicle shape which is an entropically favorable structure in terms of hydrophobic interactions.[3] They are classified based on their size as small, large, and giant; and the number of layers as unilamellar and multilamellar liposomes.[4]

To date, liposomes have been widely used in drug delivery, tissue engineering, cosmetics, and agriculture with their unique properties.[2] In fact, they can encapsulate several types of therapeutic agents including hydrophilic, hydrophilic, and lipophilic drugs providing a protective effect from the metabolic processes.[5] The surface of the liposomes can be engineered to bind several molecules such as antibodies, vitamins, carbohydrates, peptides, and enzymes to further improve the treatment of serious diseases such as tumors, or cancer by presenting localized, stimuli-based and dosage-controlled delivery to overcome the physiological and biological barriers.[6] Despite their advantages, they have several drawbacks such as low stability in aqueous mediums, rapid clearance from the blood due to the interaction between plasma proteins, short lifetimes. Thus, a new liposome formulation called "stealth liposomes" have been developed by coating the surface of the liposomes by polyethylene glycol (PEG) as a novel way to limitations.[7]

Apart from the drug delivery applications, liposomes are used as model membrane systems due to their similarities between biological membranes. Cell membranes are complex and dynamic barriers separating the livings and non-livings. It is made up mainly phospholipids (~50%) which play an essential role in many cellular processes such as the storage of membrane compounds, signaling, and fusion.[8, 9] In structural manner,

liposomes are well-matched models of the protein-free parts of cell membranes. The self-assembly of the lipid molecules provides membrane a thermodynamically stable and selective barrier enabling the chemical reactions to occur efficiently and protecting the genetic information.[10] Since the interactions of lipids is controlled by Van der Waal's and hydrophobic forces, the cell membrane is sensitive to physical and chemical changes of its surrounding medium resulting in conformational changes.[11] Such modifications in the structure of membrane leads to serious human diseases such as cancer, infection, and neurodegenerative diseases.[12] To find novel and effective ways to these disorders, it is essential to a deeper understanding of the structure and dynamics of cell membranes which can be achieved by creating simpler models with liposomes.

In this thesis, we used liposomes as cell membrane and drug nanocarrier models through elucidating their structural dynamics and interactions between surrounding polymeric medium. The thesis is organized as follow:

In Chapter 2, we first introduced the structure of liposomes by defining the self-assembly mechanism and the classification of liposomes based on their size and lamellarity. Then, we continue with reviewing the applications of liposomes in cell membrane modeling and drug delivery applications combined with hydrogels.

Chapter 3 contains materials and methods, results, and discussion sections of the first project titled as "Multiscale Dynamics of Lipid Vesicles in Polymeric Microenvironment". We utilize liposomes as cell membrane models and PEG chains to mimic macromolecularly crowded medium of the cells. The effect of PEG chains on structure and dynamics of liposomes was investigated using from bulk to nanoscale.

Chapter 4 includes the materials and methods, results, and discussion sections of the second project named as "Shear-Triggered Release of Lipid Vesicles from Tissue-Mimetic Hydrogels". We used liposomes as drug nanocarrier models and produced ECM-mimetic PEG hydrogels with five different elasticities. The structure and dynamics of liposomes in hydrogel environment and then time-dependent and shear-responsive release of liposomes was investigated.

In Chapter 5, we summarized the key findings of the two projects, and draw all conclusions.

To the best of our knowledge, both concepts have not been examined in literature, and serve a basis through a deeper understanding of structure and dynamics of liposomes, and rationale design of liposome-based drug delivery systems.

Chapter 2:
LITERATURE REVIEW

2.1 Liposomes – General Overview

During recent decades, important developments in pharmaceutical industry and nanotechnology bring the discovery of contemporary drug delivery systems and the developments in clinical studies. In 1960s, with the first discovery of Alec Bangham, liposomes became one of the oldest and most widely used nanoparticles in pharmaceutics, tissue engineering, cell membrane modelling, cosmetics, as well as agriculture.[2] Bangham obtained high resolution images of the lipid-water mixtures showing that lipids form vesicles filling with water which he called *liposome*.[13] To date, several studies have been conducted to understand the biophysical and biochemical aspects of liposomes.[14] Thus, to understand the structure and dynamics of the unique self-assembled and multi-component structure of liposomes is the key for the rationale applications of lipid-based systems.

2.1.1 Self-assembly mechanism and Structure of Liposomes

Self-assembly is defined as the transformation of pre-existing disordered systems into an organized structure because of the local interactions between components without any external force.[15] For self-assembling to take place, the process must result in a lower Gibbs free energy, thus, the assembled structures become thermodynamically more stable than the unassembled single components. Since the molecules form non-covalent interactions (*i.e.*, hydrogen bonding, electrostatic interactions, Van der Waals forces, hydrophobic force), self-assembled structures are flexible, and reversible that makes obtaining a large variety of shapes and functions on several length scales advantageous. Together with liquid crystal phases, Langmuir monolayers from surfactant molecules, and micelles; liposomes are one of the common examples of self-assembled structures.[16, 17]

The word *liposome* originally derives from two Greek words; *lipo* (fat) and *soma* (body) since its composition is mainly composed of phospholipid as seen in Figure 2.1 a. Phosphatidylcholines (PC) and sphingomyelins are two types of phospholipids primarily involved in the liposome structure.[18] They are responsible for many vital cellular processes such as control of cell shape, the storage of membrane compounds, cell signaling, and cell fusion.[8] Phospholipids are amphiphilic molecules consisting of glycerol linked to phosphate group (hydrophilic) and two fatty acid chains (hydrophobic), and classified as natural and synthetic phospholipids.[19] Natural ones can be obtained from several sources such as soya bean and egg yolk, phosphatidylcholine (PC), phosphatidylethanolamine (PE), phosphatidylserine (PS), phosphatidylglycerol (PG) and sphingomyelin (SM).[20] Whereas synthetic ones can be produced from the modification of the natural phospholipids allowing the creation of a variety of well-controlled phospholipids. Dipalmitoyl phosphatidylcholine (DPPC), dimyristoyl phosphatidylcholine (DMPC), distearoyl phosphatidylcholine (DSPC), hydrogenated soy phosphatidylcholine (HSPC), 1-palmitoyl-2-oleoyl-sn-glycero-3-phosphocholine (POPC) are the examples of synthetic phospholipids.[21] The nature of the phospholipids is also determined by the length of fatty acid chains which differ in the number of carbon atoms and the degree of unsaturation.[22] If a double bond between carbon atoms (C=C) exists, the chain is unsaturated. While the absence of double bonds (C-C) represents the saturated structure. Generally, unsaturated fatty acids are found in the natural phospholipids such as PC.[21]

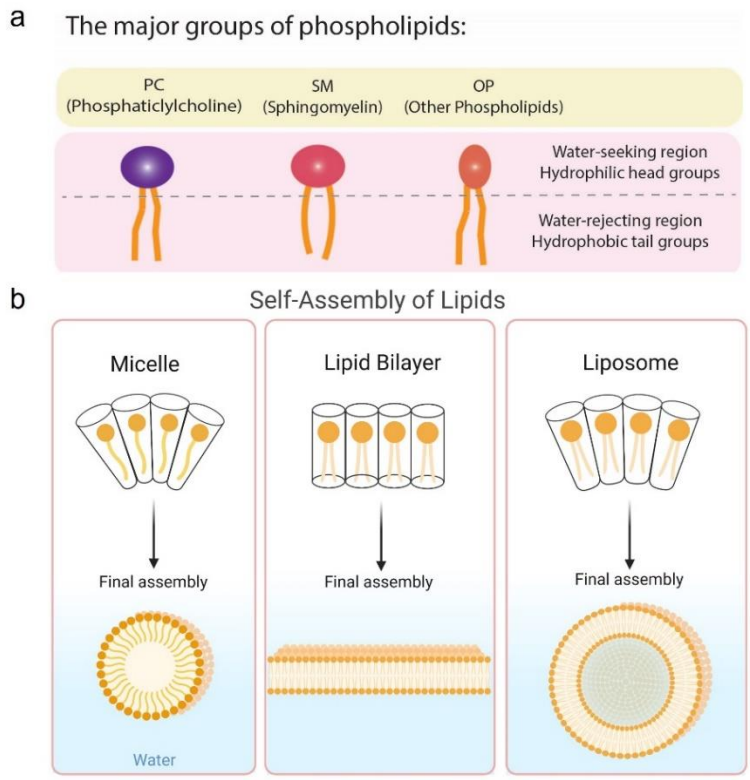

Figure 2.1 a. The types of phospholipids constructing the lipid bilayer, and their hydrophilic and hydrophobic regions. b. Different self-assembly mechanisms of lipids; micelle, lipid bilayer, and liposome formation.

Besides, liposomes may contain other types of molecules such as cholesterol involving the regulation of liposome fluidity, charged phospholipids (stearyl amine, and dicetyl phosphate), and polymers increasing the circulation time and intracellular uptake of liposomes.[23-25]

In aqueous mediums, lipids have the ability to self-assemble. They form hydrophilic interactions between polar head groups, and Van der Waals interactions between hydrocarbon chains and water which enable them to form lipid-based structures such as micelles and liposomes.[3] (Figure 2.1 b) Phospholipids having shorter and compact tails have a tendency to form micelles, whereas the ones with longer tails can form liposomes.

Liposomes can be classified based on their size and the number of bilayers present in vesicle as shown in Figure 2.2. Multilamellar liposomes are found to be in onion-like

structure with more than one bilayer.[4] Whereas, unilamellar liposomes contain one single bilayer enclosing the inner core. They can be also specified into three categories as small, large, and giant unilamellar vesicles as their size varies from nanometers to micron scale. Since unilamellar structure resembles into the structure of cell membranes with the well-controlled and adjustable properties, they are more preferred for the biological applications.[2]

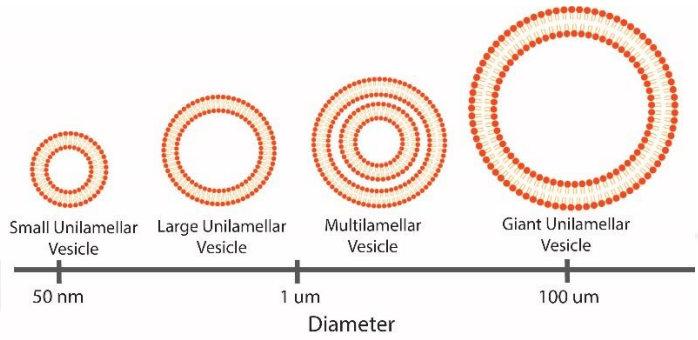

Figure 2.2 Classification of liposomes based on their size and lamellarity

The size and lamellarity of the liposomes strongly affect the circulation half-life, encapsulation efficiency, and stability of liposomes.[26] Also, as different lipid components can affect the physicochemical properties, it is essential to choose suitable composition and liposome type to reach the expected and optimum formulations.[27]

2.1.2 Dynamics of Liposomes

Understanding the dynamics of lipid membranes bring important features for rational design of drug delivery systems and understanding the complex mechanism of cell membranes. Since even the small changes in dynamics can affect several properties of liposomes such as fluidity, permeability, drug encapsulation, and stability, it is a key to unravel the fundamentals of this self-organized complicated system.

The lipid bilayer is a selective barrier which internal environment of a liposome differs from the outer surface.[28] It allows small non-polar molecules to pass across the membrane faster, while large and charged molecules can pass through the membrane slower. The fluidity and mobility of each individual lipid molecule constituting the lipid bilayer, thus, affect the permeability of membrane, and mobility of the whole lipid vesicle.[29]

The most significant parameter affecting the dynamics of liposomes is temperature.[30] The unique molecular structure of the membrane is extremely sensitive to temperature in a way that it exhibits both liquid-like viscous and elastic-like crystalline structure. Phospholipids do not undergo a usual phase transition from solid to liquid form as temperature increases, rather they make conformational changes. Below the melting temperature, phospholipids are found in a closely packed and ordered structure, called as gel phase.[31] Acyl tails of lipids exist in a fully extended and rigid state with low mobility. As the temperature increases further, the ripple phase where the first disorderness of acyl tails starts is observed and completely disappeared at the fluid phase.[32] The lowest permeability is observed in the gel phase of liposomes where the bilayer fluidity is in its lowest as well, since the hydrophobic tails of the phospholipids pack more tightly. As the lipid phase transforms into the fluid phase, the hydrophobic tails can move faster increasing the bilayer permeability.[29]

As mentioned in the previous section, the structure of phospholipids can differ with respect to the degree of unsaturation which is another parameter affecting the fluidity level of the bilayer. Since the free energy of C-H bond is relatively higher than the free energy of C=C bonds, saturated lipids have greater chemical energy compared to unsaturated ones. The double bond creates more spaces in the tightly packed lipid tails, thus, bilayers containing more unsaturated lipids have more gaps and more permeable to other molecules.[33]

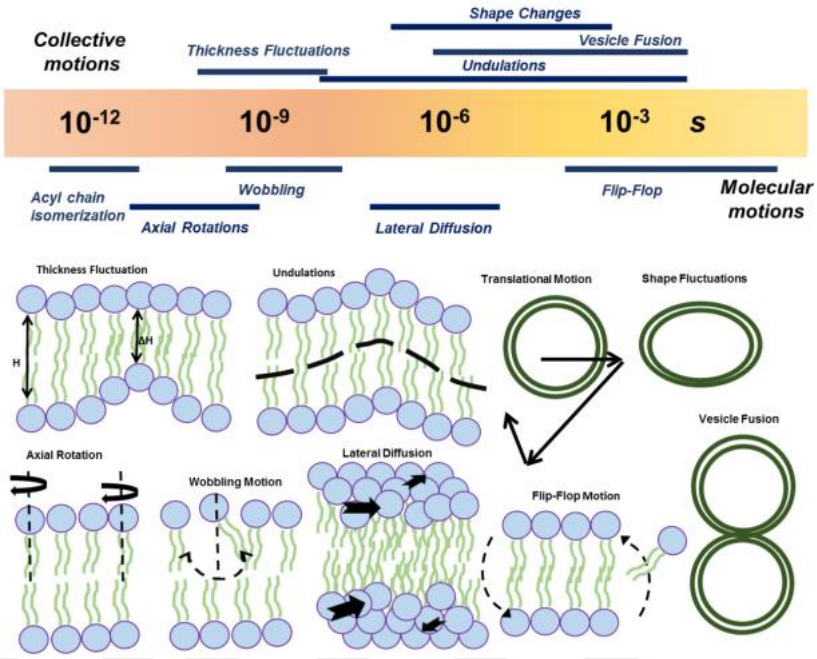

Figure 2.3 Dynamics of liposomes at different time scales.[34]

Liposomes undergo several processes from collective motions to molecular motions in macro levels although the spherical morphology is assumed. Bilayer motions can differ from picoseconds to several hours as the time scale is shown in Figure 2.3, thus, several techniques are needed to elucidate the membrane dynamics.[35]

They are assumed as spherical colloidal vesicles that undergo a Brownian motion in aqueous environments, therefore, the largest length scale and the simplest morphological case is the translational diffusion of liposomes.[36] Dynamic Light Scattering (DLS) is one of the common methods to measure the translational diffusion constant, D_T.

The Stokes-Einstein equation related D_T with the length scale which is hydrodynamic radius R_H. The thermal energy due to the thermal fluctuations is expressed with k_BT where k_B is the Boltzmann constant, and T is the temperature. η_s refers to the viscosity of the medium. Although the size of the liposomes can vary from 20 nm to 50 microns depending on the preparation methods, the D_T of the liposomes can be estimated as between 1.2×10^{-11} and 5×10^{-15} m^2/s.[34]

As a result of thermal excitations, lipid bilayer undergoes membrane undulations or fluctuations in 2D plane.[37] Various physiological processes such as fusion of the liposomes, endocytosis, exocytosis, and cell adhesion are driven by membrane

fluctuations representing collective motion of the bilayer.[38] Besides, membrane fluctuations are also responsible for stability, and shape of the lipid vesicles, and interactions of liposomes with drugs, nanoparticles, and polymers etc.

The alignment of the lipid chains is associated with both thermodynamic and mechanical properties of the membrane.[39] A lipid bilayer fluctuates continuously around its average shape when subjected to a thermal excitation. In turn, these fluctuations give important properties including correlation length, and amplitude to elucidate the membrane mechanical properties and the interaction with the surroundings.[40] Membrane fluctuations cause some mechanical deformations which are bending, stretching, shear and thickness changes. Since the internal fluid of the membrane is considered as a viscous liquid, and the viscous membrane is generally characterized by incompressibility, peristaltic and thickness fluctuations are far from phase transition. [41-43]
Apart from membrane undulations and fluctuations, thickness fluctuations of the membrane were suggested to represent the individual motions of the leaflets leading to fluctuation perpendicular to 2D plane.[44] The deformation mechanism is regulated by membrane curvature. After a critical value of deformation, the diffusion of the lipids becomes limited which leads to the formation of open areas in the membrane. In turn, vesicles can form pores to reduce the curvature stress which is also responsible for passive permeability and release mechanism of liposomes.[45] [46-48]

At faster time scales, the movements of the individual phospholipids are visible. By labelling the single particles, it was discovered that lipids do not move via Brownian motion, rather they move via hop diffusion. The movement types can be distinguished into three categories which are rotational (lipids rotate on their axis to interact with neighbor lipids), lateral (lipids move around one leaflet), and flip flop (lipids move between leaflets in transverse movement).[34] Flip flop motion occurs in slower time scale since it requires more energy to diffuse through other leaflet. In real cell membranes, protein constituents help with the transverse diffusion of the lipids.[49] On the other hand, lateral and rotational movements occur shorter times because they can happen with less energy.

In macro scale dynamics, the viscosity of the liposome solutions has a crucial role on the long-term storage of liposomes, and it is also one of the important factors of stability and drug release. Liposomes exhibit unique rheological properties since they display several morphologies related to the mobility of lipid molecules.[30] As phospholipids make conformational changes with temperature, it is expected to observe different flow behaviors of liposome solutions depending on the temperature and applied shear rate to the system.

For example, the viscosity of the DMPC/DHPC dispersion, having Tm at 20°C, was investigated at shear rates between 0.1 to 300 s^{-1}.[50] Below the melting temperature, the flow curves of liposome solution were linear indicating a Newtonian behavior, and a characteristic of the isotropic phase.[50] The viscosity decreased smoothly in gel phase due to the entropic repulsion between the molecules. During the ripple phase, shear viscosity decreases significantly then recovers itself above the transition.[51] At higher temperatures, the liposome solution starts to exhibit shear-thinning behavior.

The dependence of the shear viscosity of DPPC dispersion on shear rate was investigated.[51] It was interesting that gel and fluid phases showed distinct shear thinning behavior, whereas the ripple phase exhibited Newtonian behavior, constant shear viscosity. Since the bending elasticity of the membrane did not change remarkably in gel and ripple phases, the increase of distance between bilayers occurred as a result of out of phase configurations instead of dynamic roughing.[52] The Newtonian behavior was attributed to the suppressed approach of bilayers causing lower aggregation.

2.2 Polymers – General Overview

2.2.1 Molecular Weight and Degree of Polymerization

One of the first things in consideration of the "size" of the polymer is the molecular weight, Mw. It typically ranges from 10^3-10^7 and beyond and is expressed mainly in the unit of g/mol or Dalton (Da).[53] By covalently connecting only one or two types of repeat units together, numerous polymer molecules can be created. These units are the building blocks from which chains are formed; they are referred to as monomers as a type of compound. A polymer's molecular weight and distribution affect almost all of its

properties; hence low and high-molecular-weight polymers will have very distinct mechanical and thermophysical characteristics. For instance, polymeric materials with a low number of repeat units will be soft or rubbery solids or low viscous liquids and will have little to no strength, whereas polymeric materials with a high molecular weight will be solid and have significantly better mechanical properties.[54] Once a particular molecular weight is attained, the mechanical and viscoelastic properties often grow steeply with increasing molecular weight until they become almost independent of chain length, meaning that all properties finally reach an asymptotic value. A high molecular weight improves a material's ability to resistance to flow which is viscosity. Because more polymer bonds must be broken for the polymer to rupture due to the increased degree of entanglement, the polymer can withstand more energy before breaking, and it is harder to get it to flow.[54]

Another definition related to the length of the polymer chain is the degree of polymerization, N, which is the number of monomer units in a polymer chain. It is expressed as $N = Mw / M_0$ where M_0 is the molecular weight of a monomer unit and simply indicates the average number of monomeric units; it does not account for the variation in polymer molecule size.[55]

2.2.2 Polymer Configurations

The physical positioning of monomer residues along the chain's backbone determines a polymer's microstructure, also known as configuration.[54] These are the aspects of polymer structure that can only be altered by breaking a covalent bond. According to the monomers and the reaction conditions, several polymer structures can be made linear, branched, crosslinked, and networked. Linear polymers are similar to spaghetti with long chains held together by Van der Waals forces or hydrogen bonding. Since these bonds are easy to break, they are typically thermoplastic. With the addition of shorter chains to long chains, branched polymers are formed. Branched polymers typically have a lower density than comparable linear polymers because these shorter chains may prevent the polymers from being packed efficiently. They can have different forms such as star polymers, comb polymers, and polymer brushes as presented in Figure 2.4. Crosslinked polymer chains link from one backbone to another. They are bonded and tied together by

covalent bonding resulting in a stronger structure. Complex polymers that have been intricately connected together to create a complex web of three-dimensional links are known as networked polymers.

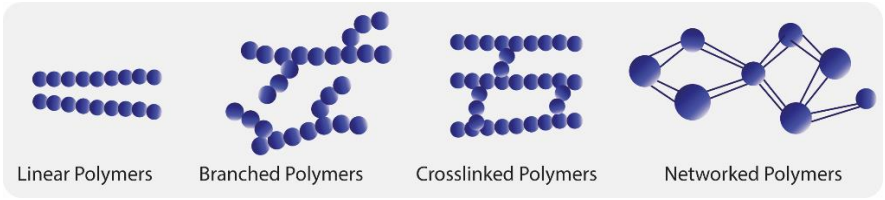

Figure 2.4 Structure of polymers

2.2.3 Polymer Conformations

The spatial arrangement of the constituent atoms or atomic groups for a certain, defined connection is referred to as polymer conformation.[53] The rotational degree of freedom around the few chemical bonds connecting the backbone atoms of most polymers is what allows them to take on many conformations. There are several methods to curl a chain into a relatively small form, resembling a ball of unraveling twine with lots of open space, but comparatively few ways to extend it out more or less. Therefore, chains are considerably more likely to be ball-like than they are to be extended if each conformation has an equal probability or statistical weight, which is an entropic effect. If a linear polymer with freely jointed chains of n subunits, each of length l (occupying zero volume) is considered, there is not a part of the chain excluding another from any location, which results in a random walk in 3D. This is the ideal chain or Gaussian chain model. The end-to-end distance, h, is expressed as: $\vec{h} = \sum_{i=1}^{n} \vec{l}_i$

However, end-to-end distance is generally difficult to measure experimentally, and it cannot be defined exactly for many interesting polymer structures. Another useful way is to calculate the average distance of all monomers from the center of mass. The root mean square, the mass-weighted average distance of any monomer in a polymer coil from its center of mass, is defined as the radius of gyration, $R_g = \frac{< h^2 >_o}{6}$ It can be defined for all polymer architectures and measured by light scattering techniques directly and by various solution dynamics indirectly. Since the scaling of size with molecular weight of

the polymer can be different in each case, Rg is expressed as a function of the degree of polymerization generally: $R_g \sim N^v$

Polymers can respond to environmental changes by changing their conformations. They can undergo various transitions, which are globule, coil, and rod. As shown in the table below, the exponent, v, is dependent on the structure of the macromolecule. For a globule, and dense object, v=1/3, and for a rod, v=1. However, for a polymer coil, the exponent depends on the solvent quality due to the excluded volume effects. There is an associated energy of interaction that might be positive or negative for the interactions between coordinated solvent molecules and polymer chain segments.[56]

Table 2.1 Types of Polymers and Corresponding Exponents

Coil	*v*=0.6 (good solvent), *v*=0.5(theta solvent), *v<0.5*(poor solvent)
Globule	*v*=1/3
Rod	*v*=1

When a solvent is good, interactions between polymer segments and solvent molecules are energetically favorable and lead to the expansion of polymer coils by swelling, v=0.6. Polymer-polymer self-interactions are preferable for a poor solvent, and the polymer coils will contract, and v<0.5. If the solvent is poor enough the counteract the excluded volume expansion effects, the theta (θ) condition is satisfied, and v=0.5.

2.2.4 Concentrations

In dilute polymer solutions, it is assumed that single chains are well separated so that they do not overlap with each other. As the concentration of the polymer increases, the chains tend to overlap. The concentration value determining solution regime is overlapping concentration[56], c*, defined as: $c^* \sim \frac{N}{4\pi R_g^{\,3}/3}$ where N is degree of polymerization and Rg is radius of gyration. The solutions are assumed in dilute regime when the concentration is lower than the c*. The chains start overlapping if the concentration is equal to c*. In the case of exceeding c*, the chains start entangling and the solution is in semi-dilute or concentrated. (Figure 2.5)

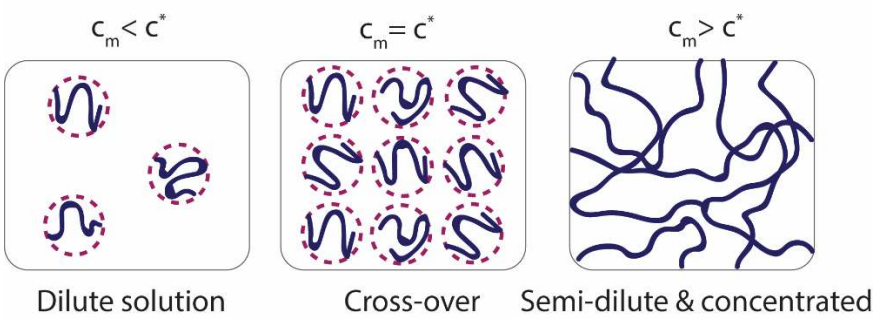

Figure 2.5 Solution Regimes with respect to Overlapping Concentration

2.2.5 Hydrogels

Crosslinked hydrophilic polymer structures known as hydrogels that can absorb huge volumes of water or biological fluids.[57] Hydrogels have a wide range of biological and pharmacological uses. They present good prospects as protein delivery systems or scaffolds for tissue engineering because of their high biocompatibility. Their hydrophilic, rubbery, and soft properties provide low tissue irritation and a low tendency for cells and proteins to adhere to the hydrogel surface.

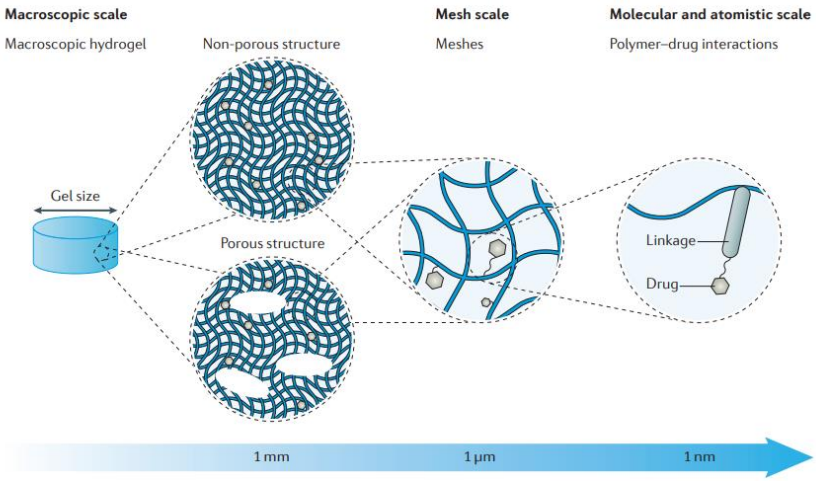

Figure 2.6 Multiscale Properties of Hydrogels[58]

The size, design, and functions of hydrogels vary, and these characteristics collectively determine how hydrogels are employed for drug delivery.[58] There are elements in hydrogels with length ranges ranging from centimeters to sub nanometers as shown in Figure 2.6. Hydrogels can be formed to have any shape and size. If present, micropores have a significant impact on the overall physical characteristics (such as deformability) while permitting convective drug transport. The water contained in the

hydrogel network is surrounded on a scale of several nanometers by a crosslinked polymeric network. Different chemical interactions between the drugs and the polymer chains may take place at the molecular and atomistic scale. The polymer chains may have a variety of sites for binding interactions with the drug, and these sites may be pre-designed utilizing a variety of physical and chemical techniques. For regulated drug release, characteristics at the molecular, atomic, and mesh scales are crucial.

2.2.5.1 Crosslinking Types

Based on the crosslinking mechanism, hydrogels can be categorized as either physical or chemical.[59] Entangled chains, hydrogen bonds, hydrophobic contact, and crystallite formation are a few examples of physical crosslinks. Even though these physical crosslinks are not inherently permanent, they are enough to make hydrogels insoluble in aqueous conditions without the addition of crosslinking entities and chemical modification. Chemical hydrogels are produced by covalent bonds between the functional groups of polymer chains and enable tuning the properties of hydrogels, such as gelation time, pore size, degradation, or dissolution. Small cross-linker molecules, polymer-polymer conjugation, photosensitive agents, or an enzyme-catalyzed reaction are used to form the chemical crosslinked hydrogels.

2.2.5.2 Mesh Size

A crosslinked polymer network and open gaps (i.e., meshes) between the polymer chains make up a hydrogel. Typical mesh sizes change from 5 to 100 nm, and mesh size can be determined by various experimental techniques such as confocal and electron microscopy, small-angle X-Ray scattering, and small-angle neutron scattering.[58] It can be calculated also theoretically with mechanical tests. $\xi = \left(\frac{k_B T}{G_0} \right)^{\frac{1}{3}}$, where k_B is Boltzmann's constant, T is temperature, and G_0 is the constant elastic modulus at low frequency. The meshes allow liquid and small solute diffusion; in other words, they control the diffusion of drugs within the hydrogel network. If the mesh size is larger than the size of the drug, diffusion dominates the drug release. Small molecules can migrate through the hydrogel

network and diffuse independently from the mesh size. For the other cases in which the mesh size is equal to or smaller than the drug size, the release is hindered by steric hindrance. Polymer chains apply frictional drag on diffusing drugs leading to slower diffusion.

2.2.5.3 Rheological Characterization

One of the crucial factors in the engineering design of hydrogels for medical applications is their mechanical properties. The ability of scaffolds to control cell behavior at both the macroscopic and microscopic levels is crucial in the science of tissue engineering. Time-independent and time-dependent viscoelastic theories are mainly used to examine the structure of the hydrogel and calculate the effective crosslinking ratio when defining the mechanical properties of hydrogel biomaterials.[60]

Hydrogels naturally display dominantly elastic and less viscous behavior since they are viscoelastic materials. Dynamic oscillatory rheology experiments help to analyze these mechanical properties of hydrogels placed between two plates by deforming sinusoidally when one plate is stationary, and the other is moving. This deformation causes stress on the gel with two components. Since it reflects the storage of energy, the elastic component is known as the storage modulus (G'), whereas the viscous component indicating energy loss is known as the loss modulus (G").[61] Therefore, hydrogels have a higher storage modulus than loss modulus, G' > G". Amplitude sweep tests are used to describe the deformation behavior and the deformation limit, which is called linear viscoelastic region (LVER), and are occurred with a constant frequency and varying strains. Frequency sweep tests provide the time-dependent behavior of the material with increasing or decreasing the frequency before the LVER.

2.2.5.4 Swelling Behavior

The ability to swell is one of the favorable properties of hydrogels when they are in contact with a solvent which is thermodynamically compatible. Swelling rate and swelling ratio of hydrogels control the release patterns of drugs or solvents from the hydrogel networks, and result in dimensional changes due to uptake of the solvent.[62]

Swelling is not a continuous process, since there is an elastic force balancing the stretching of the matrix and preventing deformation against the opposite osmotic force. When these two forces balance each other, swelling reaches an equilibrium and hydrogel can no longer uptake solvent. Swelling behavior and swelling equilibrium are affected by several parameters such as the degree of crosslinking, molecular weight of the polymer which belongs to hydrogel itself, and some external parameters such as temperature, pH, and light.[57]

2.3 Liposomes and Polymer Complexes as Artificial Cell Membranes

Cell membrane, which protects cytoplasm from the extracellular environment and acts as a barrier of life, is one of the vital components of living systems. There have been lots of artificial models have been made to mimic the biological membranes to understand this dynamic and unique structure as the major goal of the synthetic biology is unraveling the interaction between livings and non-livings. Therefore, elucidating and recreating the interactions of the cell membrane with the external environment will clarify our understanding of life.

2.3.1 Structure of Cell Membranes and Similarities Between Liposomes

Cell membrane, which protects cytoplasm from the extracellular environment and acts as a barrier of life, is one of the vital components of living systems. It has a dynamic and complex structure enabling cells '*to feel'* their physical environment while maintaining important cellular functions. In 1970s, the structure of the cell membrane is explained for the first time with the fluid-mosaic membrane model (F-MMM).[63] It has a thickness of ~7-8 nm and is made up of mainly self-assembled lipid membrane (~50%), also includes proteins (40%), and carbohydrates (2-10%).[9] Cells need to be responsive to the alterations in the external environment and produce signals through their membrane as a requirement of mutual functions such as migration, endocytosis, cell division, cell growth. To continuously perform these processes, cells should adjust their shape dynamically in accordance with the changing conditions. Therefore, the cell membrane has two distinct properties: asymmetry, and fluidity.[63] As mentioned in the previous sections, phospholipids have asymmetric structures due to some rotational, lateral and flip-flop motions. In the biological membranes, this asymmetry comes from not only

phospholipids but also receptors, enzymes, proteins, and other structures. From the view of life activity, the cell membrane provides a stable environment that several biochemical reactions can take place properly although it has a dynamic and fluidic structure. The self-assembling of lipid molecules helps to form thermodynamically stable biological membranes as they prevent interacting with water but also facilitate the material transportation, and exchanging energy between cell and surrounding.[10] Therefore, liposomes are well-suited models for the protein-free parts of the biological cell membranes with many similarities in structural manner. However, to understand the complex and dynamic interactions of cell membranes with extracellular matrix (ECM), there have been various synthetic polymeric materials used for ECM models.[64] ECM is a non-cellular component providing physical scaffolding and facilitating crucial biomechanical functions such as tissue morphogenesis, homeostasis, and differentiation.[65] It has a semi-polymeric medium with polysaccharides and collagen fibers in its structure. Various polymers including polyethylene glycol (PEG), chitosan, alginate etc. have been used for the mimicking macromolecularly crowded environment of ECM with its non-toxic, biodegradable, and tunable properties.[66] (See Figure 2.7) They are more favorable compared to ECM biomaterials since their synthesis can be well-tuned, reproducible, and they are easily applicable cost-efficient carriers.[65]

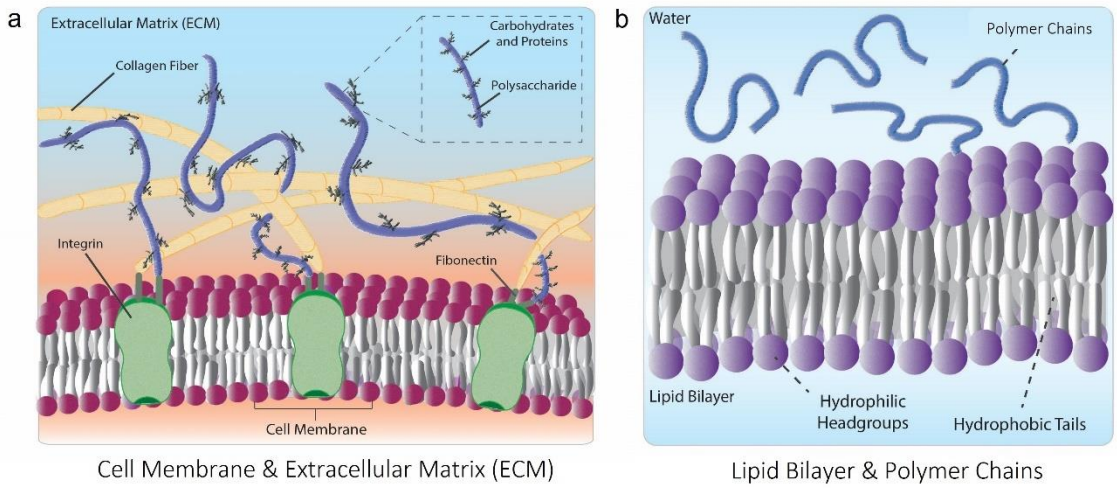

Figure 2.7 a. The structure of cell membrane and extracellular matrix (ECM) b. Lipid bilayer as the cell membrane model, and polymer chains as ECM model.

2.3.2 Membrane-related Diseases

The interaction of phospholipids constructing the cell membrane is not controlled by covalent bonds, instead the membrane lipids are held together by weaker forces such as Van der Waal's and hydrophobic interactions,[11] making the membranes susceptible to the physical and chemical changes in their microenvironment and adjust accordingly their fluidity, stiffness, and thickness.[67, 68] Such modifications in membrane structure and mechanical properties have been linked to several human diseases.[69-73] For instance, there are numerous evidences that membrane flexibility, which is directly related to permeability and cell motility, is significantly modified in tumor cells and is highly related to their invasive potential and drug resistance. [74, 75] Changes in membrane lipids and lipid composition can cause many other diseases such as cardiovascular problems, schizophrenia, obesity, infection, type-2 diabetes, cancer, Huntington diseases. In neurodegenerative diseases such as Alzheimer's, and Parkinson's diseases, a transition of the proteins amyloid-B and a-synuclein from monomers to unfolded aggregates is observed.[12] The alterations in the protein-lipid interactions results in conformational damages in lipid membrane through protein incorporation into the bilayer. Thus, increasing surface pressure and membrane rigidity promote the membrane deformation and membrane thinning affecting mainly the transportation of ions across the membrane. (Figure 2.8)

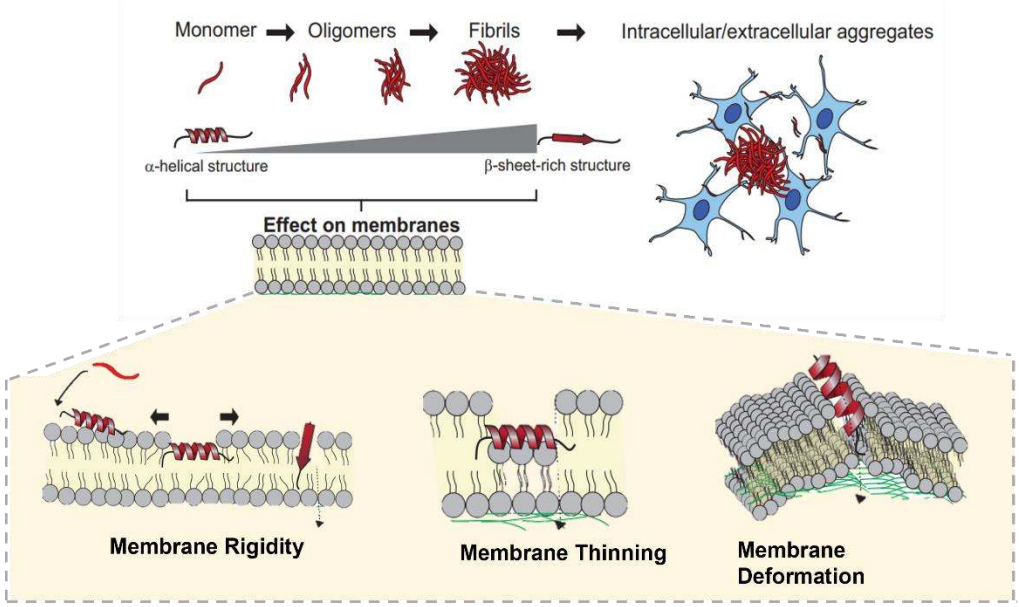

Figure 2.8 A transition of the proteins amyloid-B and a-synuclein from monomers to unfolded aggregates is observed in case of neurodegenerative diseases such as Alzheimer's, and Parkinson's diseases, leading to structural changes in membrane.[12]

Accordingly, the ability to control the lipid membrane dynamics in selective tissues appears to be a novel way of treating membrane-associated diseases. So far, current strategies developed to tune the membrane fluidity/stiffness are based on changing the chemical composition of the lipid bilayers, membrane lipid therapy being the most attractive approach.[76] It aims rational design of drugs to target the membrane lipids to change their composition, structure, and conformation. However, all these methods are essentially cell-specific and, thus, not translatable to other tissues. In order to create a more generic and mechanistic way for altering membrane structure and dynamics, from nanoscale to bulk, the influence of the mechanical properties of the ECM needs to be clarified.

2.4 Liposomes and Polymer Complexes as Drug Carriers

Over the past decades, liposomes have been promising drug delivery particles. As they are biocompatible, biodegradable, and non-toxic, they protect the encapsulated drugs from external degradation.[77] They have several pharmacokinetic advantageous, for example, delayed drug absorption, sustained drug metabolism, high encapsulation efficiency etc. Consequently, there are many liposome-based commercial products approved by United States Food and Drug Administration (FDA).[78]

2.4.1 Drug Encapsulation

As having an amphiphilic and non-ionic structure, liposomes are capable of delivering both water-soluble and lipid-soluble drugs which is an important priority in drug delivery applications to improve formulations.[5] (See Figure 2.9) Therefore, the structure and properties of liposomes (rigidity, permeability, solubility, stability) can be engineered for the desired applications. Since they have a flexible structure, liposomes can easily bind with specific ligands for active targeting.[79] Besides, the efficacy and the therapeutic index of drugs are increased by liposomes.

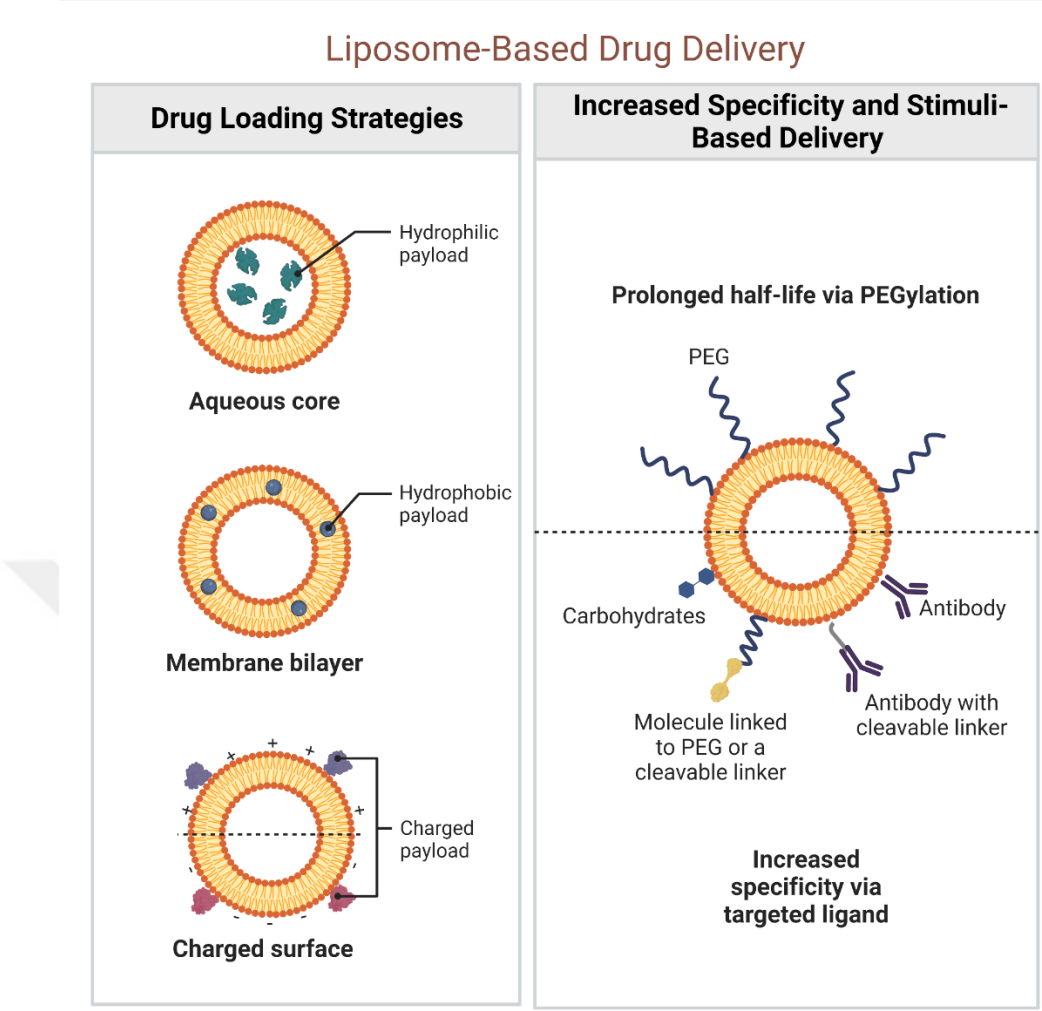

Figure 2.9 The ability of liposomes to encapsulate different types of drugs. Also, the release can be modulated by different trigger mechanisms such as temperature, pH, chemical and mechanical stimuli.

Pay load (PL) and encapsulation efficiency (EE) are two important terms to represent the amount of drug incorporated into liposomes. There are mainly two different ways to encapsulate the drug molecules; passive loading which the loading occurs during the formation of liposomes, and active loading which the drug is encapsulated after the formation of liposomes.[80] Active loading is advantages since the process can be performed with no dependency on the time and the site of the liposomes.

The properties of liposomes also affect the drug encapsulation capabilities. Multilamellar vesicles have higher EE compared to unilamellar liposomes since it contains more than one bilayer. Likewise, as the size of the liposomes increased, EE of liposomes increased due to increased encapsulation area.[81] Also, the degree of

unsaturation significantly affects the drug loading. Saturated lipids showed lower EE than the unsaturated lipids since the EE is more dependent on the unsaturated bonds than the length of the phospholipid molecule.[82]

Despite all advantages, liposomes have some disadvantages such as low solubility in aqueous solutions, leakage and fusion of the encapsulated drugs, oxidation of phospholipids which are mainly the consequences of low stability of liposomes. The physical and chemical instability of liposomes can bring undesired side effects and decreased the efficiency of the delivery.[83] To overwhelm the limitations, one approach is coating the liposome surface with polymers. The usage of polymer increases the protection on drug molecule, the stability of vesicles and also the circulation time[84]. Also, liposome-polymer hybrid vesicles have lower antigenicity which prevents them to be in the circulation of the reticuloendothelial system (RES).[85, 86] Several polymers have been used for the drug delivery applications. Chitosan, hyaluronic acid, gelatin, and alginate are examples of natural biopolymers[87-91], whereas polyethylene glycol, polyenes, polyvinyl alcohol, polyacrylic acid[92-96] are synthetic polymers used for surface modification of liposomes. Among them, PEG has been studied comprehensively in order to produce stealth liposomes[97]. Liposome membranes including PEG-lipids are commonly described as stealth liposomes due to the properties coming from PEG. Stealth liposomes not only have long circulation time and more bio distribution in vivo. PEG located on the surface of liposomes creates a hydration shell so that water molecules link to the hydrophilic chains of PEG. Therefore, liposomes could not interact with the components of blood, and they can overwhelm the Van der Waals interactions between lipid surfaces which leads to aggregation and membrane fusion.[86, 98-100]

2.4.2 Liposome-Hydrogel Complexes

Due to easily tunable physicochemical properties, hydrogels have been widely investigated and explored in a broad range of biomedical applications, and drug delivery.[101] The major drawback of hydrogel-based systems is rapid and uncontrolled release properties.[102] The combination of liposomes and hydrogel systems, thus, have important properties with respect to hydrogel or liposome only drug delivery systems. The crosslinked polymer environment provides mechanical support to bilayer and

increases the stability of liposomes. Also, liposomes facilitate a well-controlled, and sustainable release from hydrogels. There are evidences that polymeric network can modify the structure of liposomes with high osmotic pressure reached by crosslinking.[103] The composition, concentration, and surface charge have been found to regulate the hydrogel properties such as increased gelation and relaxation time.[104] Hurler *et al.* studied the release mechanics of chitosan-based hydrogels with pH-dependent rhodamine derivatives.[105] The results revealed that the lipid composition as well as the surface charge of the liposomes strongly influenced the release kinetics. The results revealed that the size of the liposomes had a minor effect compared to the surface charge of the liposomes and drug lipophilicity.

The viscoelastic behavior of the hydrogels assessed by rheology depends on several factors such as the composition, concentration, and the type of the dispersed materials.[106] The rheological properties of hydrogels are therefore expected to be affected significantly by the addition of liposomes into them as shown an enhanced elastic behavior in the presence of liposomes in the literature.[107, 108] Liposome concentration and liposome size are found to be important parameters controlling the mechanical behavior of hydrogels. Elasticity of the hydrogel is proportionally dependent on the interactions of polymer chains with liposomes.[107] Since an increase in the concentration of liposomes increases the surface area between liposomes and polymer chains as well as the interactions between them, in turn, enhanced rheological properties are observed. Inversely, an increase in the size of the liposomes decreases the surface area, thus, the interactions.

Another drawback of polymer-based systems is the restricted control over the gelation kinetics that can cause the loss of uptake and rapid crosslinking, resulting in clogging during an injection.[102] To address this issue, hydrogels are also designed to be injectable in minimally invasive drug delivery, and site-specific therapies into the poorly reachable tissues where wound healing takes longer time.[109] The administration of hydrogels to the body by a needle without any surgery makes them good candidates for biomedical applications. Similar to 3D or 4D printed hydrogels, injectable hydrogels should be designed to flow as a result of large shear stresses applied during injection (*i.e.* must be a shear-thinning material) and recover (at least partially) its initial mechanical properties to a solid-like structure upon removal of the shear stress (*i.e.* must be self-healing).[110] Hydrogels should contain dynamic bonds that can be broken under stress and

then recovered after the removal of the stress to have injectable properties. Although there have been many studies on the covalently bonded liposome-hydrogel systems due to the enhanced mechanical stability and controlled release properties, these dynamic bonds can be formed between liposome and polymer chains facilitating and enhancing the shear-thinning and self-healing behavior of the hydrogels.[111, 112] The Kechai *et al.* tested the rheological and syringeability properties of hyaluronic acid (HA) hydrogels with the addition of neat and PEG-covered EggPC liposomes.[107] The results revealed that PEG-covered liposomes strengthen the gel network and the highest viscosity and elasticity, which is attributed to the increased dynamic bonds between liposomes and PEG chains. Also, there was not any modification of the zero-shear viscosity of the gels after the syringeability test via 29G needle. Similarly, Z. Rao et al. modified PEGs with cholesterol to have hydrophobic end groups which were preferentially located within lipid bilayers of different liposomes resulting in a thermoresponsive hydrogels with dynamic bonds. The strength of the gels was found to be both liposome and polymer concentration dependent since they affect directly the crosslinking density and injectability properties.[113]

2.4.3 Stimuli-Based Drug Release

The purpose of the drug delivery is increasing therapeutic efficacy by reducing the toxic side effects. Although drug delivery vesicles are promising candidates in this context, localized delivery to desired locations while not causing a damage on healthy tissues still remains a challenge. Through addressing this issue, stimuli-responsive materials (*e.g*. liposomes, polymer nanoparticles, metallic nanoparticles, quantum dots, carbon nanotubes) have been developed to be triggered externally by light[114], heat[115], ultrasound[116], and mechanical stimuli[117], which significantly increased the precision of controlled drug delivery.[118-120] More importantly, such materials can also react towards internal stimuli which utilize physiological differences between healthy and unhealthy tissues, *e.g.* pH,[121] hypoxia[122], enzymes[123], temperature[124], and mechanical stress[125]. Since the structure of liposomes is suitable to be engineered by attachment of antibodies, ligands, or other responsive materials, these smart liposomes can perform triggered drug release on various environments.

As mentioned in the previous sections, the permeability and fluidity of liposomes which critically affect the drug release properties are extremely sensitive to temperature. Temperature is also essential for the metabolic activity of the cells. The body temperature of mammalian cells is 37℃ at which the intracellular chemical reactions occur ideally. Thermosensitive liposomes are designed mostly to higher fever temperatures ~40-42℃, which is called hyperthermia.[126] Besides, by changing the transition temperature of the bilayer with different lipid compositions, the thermosensitivity of liposomes can be modulated. One of the most well-known examples of thermo-responsive liposomes is loading of sodium bicarbonate into liposomes, it facilitates a pH gradient to doxorubicin and also enhanced release with heat.[127] Hyperthermia causes to decomposing of sodium bicarbonate into ammonia and carbon dioxide which in turn results in a damage in the membrane and the leakage of the drug. Past research showed the success of this application on tumor-selective chemotherapy until heating with high biostability and biocompatibility.

Light is another stimulus used to trigger liposomes since drug release can be modulated with a variety of parameters including wavelength, the intensity and size of the beam, and duration.[128] Electromagnetic light wavelengths, below 650 nm, cannot penetrate into deep tissue due to scattering and absorption by water, lipids, and hemoglobin. Even though UV light can be used to trigger lots of chemical reactions, it can be applied only to the skin and mucosa.[129] A deeper light penetration, thus, can be achieved by near-infrared (NIR) light (650-1000 nm) by causing less damage to cells. The drug carrier materials should have a chromophore, a chemical having the ability of capturing light energy.[128] The light sensitivity of liposomes is induced by three mechanisms: photo crosslinking, photochemical triggering, and photoisomerization. Each mechanism is working to change the chemical structure of the liposomes.[128] Light-sensitive materials can be introduced to lipid bilayer generally by chemical synthesis. Different regions of phospholipids (head, fatty acid tails, and glycerol backbone) are modified with additional groups, or the existing chemical bonds are changed. Azobenzene, spiropyran, and coumarin are the most studied examples of important photo sensitive chemical groups.[128]

Cancer cells have relatively low pH values compared to healthy cells and tissues that can be taken as an advantage of pH-sensitive drug delivery. The acidification of the surface of the liposomes facilitates selective destabilization of the membrane to pH.[130] pH-sensitive liposomes contain a neutral lipid, usually a phosphatidylamine derivative, and a weak acid amphiphile such as cholesteryl hemisuccinate (CHEMS).[130] The negatively charged group of phospholipids destabilizes in acidic medium, in turn, membrane fusion or pore formation on the membrane leading to release of the content occurs. Although several types of liposomes having anionic/cationic composition have been developed, the surface of the liposomes can be modified with pH-labile polymers, target-specific ligands to increase the efficiency of the delivery.[131]

Mechanical stimulus is another common mechanism for targeted delivery due to easy access, measurement, and applicability. A mechanical force applied on an object result in a distribution of internal forces, causes shape change or deformation, and is divided into three major categories; compression, tension, and shear forces. The human body is exposed to several internal and external mechanical forces continuously and repeatedly from cellular to skeletal muscle level in the range of 10^{-9} – 10^{3} N. Since mechanical forces are ubiquitously achieved in the body or externally and facilitate a quick treatment in several conditions, they can be taken as an advantage for the drug and protein delivery systems responding to mechanical/shear triggers.[132] More importantly, they may serve as creative approaches since controlled direction and adjustable dose delivery that increased therapeutic efficiency have been demonstrated.[133] Owing to their soft and flexible nature, liposomes are the most widely used as mechanically triggered nanoparticles. Under sufficiently large stress, hydrodynamic effects can lead to deformations on the membrane. Any structural change such as size and lamellarity can modulate the drug release and encapsulation properties of liposomes.[134, 135] Under compression and tension, the release rate of the drugs from liposomes increased due to the rearrangement and destruction of the structure of lipid bilayer.[136, 137] Also, enhanced release properties were obtained under shear, since it causes pore formation on the membrane and leakage of the drug. .[138-140]

Chapter 3:
MULTISCALE DYNAMICS OF LIPID VESICLES IN POLYMERIC MICROENVIRONMENT

3.1 Introduction

Liposomes have been widely studied as artificial cell membranes to understand the complex relationship of the cells with their environment and understand membrane dynamics at macroscopic and molecular levels.[80] As they are formed by self-assembling of individual phospholipids in aqueous environments, they reflect the similarity of the protein-free parts of the real membranes.[3] The interaction between lipid molecules constituting the membrane is controlled by weaker forces such as Van der Waal's and hydrophobic interactions,[11] making the membranes susceptible to the physical and chemical changes in their microenvironment and adjust accordingly their fluidity, stiffness, and thickness.[67, 68] Meanwhile, polyethylene glycol (PEG) is a widely studied synthetic polymer in mimicking the crowded macromolecular medium and ECM due to its non-toxic structure, tunable properties, and flexible conformation.[141] The liposome-PEG complexes, thus, have found unique applications in drug delivery and tissue engineering.[142-144] One of the recent example of this composite systems is mRNA-based COVID-19 vaccines. PEG is used to modify the surface of the liposomes to facilitate the stability and enhanced biodistribution.[145, 146] Despite controversial evidence, the reason behind the rare allergic responses in vaccines was shown to be the conjugated PEG chains on liposomes, and this allergen effect was claimed to be highly molecular weight dependent.[147]

As the local viscoelasticity is strongly affected by the length of the polymer chains attached, lipid vesicles can experience a very different microenvironments compared to their bulk dynamics, which affects the drug delivery properties significantly. the segmental and collective chain relaxation of the polymers occur at timescales comparable to those of the single lipid motion and membrane undulations, the dynamics of the flexible polymer chains and the liposomes are expected to be coupled.[148] Nevertheless, a thorough

understanding of the effect of polymeric microenvironment on the membrane dynamics is still lacking.

Lipid bilayers can form hydrogen bonds intermolecularly to bind the specific areas of proteins enabling protein-lipid coupling.[149] Likewise, hydrogen binding between PEG and lipid molecules is favored due to the ether oxygen groups of PEG, and hydrophilic headgroups of the lipids.,[150] Such an attractive interaction may lead to a highly molecular-weight dependent, and stable polymer-bound layer on lipid bilayer. Although some macroscopic effects of PEG have been reported, the effect of it on the structural dynamics of liposomes has not been explained yet. As being a highly hydrated polymer, PEG can induce lipid fusion by disrupting the packing of membrane.[151] According to MD simulations, it locates into the bilayer/water interface rather than penetrating inside the membrane.[152] PEGs with lower molecular weights can destabilize the membrane due to the osmotic pressure. It can further alter the bilayer curvature leading to modifications in thermal behavior of liposomes.[153] It was shown that the concentration of PEGs is as important as the molecular weight on the phase transition.[154] In one study, the interaction of multilamellar DMPC, DPPC, and DSPC liposomes and PEG molecules, it was suggested that the main phase transition temperature is affected faster than the pretransition temperature as PEG concentration increases.[155] Lipid membranes dehydrate with the increasing concentration and decreasing molecular weight of the PEG, since the microviscosity of the membrane increases gradually as the molecular weight changes from 400 to 6,000 Da.[156]

The microviscosity of the lipid membrane is one of the crucial properties related to membrane permeability, and fluidity affecting the transport properties and contributing the many vital cellular activities.[157] It has been measured by various fluorescence techniques, which are time resolved fluorescence spectroscopy, fluorescence anisotropy, and determination of fluorescence quantum yield.[158] Microviscosity of DMPC membranes was estimated to change from 1.5 mPa.s to 97 mPa.s after phase transition to the gel state. [159] At the macroscopic level, the diffusion of the liposomes is closely related to the bulk viscosity of the surrounding medium.

All these studies strongly indicate that lipid membrane interaction with the surrounding polymeric media can modify the membrane structure and dynamics. Although liposome-polymer complexes have been widely utilized in drug delivery and tissue engineering applications in the past[160, 161], the key fundamental question, that is how the polymeric microenvironment affects the bulk viscous properties and microviscosity of the membranes, remains unanswered. In this work, we used aqueous solutions of poly (ethylene glycol) (PEG) with a wide range of molecular weight (from 1.5 kDa to 400 kDa) to mimic the viscous medium of the cells, and nearly monodisperse unilamellar vesicles of DMPC/DMPG liposomes to model the cell membranes. Using small-angle X-ray scattering (SAXS), dynamic light scattering (DLS), temperature modulated differential scanning calorimetry (DSC), bulk rheology, and fluorescence lifetime spectroscopy (FLS), we investigated the structural phase map and dynamics of the liposome-polymer mixtures from the nanoscale to the bulk. The results show that the microviscosity of the lipid bilayers is strongly influenced by the relaxation of the whole chain, resulting in accelerated dynamics of the lipids within the membrane (even in the gel state) compared to the polymer-free liposome case. At the macroscopic level, the gel-to-fluid transition of the bilayers causes an unprecedented thermal-thickening behavior of the polymer-liposome solutions, which is controlled by multilamellarity, size, and concentration of the liposomes.

3.2 Experimental Methods

3.2.1 Materials

Lipids, 1,2-dimyristoyl-sn-glycero-3-phospho-choline (DMPC), and 1,2-dimyristoyl-sn-glycero-3-phospho-(1'-rac-glycerol) (sodium salt) (DMPG), and mini-extruder were purchased from Avanti Polar Lipids (AL, USA). Poly (ethylene glycol) (PEG) with four different molecular weights (1.5 kDa, 20 kDa, 100 kDa, 400 kDa), and Oil-Red-O were purchased from Sigma-Aldrich and used as received.

3.2.2 Preparation of Liposomes

Unilamellar liposomes were obtained by thin-film hydration followed by extrusion method. A schematic of the procedure was presented in Figure 3.1. Lipids containing (5%

w/w) DMPG and (95% w/w) DMPC were dissolved in chloroform and mixed for one hour for complete dissolution. DMPG, a charged lipid, was used to increase the liposome stability and the dispersion of the solution. Chloroform was evaporated in a vial and kept under vacuum at 80℃ for 24 hours to have a thin film of the lipids. Then, the film was hydrated with DI water to obtain a final lipid concentration of 20 mg/mL. Lipid solution was mixed at 40℃ using a vortex for 2 hours, and was extruded using a mini extruder after waiting 15 min for the temperature equilibration. Temperature of the system was kept constant at 40℃, above the transition temperature of the lipids, by using a heating block. The solution was subsequently extruded 15 times through 400 nm and 200 nm membranes, respectively, and 41 times through 100 nm membranes. Extruded solution was used immediately after preparation or stored at 40℃ while mixing in a vortex. The stability and size of the liposomes were confirmed using dynamic light scattering (DLS) before each experiment.

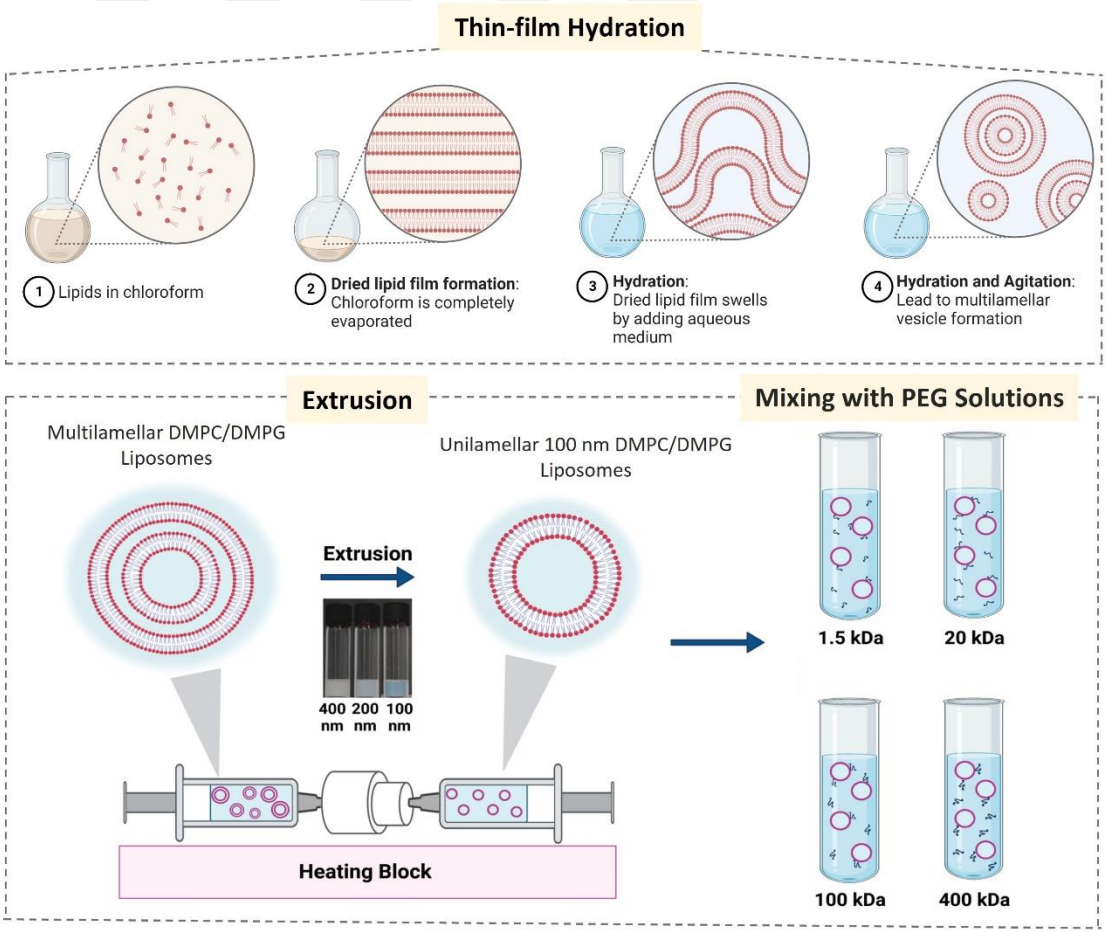

Figure 3.1 The schematic of the sample preparation procedure. 100 nm unilamellar liposomes were prepared by thin-film hydration method (top) followed by extrusion

method (bottom-left). Then, the liposome solutions were mixed with PEG solutions with different molecular weights (1.5, 20,100, and 400 kDa) (bottom-right).

3.2.3 Preparation of Liposomes Containing Oil-Red-O

For the microviscosity estimation experiments with Fluorescence Lifetime Spectroscopy (FLS), liposomes were stained with Oil-Red-O. Liposomes were prepared with the same procedure above. 2×10^{-5} uM Oil-Red-O was added to the solution of lipids in chloroform in the beginning of the preparation.

3.2.4 Preparation of Liposome-Polymer Mixtures

Stock solutions of polymers were prepared at a PEG concentration of 100 mg/mL for the molecular weights of 1.5, 20, and 100 kDa. PEG 400 kDa solutions was prepared at 50 mg/mL due to its high viscosity. The required amounts of PEG solutions were added to the extruded 100 nm liposome solution slowly, and the final concentration of polymers in the composite solution was kept the same with lipids, 20 mg/mL. After mixing, the composite solution including 100 nm liposomes and polymers was vortexed for 15 min prior to use.

3.2.5 Dynamic Light Scattering (DLS)

Hydrodynamic size, polydispersity index and diffusion constants of liposomes were determined by Dynamic Light Scattering (DLS, Malvern ZS Zetasizer) with backscatter detection at a scattering angle of 173° and a wavelength of 633 nm. Since low concentrations are required for DLS measurements, the solutions were diluted to have a concentration of 0.2%. Each measurement was repeated three times and averaged.

3.2.6 Differential Scanning Calorimetry (DSC)

TA Instrument's Q25 AutoDSC was used to obtain the phase transition temperature of liposomes. The 10-15 mg of samples were sealed in Tzero pans with Hermetic lids. An empty pan was measured as reference. Samples were first heated to 60℃ and equilibrated for 5 min. Then, they were cooled down to 5℃ with a rate of 2 ℃/min. The crystallization temperatures of liposomes were obtained using the cooling curve for each case. Enthalpy

values are calculated from the area of exothermic peaks. The cycles were repeated several times to ensure reproducibility of the data.

3.2.7 Rheology

Viscosity of liposomes-PEG solutions were measured using Anton-Paar rheometer (MCR-302). CP50-1, a conic plate having 50 mm diameter and a cone angle of 1° was used. Temperature was controlled using a Peltier control device. A hood coupled with Peltier was used to prevent evaporation during measurements. Temperature of the system was changed from 10 ℃ to 40 ℃ continuously with a heating rate of 1 ℃/min. Data was collected every 60 s at a constant shear rate of 30 s^{-1}.

For microviscosity estimation, viscosity of glycerol-methanol- Oil-Red-O solutions with varying ratios was measured with CP50-2, a conic plate having 50 mm diameter and a cone angle of 2° at 35℃. Shear rate was changed from 1000 s^{-1} to 1 s^{-1}, and the viscosity data was taken at a shear rate of 10 s^{-1} for all solutions.

3.2.8 Small Angle X-Ray Scattering (SAXS)

SAXS data was collected using Anton Paar SAXSpoint 5.0 at the sample to detector distance of 500 mm. Quartz capillary sample holder was used to seal the samples, and placed on a heated cooled sampler holder for temperature control. Over a total duration of 1.5 hours, each frame was collected for 3 minutes. Background (water only) was subtracted from the data. Data reduction was performed using SAXS analysis program of the SAXSPoint 5.0.

3.2.9 Cryo-TEM

Sample was placed on a 400-mesh copper grid and transferred to Gatan cryo transfer holder containing liquid N_2 in it. Sample was investigated by cryogenic transmission electron microscopy (cryo-TEM) operated at 120 kV (Hitachi HT7800, Japan).

3.2.10 UV-Vis Spectroscopy

UV-Vis spectra was obtained by a Shimadzu UV-3600 -UV-VIS-NIR Spectrophotometer in transmission mode using quartz cuvettes from 400 nm to 700 nm at 35 ℃. 5 minutes

was waited before each experiment for the temperature equilibration. DI water, and neat PEG solutions with appropriate molecular weights were taken as reference of the neat liposome solutions, and liposome-polymer solutions, respectively.

3.2.11 Time-Resolved Photoluminescence

Time-resolved spectroscopy measurements were carried out by Picoquant MicroTime 100 time-resolved confocal fluorescence microscope. The picosecond diode laser (λ_{ex} = 375 nm) pulsed at 10 MHz repetition rate with 8mW power was used as the excitation source via a 40X objective lens. A single photon sensitive detector (PMA Hybrid 50) based on a photomultiplier tube (R10467 from Hamamatsu) and the time-correlated single photon counting system (HydraHarp 400) were utilized. The data were analyzed in fluorescence lifetime imaging (FLIM) mode with SymPhoTime 64 (Picoquant) software. PL decays were fit by a two-exponential decay, and the average lifetime was calculated from an intensity-weighted mean.

3.3 Results and Discussion

3.3.1 Structure of Liposomes in Their Neat Form

We first investigating the structure of liposomes first in their neat form, and then in polymer solutions. We start by measuring the hydrodynamic size of the neat liposomes through extrusion process, and neat polymers by DLS, as shown in Figure 3.2. The extrusion process was gradually decreased the size of the liposomes to 119.9 $\pm$ 2.54 nm. The polydispersity index of 0.075 $\pm$ 0.010 yields a monodispersed vesicle solution.

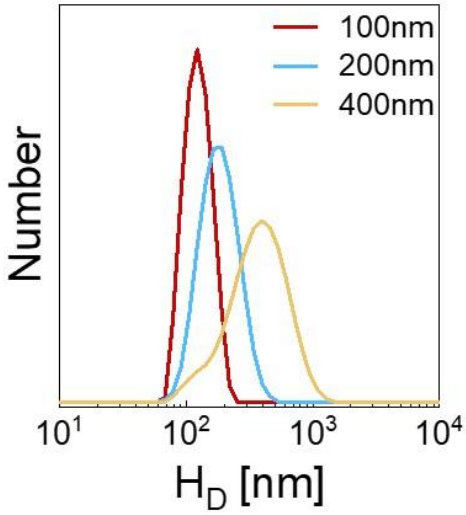

Figure 3.2 Hydrodynamic diameters of 400 nm, 200 nm, and 100 nm liposomes through extrusion.

To confirm the unilamellar liposome structure, the lamellarity analysis was performed by DSC and SAXS. Figure 3.3.a shows the DSC traces of obtained for liposome solutions during extrusion process. DMPC and DMPG lipids have identical hydrophobic tails, and a transition temperature from gel to fluid state was observed at ≈ 24℃.[162] We observed a sharp and intense peak for the unextruded liposomes as the solution contains high fraction of multilamellar vesicles with highly ordered lamellar structures at ≈ 22.4℃. The intensity of the peaks decreases gradually through extrusion, and a broad transition ≈ 23 ℃ is obtained for 100 nm liposome solution suggesting a transition from multilamellar to unilamellar structure. Due to the interbilayer interactions in membrane, unilamellar structures have higher curvature, and lower lateral packing which causes a broad transition in agreement with our observations.[163, 164]

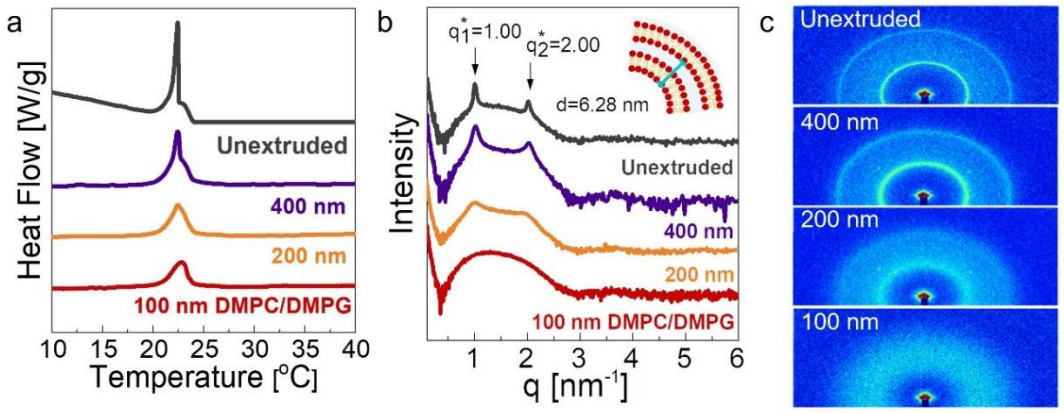

Figure 3.3 a. DSC traces of 20 mg/mL unextruded, 400 nm, 200 nm, and 100 nm lipid solutions. b. SAXS analysis of unextruded, extruded 400 nm, 200 nm, and 100 nm liposomes and c. raw detector data.

SAXS offers more direct evidence for lamellarity compared to DSC. Scattering intensity versus wave vector, q, for unextruded and extruded liposome solutions are represented in Figure 3.3.b. The repeat distance of the stacked lipid bilayers including water in between (see the sketch in the inset) can be calculated by $d=2\pi/q_1^*$. We obtained a characteristic set of equally spaced two peaks was observed for unextruded multilamellar liposomes at q_1^*=1.0 nm^{-1}, q_2^*=2.0 nm^{-1}, corresponding to the Bragg spacing of 6.28 nm in agreement with the reported values for multilamellar vesicles.[165] As the size of the liposomes decreased to 400 nm and 200 nm, the intensity of the peaks decreases without changing the q positions. The disappearance of the peaks for 100 nm vesicle solution confirms the unilamellar structure. Since unilamellar vesicles are representative of the protein-free part of the cell membranes, and their properties such as permeability, and viscosity are well-controlled, we continue our further analysis mostly based on 100 nm unilamellar liposomes.

3.3.2 Structure of Liposomes in Polymer Solutions

It was shown that transition behavior of liposomes can be molecular weight dependent, implying that the structure and dynamics of the membranes can change with the length and size of the polymers.[154, 166] Therefore, we choose a wide range of PEG molecular weights from 1.5 to 400 kDa for this study. Table 3.1 shows the hydrodynamic sizes measured by DLS and calculated radius of gyration (Rg) values of PEGs. Rg is calculated according to the following equation; $R_g = \frac{< h^2 >_o}{6}$ where $< h^2 >_o$ (is the actual mean-square end-to-end distance of the polymer chain. $\frac{< h^2 >_o}{M}$ value is taken as 0.805 for PEG, and M is the molecular weight of the polymer.[167] Rg and hydrodynamic radius values are close to each other, suggesting that the polymers do not form clusters in water.

Table 3.1 Calculated Radius of Gyration of PEGs with various molecular weights

	Radius of Gyration (nm)	Hydrodynamic Radius(nm)
PEG 1.5 kDa	1.41	0.78±0.10
PEG 20 kDa	5.18	6.50±1.70
PEG 100 kDa	11.5	10.10±2.13
PEG 400 kDa	23.16	18.17±3.28

We then prepared the liposome-polymer solutions containing 1.7 w% lipids and 1.7 w% polymer in water. Figure 3.4.a shows the hydrodynamic sizes of 100 nm DMPG/DMPC liposomes in polymer solutions. The diameter of the liposomes increased gradually as the polymer molecular weight increases, suggesting an attractive interaction between lipid bilayer and polymer chains, illustrated in Figure 3.4.b. The interaction between PEG and lipids is shown to be hydrogen bonding between the ether oxygen of PEG and hydrophilic headgroups as recently shown by Zhang *et al.*[150] Moreover, as PEG has terminal OH^- end groups which make it hydrophilic, it prefers to stay in the bilayer/water interface due to energetic barrier as was also shown by MD simulations. [152] Also, the penetration of the PEG chains into bilayer is possible only if the terminal groups of polymers are modified to contain hydrophobic groups.[168] Therefore, in our case, it is expected to observe a bound layer of polymer on the outer surface of the membrane as suggested by DLS. The thickness of this bound layer, δ, can be calculated by comparing the size increase in liposomes. Figure 3.4.c shows the dependence of δ on the PEG M_w, and its value ranges from ≈1 nm to ≈20 nm. δ values are in agreement with Rg values of polymers, and also a linear relationship with $\log \delta \propto \log M_w$ is observed with slope of 0.58, in agreement with good solvent condition for PEG-water system.[169] This suggest that the adsorbed PEG chains on DMPC/DMPG bilayers exhibit nearly Gaussian statistics with no strong collapsing, flattening or stretching due to high entropic barrier, similar to the case of attractive polymer nanoparticle mixtures.[170]

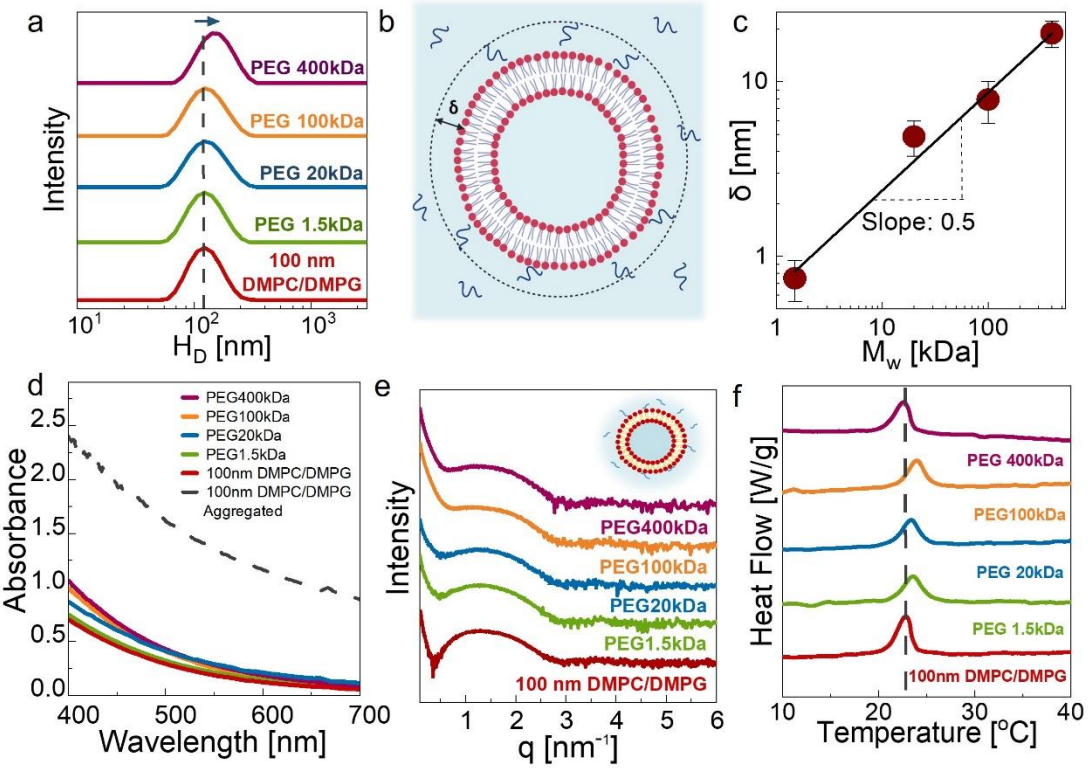

Figure 3.4 a. Hydrodynamic diameter of 2 w% 100 nm DMPC/DMPG liposomes mixed with 2 w% PEG solutions with the molecular weights of 1.5, 20. 100, and 400 kDa at 35℃ b. Schematic representation of the attachment of PEG chains on lipid bilayer surfaces. δ represents the thickness of the adsorbed layer. c. Molecular weight dependence of δ in PEG-liposome solutions. d. UV-vis spectroscopy results of 2 w% 100 nm DMPC/DMPG liposomes and mixed with 2 w% PEG solutions at 35℃. The dashed line represents aggregated vesicles after 1 week of preparation. e. DSC results of neat 2 w% 100 nm DMPC/DMPG liposomes and 2 w% 100 nm DMPC/DMPG liposomes mixed with 2 w% PEG solutions at 35℃. f. SAXS results of neat 2 w% 100 nm DMPC/DMPG liposomes and mixed with 2 w% PEG solutions at 35℃. Inset shows the attachment of PEG chains into lipid bilayer.

Figure 3.4.d shows the absorption spectra of liposomes in neat form and in polymer solutions. The absorptions represent a typical spectrum of individually dispersed nanoparticles in solution and increase slightly in the PEG solutions, which is due to the size increase of the liposomes. The SAXS results in Figure 3.4.e show that 100 nm unilamellar liposomes did not change their structure in the presence of PEGs as no Bragg peaks are observed. In the crosslinked PEG chains, the transition from unilamellar structure into multilamellar structure was observed previously due to osmotic pressure exerted on the membrane.[103] However, in the uncrosslinked solution state, we did not observe such a structural change for liposomes even in the highest osmotic pressure with PEG 1.5 kDa. This shows that not only the osmotic pressure but also the elastic stresses

and confinement can play significant role on the multilamellarity of the liposomes. The unilamellar structure was also evidenced by DSC results in Figure 3.4.f as no characteristics peaks of the multilamellar structure was observed. The change in T_c (≈1℃) with PEG molar mass is negligibly small. However, Table 3.2 shows ≈ 30% decrease of the specific enthalpy for all polymer-liposome solutions with respect to the neat liposome case. A reduction in enthalpy suggests that PEG caused a change in lateral packing of membranes, [171] confirming the physical attachment of the PEG chains on the bilayer surfaces.

Table 3.2 Hydrodynamic Diameter, Polydispersity Index (PDI), Crystallization Temperature (Tc), Translational Diffusion Constant (DT) at 35℃ and 15℃ of neat 20 mg/mL 100 nm DMPC/DMPG liposomes and in PEG solutions with varying molecular weights.

	H_D (nm) (35 ℃)	PDI	Tc (℃)	Specific Enthalpy (J/g)	D_T (m^2/s) (35 ℃) (x 10^{-12})	D_T(m^2/s) (15 ℃) (x 10^{-12})
Liposome only	119.9± 1.11	0.075 ± 0.010	22.84±0.11	0.335±0.013	5.21	3.73
In PEG 1.5kDa	121.4 ± 0.20	0.074±0.009	23.55±0.19	0.242±0.015	5.12	3.61
In PEG 20kDa	129.6± 1.10	0.077±0.014	23.39±0.02	0.241±0.017	5.03	3.58
In PEG 100kDa	135.7 ± 2.13	0.113±0.022	23.95±0.32	0.234±0.020	5.02	3.21
In PEG 400kDa	157.7± 3.28	0.150±0.025	22.58±0.07	0.256±0.012	4.40	2.72

We finally investigated the stability of liposomes by DLS in the presence of PEGs in Figure 3.5. Neat liposomes and liposomes in PEG 1.5 kDa solution are stable for 20 hours. Since the number of hydrogen bonds between lipid bilayer and polymer chains increases with the increasing molecular weight, the highest stability, 3 days, in PEG 100 kDa and 400 kDa is an expected result.

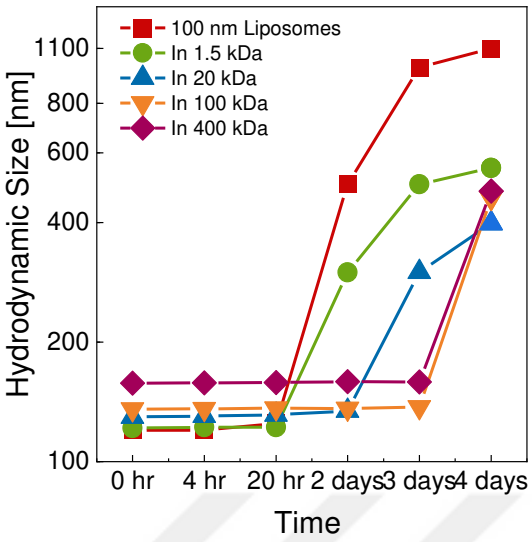

Figure 3.5 The stability of liposomes in terms of their size in their neat form and in PEG solutions obtained by DLS at 35°C.

3.3.3 Dynamics of Liposomes

In the dynamics section, we elucidate how PEG chains affect the dynamics of 100 nm liposomes at different time scales. First, the translational bulk diffusion of vesicles in the presence of PEG chains are examined at 35°C where liposomes are in fluid phase, and at 15 °C where they are in gel phase. Then, we investigated bulk viscosity of the solutions by rheology to understand the effect of particle softness of liposomes on the viscosity of the composite system., and microviscosity of lipid bilayer by FLS to show how the lipid bilayer dynamics is correlated with the viscosity of the bulk medium.

3.3.3.1 Bulk Diffusion of Liposomes

Translational diffusion constants are calculated by DLS from the decay of autocorrelation functions (G_2). Diffusion constant is calculated from the fitting of G_2 which is expressed as $G_2(q,t) = A\exp(-2\Gamma\tau)$ where Γ is the relaxation rate and related to the diffusion constant by $\Gamma = -D_T q^2$ and q is the wavevector. In Figure 3.6 a and b, G2's with respect to the delay times are displayed for the liposomes in water and in dilute polymer solutions (0.2 %) at 15 °C and 35 °C. In all cases, simple diffusion behavior is observed from the single exponential decay of the relaxation behavior. For the neat liposomes,

$5.21 \times 10^{-12} \pm 0.018 m^2/s$ and $3.73 \times 10^{-12} \pm 0.013 m^2/s$ for 35 ℃ and 15℃, respectively, and in agreement with previous studies.[34, 172] Such a nearly 1.5 fold decrease at 15℃ is expected since liposomes behave as hard spheres at gel phase, whereas the bilayer turns into soft particle at fluid phase. In presence of PEGs, the diffusion constant is highly dependent of Mw as seen from the Table 3.2. However, D_T is unaffected up to 100 kDa at 35℃ although the remarkable slowdown starts at >20 kDa at 15℃. The diffusion of liposomes is not facilitated by the fast diffusion of polymer chains, instead their motion slows down by the local viscosity increase due to the adsorption of polymer at 15℃. Although PEGylated stealth liposomes are widely preferred in drug delivery applications as they increase the biodistribution and half-life of the liposomes, they affect and slow down the diffusion of liposomes with respect to temperature and chain length. These results can be useful tools for liposome and polymer-based design of drug delivery systems.

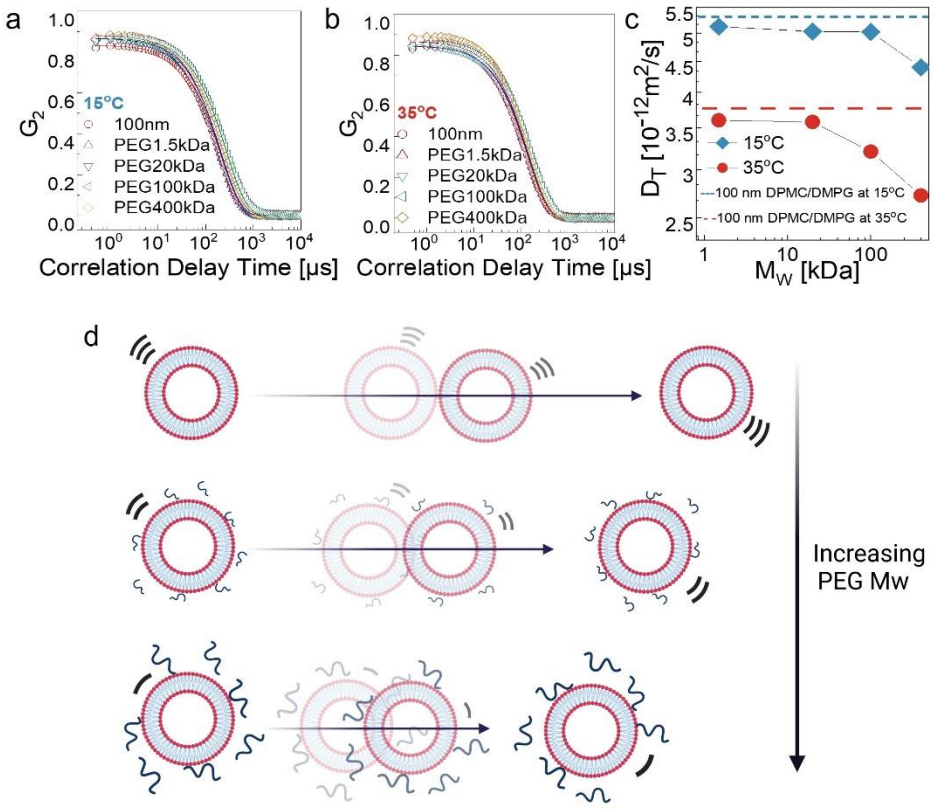

Figure 3.6 Autocorrelation functions of neat 100 nm DMPC/DMPG liposomes and 100 nm DMPC/DMPG liposomes mixed with PEG solutions at a.15℃ and b. 35℃. c. PEG molecular weight dependent diffusion constants of liposomes at 15℃ and 35℃. d. Schematic representation of the effect of PEG chains on translational liposome diffusion.

3.3.3.2 Macroscopic Viscosity of Liposome Solutions

As the structure of liposomes are highly dependent on temperature, they exhibit several morphologies at gel and fluid phases which gives unique rheological properties to them. We used rheology to observe the bulk viscosity of liposomes with respect to temperature. Figure 3.7.a shows the comparison of the temperature dependent bulk viscosities of 400 nm, 200 nm, and 100 nm liposomes in the absence of polymers from 10℃ to 40℃. For better clarification, the viscosity of DI water is added. The addition of liposomes to water increased the viscosity at all temperatures changing with size and lamellarity. Since the nominal lipid concentration is the same for all solutions, the reduction of viscosity is due to the decrease in the number of liposomes and the effective volume. The lamellarity effect becomes significant after passing across the transition which results in a thermal-thickening effect being more severe as the fraction of multilamellar vesicles increases. Owing to soft and deformable structure of liposomes, the collective lipid motion enhances the reconfiguration under deformation, thus, greater resistance to flow observed beyond transition. Also, the broadened transition through 100 nm liposomes confirms the DSC results since the structural order within a single bilayer is lost more rapidly. The results indicate that the transition behavior can be modulated based on liposome properties without any chemical constituents.

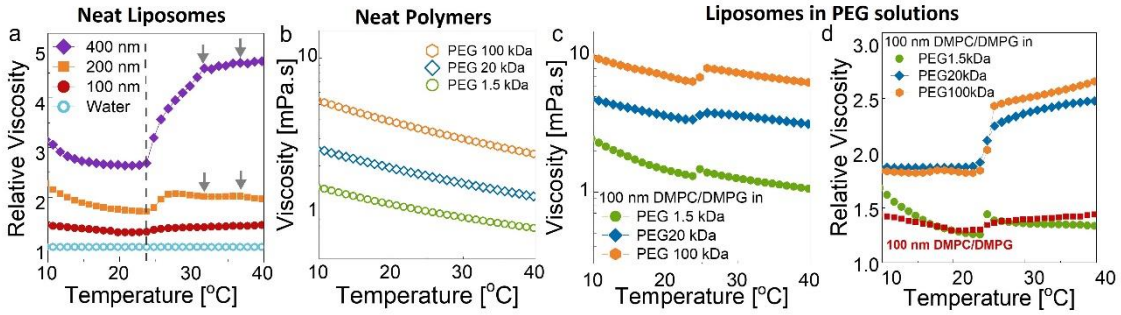

Figure 3.7 a. Relative viscosity of 400 nm, 200 nm, 100 nm liposomes with respect to water. Vertical dashed line shows the phase transition temperature. Viscosity of b. neat 1.7 w% PEG solutions with varying Mws (1.5 kDa, 20 kDa, 100 kDa) and c. composite solutions containing 1.7 w% lipids and 1.7 w% polymer in water. d. Relative viscosity of composite solutions containing 1.7 w% lipids and 1.7 w% polymer in water with respect to neat PEG solutions.

Figure 3.7.b shows the viscosity of neat polymer solutions with different Mws. They exhibit a typical polymer behavior decreasing viscosity with increasing temperature. With the addition of liposomes, viscosity values show a significant change

and increase nearly 2-fold suggesting liposomes act as reinforcing nanoparticles in the composite solution. (Figure 3.7.c) The relative viscosity of the solutions is presented in Figure 3.7.d for better analysis. In 20 kDa and 100 kDa solutions, viscosity increases compared to neat and in 1.5 kDa solutions due to the slight size increase of liposomes, and it remains nearly the same upon transition. Clearly, the magnitude of the increase is amplified with increasing PEG chain length. The interaction of the bound chains can cause a transient network (like entanglement) which results in higher viscosities at $T > T_m$. Also, as the polymer-polymer interaction is enhanced with membrane softening, higher temperatures result in enhanced polymer-polymer interaction and thermal thickening. As the chains get shorter, the interaction of the bound polymers is less likely, thus, the viscosity shift and thermal transition is less pronounced.

The reinforcing behavior of liposomes with temperature and PEG chain lengths is investigated by using two viscosity models; Einstein and Krieger-Dougherty for neat 100 nm liposome solutions and liposomes and PEG 100kDa solutions at 2.5 w%, 2 w%, 1.5 w%, and 1 w% liposome concentrations. The viscosity data is presented in Figure 3.8.a.

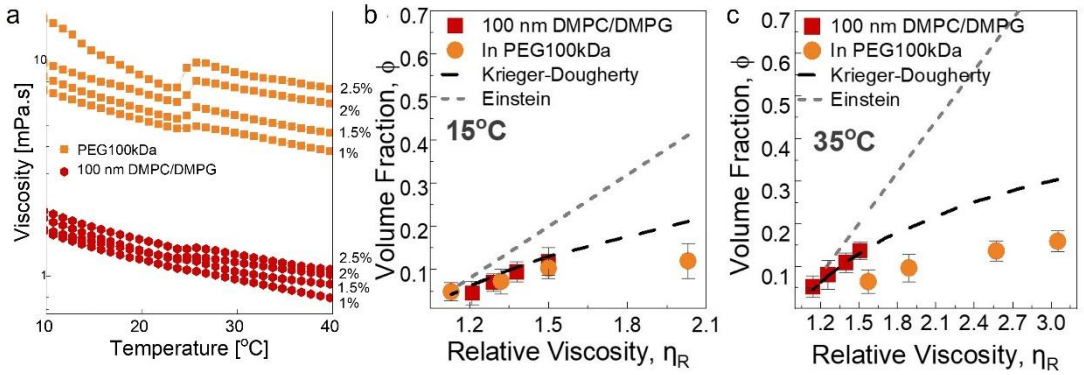

Figure 3.8 a. The viscosity of the mixture of 100 nm liposomes and PEG 100kDa solutions and 100 nm liposome solution at 2.5%, 2%, 1.5%, and 1% concentrations. Volume fractions versus relative viscosity of the neat 100 nm liposome solutions and liposomes in 1.7 w% PEG (100kDa) solutions at four lipid concentrations (2.5 w%, 2 w%, 1.5 w%, and 1 w%). The curves show the predictions from Einstein and Krieger-Dougherty viscosity models at b. 35°C and c. 15°C. Error bars represent propagated error.

Einstein model assumes rigid spheres in dilute solutions where they all have independent movements, and is given by; $\eta_r = 1 + 2.5\phi$ where η_r is the relative viscosity, and ϕ is the volume fraction of spheres in solution. Krieger-Dougherty is commonly used for

the concentrated suspensions[173] with $\eta_r = (1 - \frac{\phi}{\phi_{max}})^{-A\phi_{max}}$. Here, $-A$ and ϕ_{max} are 2.7 and 0.71, respectively for spheres in submicron sizes. [174] We measured relative viscosities by rheology and calculated the volume fractions based on nominal lipid concentration, size and area per lipid information provided in the Appendix section. The symbols in Figure 3.8 b and c show the calculated volume fractions and their corresponding relative viscosity values, and the dashed lines present the predictions from the models. Clearly, the Einstein model fails to explain the observed trend whereas The Krieger-Dougherty model reasonably accounts for the neat liposome data at the fluid and gel states. In the presence of PEGs, The Krieger-Dougherty model still fairly explains the observed behavior at 15 ℃ (except only for the solution with the largest liposome volume fraction which diverges from the prediction) whereas at 35℃ the model significantly overestimates the effective volume fraction of the liposomes at all nominal lipid concentrations, suggesting that the size increase of the liposomes in the fluid state is not alone sufficient to explain the viscosity shift; the particles turn from hard-nanoparticles to soft-nanoparticles.[175] As the model still predicts the viscosity trend in the fluid phase of the neat liposome solutions, the soft particle behavior is mainly due to the presence of PEG chains that are dynamically coupled with the flexible membrane.

3.3.3.3 Microscopic Viscosity in Bilayers

We investigated the microscopic viscosity of bilayers in the presence of PEGs by FLS at 15℃ and 35℃ in this section. Estimation of the microviscosity of the lipid membranes is a well-studied technique using fluorophores.[176-178] We stained liposomes by Oil-Red-O which is a hydrophobic fluorescent probe locating in the lipid bilayer, and used to monitor the cell membranes in biological applications.[179] Förster-Hoffman theory relates the lifetime of the probe with the viscosity of the local microenvironment by the following equation; $\ln(\tau) = A + B \ln(\eta)$ where τ is the fluorescent lifetime (FL) of the Oil-Red-O, η is the viscosity, A and B are the intercept and slope of the line, respectively.[180] A calibration curve for the probe is required to determine the changes in the lifetime of the probe in the environments with known-viscosities and to obtain the constants of the Förster-Hoffman equation. For this reason, we have used methanol-glycerol solutions in varying ratios since Oil-Red-O is soluble in both as lots of examples are found in

literature.[177, 181] The viscosity of the solutions is measured with rheometer as shown in Figure 3.9.a, and the lifetime of the Oil-Red-O in each solution is measured by FLS . The calibration curves presented in Figure 3.9b and c. The linear dependence at both temperatures indicates the validation of the Förster-Hoffman theory.

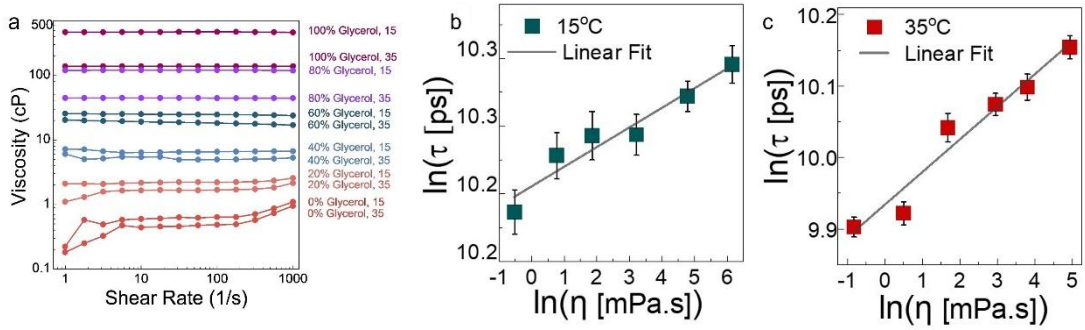

Figure 3.9 a. Viscosity of oil red o in glycerol and methanol mixtures as a function of shear rate at different glycerol compositions Average fluorescence lifetime of Oil-Red-O in methanol-glycerol mixtures at various compositions plotted against viscosity at b. 15℃ and and c. 35℃.

Then, the fluorescent lifetime measurements on 100 nm neat liposomes and liposomes in the presence of PEGs was performed as shown in Figure 3.10 a and b at 15℃ and 35℃, respectively. , the spatial identification of the measuring point and the fluorescence probe is crucial to monitor the targeted chemical and biological processes.[178, 182] As the hydrophobic nature of our probe, the Oil Red-O, maintains their localization within the membrane, which enables the estimation of microviscosity of the lipid bilayers. The average lifetime calculated from the exponential decay and the estimated microviscosities within the lipid bilayers are given in Table 3.3.

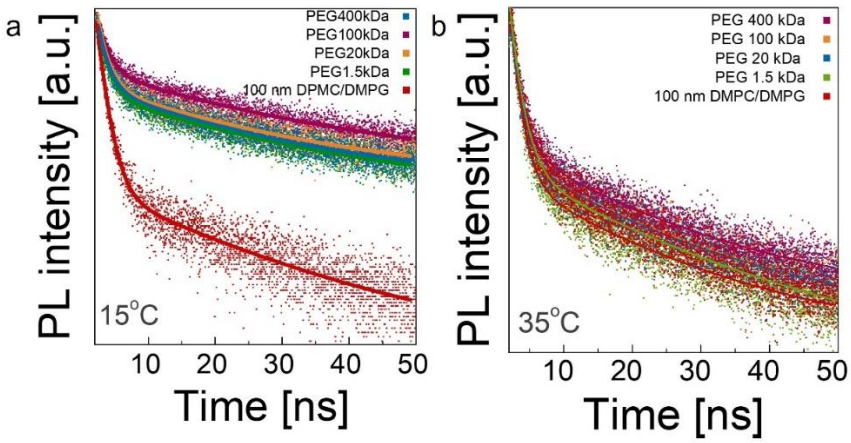

Figure 3.10 Time-resolved fluorescence decays of Oil-Red-O inside lipid bilayer in the presence of different PEG Mws at a. 15℃ and b. 35℃.

Table 3.3 Lifetime of Oil-Red-O and microviscosity of lipid membranes in 100 nm liposome solutions in the absence and presence of PEG with various Mw's.

	τ_{avg} (ns) 35℃	Microviscosity (cP) 35℃	Bulk Viscosity (cP) 35℃	τ_{avg} (ns) 15℃	Microviscosity (cP) 15℃	Bulk Viscosity (cP) 15℃
100 nm liposomes	24.01±0.032	28.75±0.85	1.414	28.91±0.038	142.82±13.54	1.546
in PEG 1.5kDa	20.61±0.013	1.02±0.01	1.156	27.38±0.033	3.36±0.29	1.827
in PEG 20kDa	21.43±0.022	2.39±0.05	3.406	27.59±0.036	5.69±0.53	4.163
in PEG 100kDa	22.72±0.019	8.59±0.15	6.874	28.42±0.029	43.93±3.2	8.247
in PEG 400kDa	23.91±0.028	26.24±0.68	23.94	28.74±0.031	95.09±7.34	53.35

The microviscosity of the neat liposomes was decreased from 142.82 cP to 28.75 cP at 15℃ and 35℃, respectively as in agreement with the literature.[159, 183] The lifetime of the probe and thus, the microviscosity is changed with respect to PEG molecular weight. In 400 kDa, the microviscosity is close to the neat liposomes, whereas it decreased with the decreasing molecular weight for the gel and fluid phase of liposomes. It is a clear indication that the microenvironment of liposomes is strongly affected by the existence of PEG chains, and tunable with changing the chain length. As the chains get shorter, the relaxation becomes faster, and the dynamical coupling between the membrane and the polymer segments is more pronounced, which may facilitate the thickness fluctuations and/or membrane undulations.

3.3.4 Osmotic Pressure Analysis

The effect of PEG on lipid bilayers is primarily known to increase the osmotic pressure, thus cause the dehydration of the membrane, and it is definitely effective for the high concentrations of PEG. Therefore, we assessed the osmotic pressure effect of PEG to observe the possible influences on the results. 1.5 and 20 kDa, the Mws applying the highest osmotic pressure are chosen and the liposome size is measured by DLS on varying concentrations of PEG (from 0.2 w% to 10 w%) as shown in Figure 3.11. Low

concentrations of PEG increase the size of the liposomes up to ~3%, however, the size starts decreasing due to dehydration. We, thus, conclude that the size increase seen in DLS for small PEG concentrations is due to the bound PEG layer whose thickness increases with the expected size dependence of PEG M_w.

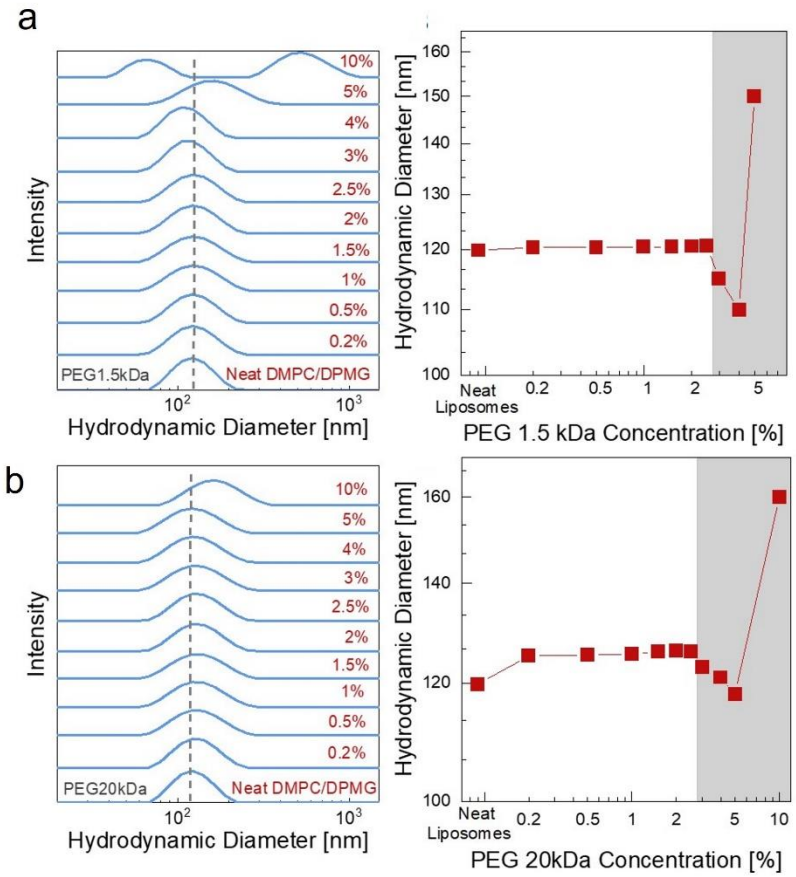

Figure 3.11 Hydrodynamic sizes liposomes in varying a. PEG 1.5kDa and b. PEG 20kDa concentrations from 0.2 to 10 w%. Gray-shaded area represents the concentration range in which the size of the liposomes starts decreasing.

In order to evaluate osmotic pressure effect on bulk thermal thickening, we prepared additional liposome-PEG solution by hydrating the lipids with 20 kDa PEG solutions to form liposomes containing PEG everywhere (inside and outside of the vesicles). The solutions were then extruded using the same protocol to obtain identical size and polydispersity of the liposomes (confirmed with DLS). Figure 3.12 shows no difference in the transition behavior of liposomes when compared to the data presented in Figure 2C (for empty liposomes at the same PEG concentration). Therefore, the observed viscosity shifts are not related to the osmotic pressure variation but due to the

hard-to-soft particle transition as discussed above. We also confirm the existence of PEG layer with respect to concentration on the liposome surface by zeta potentials as shown in Table. The PEG layer on liposome causes a shift of the hydrodynamic slip layer; the zeta potential increases from ≈ -9 mV to ≈0 with PEG addition.

Table 3.4 Zeta potential values of liposomes in varying PEG 1.5kDa and PEG 20kDa concentrations from 0.2 to 2.5 wt%.

PEG 1.5kDa		PEG 20kDa	
PEG Concentration (%)	**Zeta Potential (mV)**	**PEG Concentration (%)**	**Zeta Potential (mV)**
0	-9.78±1.32	**0**	-9.78±1.32
0.2	-9.11±1.01	**0.2**	-4.34±0.91
0.5	-2.53±0.53	**0.5**	-2.51±0.47
1	-1.05±0.23	**1**	-1.48±0.27
1.5	-0.952±0.07	**1.5**	-1.18±0.12
2	-0.360±0.04	**2**	-0.204±0.02
2.5	-0.150±0.01	**2.5**	-0.209±0.01

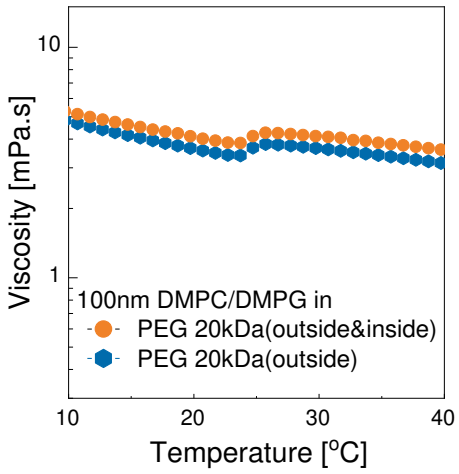

Figure 3.12 The comparison of the viscosity of 100 nm liposomes in PEG 20 kDa solution where PEG chains are outside and both outside and inside (elimination of osmotic pressure)

Recently, Sahu *et al.* suggests that the microviscosity of unilamellar DMPC vesicles increases with the addition of PEG-400 (400 Da) and PEG-6000 (6 kDa) as a result of high osmotic pressure of PEG molecules.[156] The polymer concentration used in

this study was 25 w% that is adequately high to have an effective osmotic pressure leading to vesicle aggregation and fusion according to our observations. This is unlike our study where the osmotic pressure is not as effective due to low concentration of PEGs. Instead. the addition of the PEG chains caused a dynamical coupling and accelerated lipid dynamics.

Chapter 4:
SHEAR-TRIGGERED RELEASE OF LIPID VESICLES FROM TISSUE-MIMETIC HYDROGELS

4.1 Introduction

Shear-responsive materials have received tremendous attention in drug delivery applications due to their easy access, and applicability as localized delivery while not causing damage to healthy tissues efficiently remains as a challenge.[184, 185] As one of the fundamental forces associated with blood flow, shear forces contribute to vital biological processes including proliferation, platelet aggregation, and assisting barrier formation.[186-188] Cardiovascular diseases, such as stenosis, or thrombosis, result in more than one order of magnitude higher shear stresses due to constrictions in the vessels.[189, 190] These changes in the flow field cause perturbations in local microenvironments of cells and tissues, and can be used as an advantage to design shear-sensitive drug carriers to respond only in high-shear environments; however, their dynamical features associated with the shear induced structural variations must be well-understood.

Nanoparticle-based systems have emerged as suitable platforms for precise delivery as they can be engineered to dynamically engage with their biological environment in direct physical or chemical contact.[191] The difficulty of spatiotemporal and dosage-controlled release that are not cell or tissue-specific require smarter and on-demand drug delivery systems which recognize their environment and response in a dynamic way. Among many nanoparticle based systems, liposomes with a wide range of sizes are promising candidates with their structural versatility, excellent biocompatibility and biodegradability.[3, 142] Owing to their soft and deformable structure originating from weak intermolecular interactions between lipid constituents, liposomes are also attractive candidates for shear-deformable nanoparticles alternative to solid or internally crosslinked polymer nanoparticles.[192, 193] Various studies have revealed that high shear may lead to changes in structure as well dynamics of liposomes such as increase in membrane permeability, lamellar packing, membrane fusion, and pore formation.[194-197] Thus, drug release kinetics and encapsulation properties of liposomes can be well-tuned

by shear forces. However, the stability of liposomes under high shear remains as one of the significant challenges.[138] For this purpose, the combination of liposomes and hydrogel matrices brings important benefits by providing physical stability to liposomes, and mechanical support to the whole system with strong (visco) elastic behavior.[198]

Hydrogels are commonly used as tissue scaffolds and extracellular matrix (ECM) models due to their non-toxic, biodegradable structure, and adjustable properties such as osmotic pressure, stiffness, and mesh size to be well-suited with biological environments.[198, 199] The mobility and diffusivity of liposomes depends on the membrane properties as it is known that liposomes with moderate rigidity and neutrally charged membrane can move faster in biological hydrogels.[200] Besides, hydrogel properties such as mesh size, crosslinking type, and adhesiveness significantly affect the diffusion rate of liposomes.[201] Although there have been studies of liposome-hydrogel complexes responding to increased release properties under compressive and tensile forces, all these examples are based on the rupturing and destructing the lipid bilayer within the hydrogel matrices;[136, 137] the case where liposomes diffuse out of the hydrogel environment to effectively release their cargo in response to applied (endogenous or exogenous) shear stress remains unexplored.

In this work, we took the first step towards understanding the way that the liposomes interact with the surrounding hydrogel matrix, and how the composite system respond to an applied shear deformation from linear to nonlinear regimes. We used nearly monodisperse unilamellar DMPC/DMPG liposomes as model nanocarriers and combined them with photo-crosslinked ECM-mimetic PEGDA hydrogels having different stiffnesses. Using small-angle X-ray scattering (SAXS), dynamic light scattering (DLS), differential scanning calorimetry (DSC), bulk rheology, and fluorescence lifetime spectroscopy (FLS), we first investigated the structural and dynamical features. In the presence of liposomes, the stiffness of the hydrogels could be tuned from 1 Pa to 180 Pa by changing the crosslinking density, and temperature-sensitive viscoelastic properties and swelling capacity was observed. The presence of liposomes provides composite hydrogels with temperature-controlled swelling capacity of that is sensitive to membrane microviscosity. Remarkably, increase of shear deformation from linear towards nonlinear regime results in ~2-fold increase in the liposome release under transient and cyclic stimuli with the increased gel mesh size. Considering that shear force is one of the fundamental forces associated with biofluid flow, these findings enhance our

understanding of the underlying mechanism and rational design of shear triggered liposomal drug delivery systems.

4.2 Experimental Methods

4.2.1 Materials

Lipids 1,2-dimyristoyl-sn-glycero-3-phospho-choline (DMPC) and 1,2-dimyristoyl-sn-glycero-3-phospho-(1'-rac-glycerol) (sodium salt) (DMPG); and mini-extruder were purchased from Avanti Polar Lipids (Alabaster, AL, USA). Polyethylene (glycol) diacrylate (PEGDA) 10kDa, and 2-Hydroxy-4'-(2-hydroxyethoxy)-2-methylpropiophenone (Irgacure 2959) were purchased from Sigma-Aldrich and used as received.

4.2.2 Preparation of Liposome Solutions

Liposomes were prepared with the well-known thin film hydration and followed by extrusion method. First, DMPG (5% w/w) and DMPC were dissolved in chloroform and vortexed one hour. The solution was evaporated in a vial, and then kept under vacuum at 80℃ for 24 h. The thin film of the lipids was hydrated with PEGDA solution. The final concentrations of liposomes and polymer were arranged as 20 mg/mL in the composite solution. The solution was vortexed for 2 h for complete dissolution, and then extruded via a mini extruder. The temperature of the extruder was kept at 40℃ during extrusion. The solution was subsequently extruded 15 time through 400 nm and 200 nm membranes, and 41 times through 100 nm membranes. Extruded solutions were used immediately after preparation or stored at 40℃ while mixing in a vortex and used in 24 hours.

4.2.3 Preparation of Liposome Solutions Containing Oil Red O

For Fluorescence Lifetime Spectroscopy (FLS) experiments, the same amount of lipids and 2×10^{-6} uM Oil-Red-O were dissolved in chloroform and vortexed one hour. The same protocol was followed for the rest of the preparation as described above.

4.2.4 Preparation of Liposomal Hydrogels

The stock solution of photo initiator, Irgacure 2959 was prepared in ethanol (70%v/v) and water due to low water solubility. It was added to the extruded liposome-PEGDA solutions at 4% w/w, and vortexed for 15 min. Then the solution was poured into the 8 mm disc shaped molds, and photo-crosslinked by UV lighting at 365 nm, 100 mW/cm^2 at time intervals of 75 s, 105 s, 120 s, 150 s, 165 s. The distance of the mold containing the solution from the UV source was kept constant as 8 cm for all experiments. The hydrogels containing liposomes are called *liposomal hydrogels* throughout the paper.

For the neat PEGDA hydrogels, 2%(w/v) PEGDA 10 kDa solution was prepared and Irgacure 2959 (4%w/w) was added to the solution. The hydrogels were prepared with the same protocol as described above.

4.2.5 Dynamic Light Scattering (DLS)

Hydrodynamic size, and polydispersity index (PDI) values were obtained by Dynamic Light Scattering (DLS, Malvern ZS Zetasizer) at a wavelength of 633 nm, and a scattering angle of 173^o. Solutions were diluted to 0.2% concentration for the experiments. Each measurement was repeated three times and averaged.

4.2.6 Differential Scanning Calorimetry (DSC)

The phase transition temperature of the liposomes was determined using TA Instrument's Q25 AutoDSC. The 10-15 mg of samples weighed and sealed in Tzero pans with Hermetic lids. For the hydrogel samples, the solutions were first put into the pans and then photo crosslinked. Reference was taken as an empty sealed pan. All samples were heated to 60℃, and waited for 5 min for the equilibration. Then, the temperature was decreased to 5℃ with a rate of 2 ℃/min. Using the cooling curves, the crystallization temperatures of liposomes were obtained. Enthalpy values for each sample was calculated from the area of exothermic peaks. The reproducibility of the data was ensured by repeating the cycles several times.

4.2.7 Small-Angle X-ray Scattering (SAXS)

The lamellarity of liposomes were determined using Anton Paar SAXSpoint 5.0 at the sample to detector distance of 500 mm. The solutions were put in quartz capillary holder, and then photo crosslinked. Temperature was controlled using a heated cooled sampler with the stability range of ± 0.005℃. The data was collected over a range of wave vectors, Q=0.01 to 6.86 nm^{-1}. The background (water only) was subtracted for proper reduction. SAXS analysis program of the SAXSPoint 5.0 was used for analysis and data reduction.

4.2.8 Scanning Electron Microscopy (SEM)

The surface morphology of neat PEGDA and liposomal hydrogels were observed by using scanning electron microscope (Zeiss Ultra Plus Field Emission Scanning Electron Microscope). All the samples were gold-coated for 12 s before measurement.

4.2.9 Confocal Microscopy

Confocal microscope images were captured with (TCS SP8 DLS, Leica, Wetzlar, Germany). All samples (stained with Oil Red O) were excited at 560 nm.

4.2.10 Rheology

Rheological measurements were carried out using Anton Paar rheometer (MCR 302) equipped with a parallel plate with a diameter of 8 mm. Temperature was controlled using a Peltier coupled with a temperature control hood to prevent heat loss and evaporation. To eliminate the wall slip, sandpaper was used for measuring plate, and sample plate. It was cut and sticked to be the same size as the measuring plate (8 mm diameter). Frequency sweep tests were performed in linear viscoelastic region obtained from the amplitude sweep tests (under a constant frequency of 10 1/s). Frequencies varied from 0.1 to 10 1/s. Temperature sweep tests were carried out from 10℃ to 40℃ at a heating rate of 1℃/min.

4.2.11 Time-Resolved Photoluminescence

Time-resolved photoluminescence spectroscopy measurements were carried out by Picoquant MicroTime 100 time-resolved confocal fluorescence microscope. The excitation beam was provided by an 8-mW picosecond diode laser operating at 375 nm with 20 MHz repetition rate and focused on the sample by a 40X objective lens. For the transient photoluminescence measurements, the single photon sensitive detector (PMA Hybrid 50) with photomultiplier tube (R10467 from Hamamatsu) and the time-correlated single photon counting system (HydraHarp 400) were used. The data were analyzed in fluorescence lifetime imaging (FLIM) mode using SymPhoTime 64 (Picoquant) software, where the PL decays were fitted by a two-exponential decay, and corresponding average lifetimes were calculated from an intensity-weighted mean.

4.2.12 Water Uptake Ratio

Hydrogel samples were submerged into water at 15℃ and 35℃, and then removed at predetermined time intervals. Surface water was taken with a filter paper. Swollen hydrogels were weighed, and the water uptake ratio was calculated by the following equation:

$$Water\ Uptake\ Ratio\ \ (\%) = \frac{M_s - M_h}{M_h} \times 100$$

Where M_s and M_h are the weight of swollen hydrogel and hydrogel right after UV crosslinking, respectively.

4.2.13 Time Dependent Liposome Release from Liposomal Hydrogel

Hydrogel samples were immersed a vial containing 1 mL of DI water, 200 uL of the sample was taken at determined time intervals and 200 uL fresh water was added. The samples were excited at 400 nm and the absorbance values were recorded by using a plate reader (Synergy H1-MF, Biotek). DI water was taken as reference for the analysis of released liposomes from the hydrogel since they were released through water medium. Cumulative drug release was calculated using a standard curve constructed by subtracting the background containing PEGDA and Irgacure 2959 at the same concentration. All measurements were repeated three times for different samples and averaged.

4.2.14 Shear-Stimuli Release of Liposomes from Hydrogel

Shear-stimuli release experiments were performed using a rheometer equipped with a parallel plate with 8 cm diameter. Before the release experiments, amplitude sweep tests were performed at varying strains from 1% to 1000% (at a constant frequency of 1 1/s) at 15℃ and 35℃ to determine the strain values for the experiments.

The hydrogel sample was put into a beaker which is fixed to the sample plate by tape. The bottom of the beaker and the measurement plate was covered by sandpaper to prevent wall slip. Before starting the amplitude sweep test, the beaker was filled with 1 mL DI water. 200 uL of the sample was taken at determined time points, and 200 uL fresh water was added. (See Figure 6a for experimental setup) All measurements were repeated three times for different samples and averaged. Control experiments for the sandpaper in DI water were performed by DLS and plate-reader, and we did not observe a peak in DLS or an increase in absorbance.

4.3 Results and Discussion

4.3.1 Structure of Liposomes in Hydrogels

Liposomes were produced by thin film hydration and followed by extrusion method (see Methods section for details). The thin film of the lipids was hydrated by PEGDA solution to have a final concentration of 2% 100 nm lipids and 2% PEGDA 10kDa. The polymer chains are also encapsulated within the liposomes; thus, increasing the stability of liposomes by minimizing the osmotic pressure effect. Upon addition of the crosslinker (I2959 ,4% w/w) the PEG-liposome solutions were exposed to UV light at different time intervals (75 s, 105 s, 120 s, 150 s, and 165 s) to form hydrogels with different crosslinking densities and elastic shear moduli ranging from 1 Pa to 200 Pa, mimicking various tissue environments (see Figure 4.1.a for the schematic and the rheology section). Liposome-free PEG hydrogels were also prepared with the same UV time and concentrations to compare the results. Figure 4.1.b shows the hydrodynamic size distribution of neat PEGDA 10 kDa chains, neat (polymer-free) liposomes, and the liposomes in uncrosslinked PEGDA solution in dilute regime. Nearly monodisperse liposomes with diameters 119.9 ± 2.54 nm and the polydispersity index of 0.075 ± 0.010 were formed in the neat (polymer-free) form. The liposome size increases slightly to

133.6±2.401 nm in the solution containing PEGDA but they remain nearly monodisperse with polydispersity index of 0.042±0.0041. About 6.85 nm increase in radii of the liposomes in the PEGDA solution is close to the hydrodynamic diameter of single PEGDA chain in water (≈ 7 nm) suggesting physical adsorption of PEG on hydrophilic phospholipid heads on liposome surface.[150, 202] Also, the single PEGDA peak in DLS confirms that the polymers do not form clusters in water.[203]

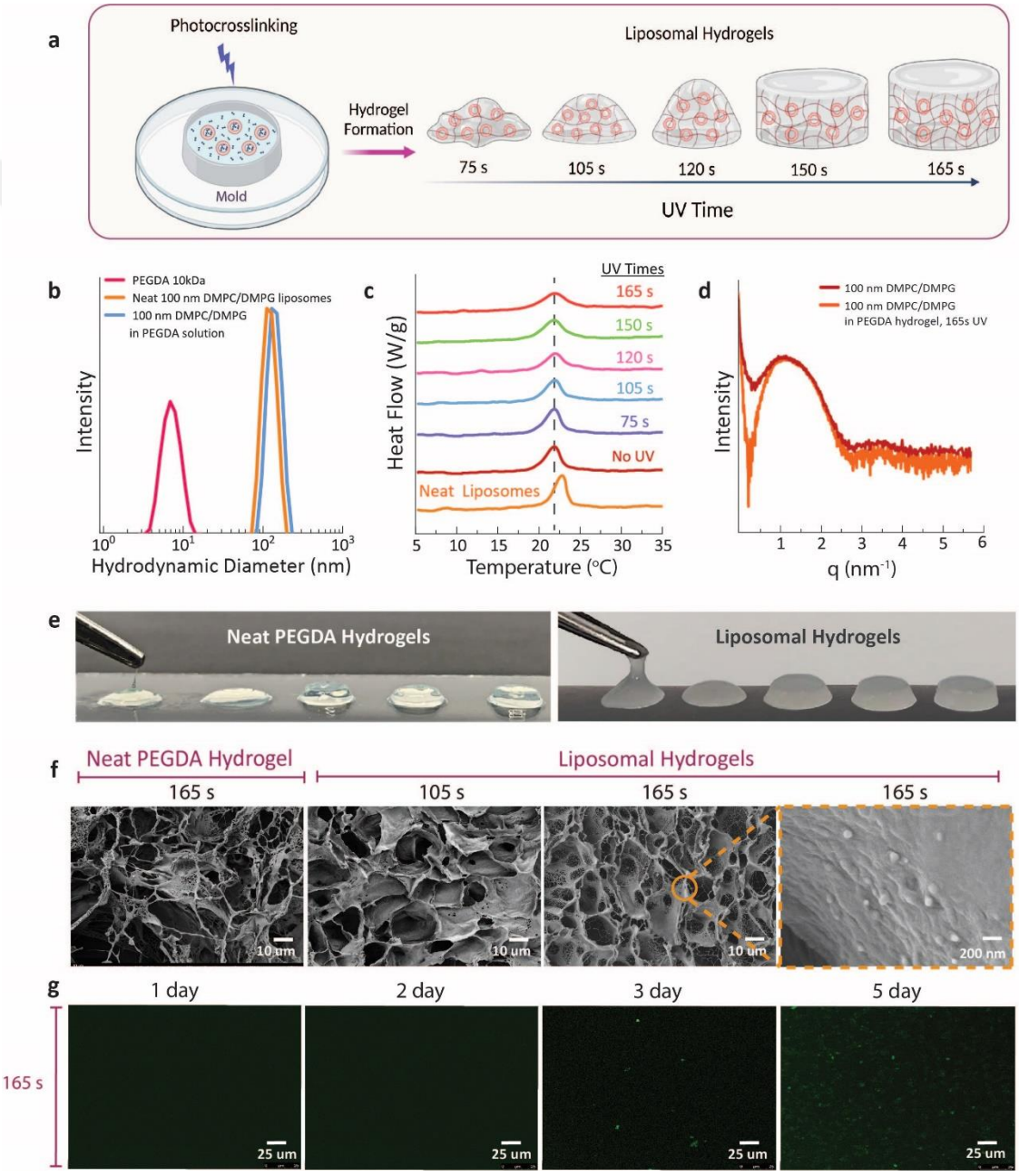

Figure 4.1 Structural characterization of liposomal hydrogels. a) Schematic image of the system. The extruded composite solution including 2% DMPC/DMPG liposomes and 2% PEGDA 10 kDa was photo-crosslinked by UV light to form liposomal hydrogels. UV exposure times were arranged as 75 s, 105 s, 120 s, 150 s, and 165 s to change the crosslinking density. b) Hydrodynamic diameters of PEGDA 10 kDa chains, neat DMPC/DMPG liposomes, and DMPC/DMPG liposomes PEGDA solution after extrusion. c) DSC traces of liposomes in uncrosslinked PEGDA solution, and in liposomal hydrogels. d) SAXS analysis of liposomes in uncrosslinked PEGDA solution, and in liposomal hydrogel with a UV time of 165 s. e) Representative photographs of neat PEGDA hydrogels and liposomal hydrogels. f) SEM images of neat PEGDA hydrogel with UV time of 75 s, and liposomal hydrogels with UV time of 75 s, 120 s, and 165 s. Inset shows the existence of liposomes. g) Stability of liposomal hydrogel with a UV time of 165 s assessed by confocal microscopy.

We then investigated the lamellarity of the liposomes in hydrogels as unilamellar liposomes can transform into multilamellar stacks at different environments.[103, 168] In our study, we first formed liposomes in uncrosslinked polymer solution, and then changed the viscoelasticity of polymeric environment by crosslinking the PEGDA solution in the presence of the vesicles. To determine if the continuous matrix of the crosslinked polymers affect the unilamellarity of the liposomes, we used DSC and SAXS whose signal are very sensitive to periodic stacking of bilayers in case of multilamellar vesicles. Figure 4.1.c shows the specific heat flow curves of 100 nm DMPC/DMPG liposomes in their neat form and in uncrosslinked PEGDA solution upon transition from fluid to gel phase of bilayers. The neat liposomes showed a phase transition with one broad peak at ≈22.84℃ corresponding to the liquid crystal formation of bilayers, but no intense and sharp peak related to the multilamellar structured vesicles (as shown previously[163, 202]) exists. Similarly, no characteristic features of multilamellar vesicles were observed in liposomal hydrogels regardless of the UV exposure time. PEG is known to dehydrate the lipid bilayer and increase the lateral packing density of between acyl chains of the lipids as the transition temperature appeared at ≈21.90℃ in polymer solution.[156] Although a ≈1℃ change was observed (see Table 4.1), PEG chains did not change the unilamellarity of liposomes. The unilamellarity of the liposomes was also confirmed by SAXS as it provides more direct structural evidence. Figure 4.1.d shows the scattering intensity as a function of wave vector, q, of liposomes in uncrosslinked PEGDA solution and in liposomal hydrogel with the longest UV time of 165 s. The absence of any Bragg peaks at q=1.00 nm-1 and q=2.00 nm-1, which would result from multilayer vesicles[165, 202], confirms that the liposomes retain their unilamellar structure even in the stiffest hydrogel and that liposome restructuring such as aggregation or fusion is not favorable in these

gels. This is in contrast to the observation by Bandara *et al.*[103] where pre-formed unilamellar liposomes were either added to the uncrosslinked gel precursors or directly injected into hydrogels and transformed to multilamellar structure mainly due to osmotic pressure across the membrane.

Table 4.1 Crystallization temperature TC (℃), and Specific Enthalpy (J/g) of 100 nm DMPC/DMPG in their neat form and in uncrosslinked PEG solutions and in liposomal hydrogels with different UV exposure times.

	UV Exposure Time	T_C (℃)	Specific Enthalpy (J/g)
Neat Liposomes	-	22.84±0.11	0.335±0.013
Liposomes in Uncrosslinked PEG solution	-	21.90±0.21	0.303±0.014
Liposomal Hydrogels	75 s	21.88±00.04	0.299±0.017
	105 s	21.85±0.34	0.287±0.023
	120 s	21.93±0.16	0.272±0.009
	150 s	21.99±0.28	0.269±0.011
	165 s	21.91±0.14	0.245±0.041

The bulk liposomal hydrogels display whitish color compared to transparent look of the liposome-free PEG hydrogels (Figure 4.1.e). The morphology of the gels was also investigated by SEM as shown in Figure 4.1.f. The SEM image of neat PEG hydrogel is also shown. The liposomal hydrogels have denser structure with more network connections compared to the PEG hydrogel at the same UV exposure time of 165 s. Although the morphology of the liposomal hydrogels with 105 s and 165 s UV time shared a similar morphology, such as uniform rounded pores, and thin wall, the size of the pores decreased with crosslinking density as expected. The individual liposomes (with diameters of ≈ 130 nm) in the hydrogel exposed are also clearly seen (Figure 4.1.f inset). The stability of liposomes in same hydrogel matrix was also evaluated using confocal microscopy by staining the liposomes with a hydrophobic fluorophore, Oil Red O (Figure 4.1.g).[179] During the first two days, no vesicle signal was detected as 100 nm lipid vesicles are lower than the resolution limit of the microscope with diffraction limit of ~200 nm at

560 nm excitation. After two days, aggregation occurs, and the larger sized vesicles became visible in the images of liposomal hydrogels observed on third and fifth days.

In summary, the structural analysis verifies that the liposomes retain their unilamellar structure in the presence of PEG hydrogels with varying crosslinking density, and stable for 2 days. It is important to obtain the structural information of the vesicles as the physicochemical properties such as packing order, environment polarity, and stability, depends on size distribution and lamellarity.[142] The obtained unilamellar liposomes are attractive in this manner with their well-controlled structure mimicking the biological membranes.

4.3.2 Dynamics of Liposomes in Hydrogel Matrixes

4.3.2.1 Viscoelastic Behavior of Liposomal Hydrogels

The viscoelastic behavior of the hydrogels assessed by rheology depends on several factors such as the composition, concentration, and the type of the dispersed materials.[106] The rheological properties of hydrogels are therefore expected to be affected significantly by the addition of liposomes .[107, 108] To measure the viscoelastic properties of liposome-hydrogel complexes, we performed dynamic (oscillatory) shear rheology. Figure 4.2.a and 4.2.b show dynamic oscillatory shear rheology measurements of the hydrogels without and with liposomes, respectively at 35℃. All hydrogels display robust solid-like behavior with greater storage moduli (G') compared to loss moduli (G'') over the entire frequency regime. Also, the G' and G'' for all samples show negligible frequency dependence-typical of gel-like behavior. As the UV exposure time increased, G' increased due to higher crosslinking densities for both type of hydrogels. For the neat PEG hydrogels, the storage modulus changed from 0.04 Pa to 55.92 Pa with the selected UV times. We did not observe an increase in storage modulus beyond the 165 s UV time where the crosslinking density reached at its maximum for our system. The addition of liposomes in the hydrogels has a significant impact by shifting the storage and loss modulus curves towards higher values. Since liposomes are soft and deformable particles, the low bending elasticity enables them to reconfigure their structure under deformation, therefore, liposomes behave as reinforcing particles and strengthen the elasticity of the PEG hydrogels. However, this effect is most prominent for the softer gels as seen in

Figure 4.2.c. As the crosslinker density increases, the free space where liposomes can move decreases in the hydrogel matrix, thus, their contribution to the elasticity became weaker. Nevertheless, the stiffnesses of the hydrogels obtained by using different UV times match with the elasticity of the real tissues such as mucus, brain, bone marrow, lung, and liver (see Figure 4.2.c)[204] ; thus modelling biological cell in different ECM environment.

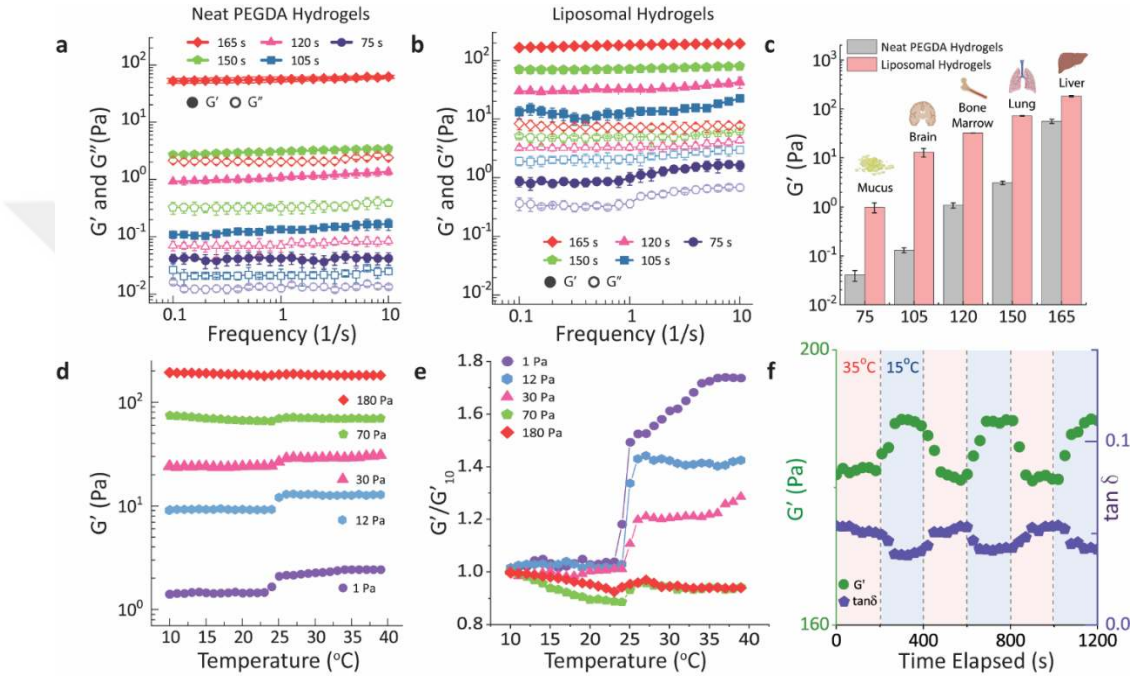

Figure 4.2 Rheological measurements of liposomal hydrogels and neat PEGDA hydrogels. Storage and loss modulus of a) neat PEGDA hydrogels and b) liposomal hydrogels as a function of frequency. c) Comparison of storage modulus values of neat PEGDA hydrogels and liposomal hydrogels as a function of UV times. Storage values were taken at the frequency value of 1 1/s. Error bars represents standard deviation, (n=3) d) Storage modulus of liposomal hydrogels as a function of temperature. e) tanδ of liposomal hydrogels as a function of temperature. f) Thermoreversibility of the storage and elastic modulus of liposomal hydrogel in the temperature range of 15℃ and 35℃.

Liposomes not only act as reinforcing nanoparticles for hydrogels but bring along interesting thermoresponsive behavior. Lipid bilayer transforms from hard spheres with impermeable particles to soft spheres with deformable structure beyond the transition which can affect the elasticity of the whole hydrogel matrix. To observe how the softness of the liposomes change the hydrogel stiffness, we performed temperature sweep experiments from 10℃ to 40℃ (below and above the melting temperature of the lipids). Figure 4.2.d represents the storage modulus of liposomal hydrogels in the temperature range from 10℃ to 40℃. We also included the temperature sweep of a neat PEG hydrogel

in Figure 4.3.a which shows a typical hydrogel behavior with slightly increasing G' and G" with increasing temperature. In the liposomal hydrogels, the storage moduli increased rapidly after the transition temperature and a thermal-stiffening effect was observed. (See Figure 4.2.e for the relative G' with respect to G' at 10℃) Besides, the effect of transition of liposomes was the most significant in hydrogel having the lowest crosslinking density, which was closer to the liquid state. In our recent previous work, we observed the similar transition behavior in the polymer-free liposome solutions and composite solutions of liposomes and PEG with different molecular weights (from 1.5 to 400 kDa).[202] We observed an increasing thermal-thickening effect on the viscosity of the liposome solutions due to enhanced dynamical coupling of PEG chains with highly mobile lipids in the fluid phase compared to rather immobile (in the time-scale of polymer relaxation time) lipids in the gel state Here, as the UV time increases, more polymer joins the gel network and the number of the free polymers that can bound together decreases. This effect can also be seen from the increasing tanδ (=G''/G') values of the hydrogels as the stiffness decreased (see Figure 4.3.b). Although the lipid dynamics get faster and resistance becomes stronger with temperature, the mobility of liposomes is suppressed by the crosslinked polymer network. Figure 4.2.f shows the evolution of storage and loss modulus of 180 Pa liposomal hydrogel with repetitive heating and cooling cycles between 15℃ (below T_m) and 35℃ (above T_m). The gel moduli display a good thermoreversibility with returned modulus values to almost original values after a short period. The tan δ values show the gels are more solid-like nature at 35℃.

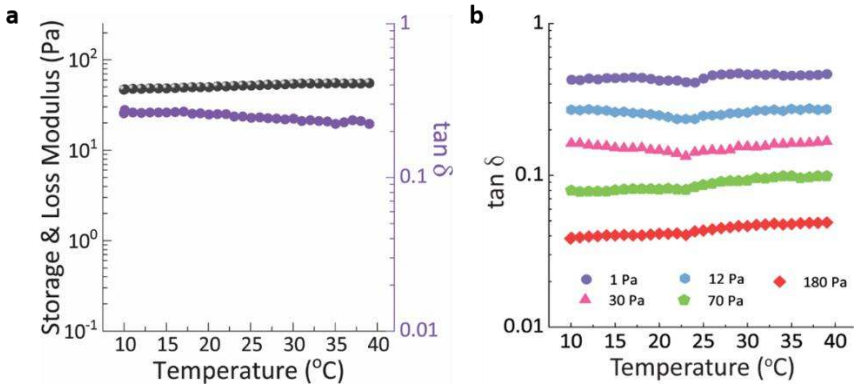

Figure 4.3 a) Storage modulus (left axis) and tanδ (right axis) of neat PEGDA hydrogel as a function of temperature. b) tanδ of liposomal hydrogels as a function of temperature.

4.3.2.2 Microviscosity Estimation of Liposomes in Liposomal Hydrogels

After evaluating the bulk dynamics of liposomes in PEG hydrogels, we further investigated the microviscosity of lipid bilayers in hydrogels to see the effect of the mechanical properties (stiffness) of the hydrogel environment on membrane using time-resolved fluorescence spectroscopy at 15℃ and 35℃ by staining lipid bilayers with Oil Red O. The microviscosity of the lipid bilayers is associated with the membrane permeability and contributes various cellular processes as an increase in rigidity decreases membrane permeability.[157] Fluorophores are widely used in the estimation of microviscosity in lipid bilayers.[176, 178] We chose Oil Red O since it is a hydrophobic fluorescent probe which locates within the membrane, and widely used in biological applications to monitor the cell membranes.[179, 205] According to Förster-Hoffman theory[180], the lifetime of the probe depends on the viscosity of its local microenvironment as expressed in the flowing equation: , $\ln(\tau) = A + B \ln(\eta)$ where τ is the fluorescent lifetime of the probe, Oil Red O, η is the viscosity, A and B are the constants. However, this equation is not valid for our system since liposomes are located in hydrogel matrices where the viscosity of the environment is assumed as infinite in gel-like structures.[206] Although it was not possible to calculate the microviscosity of lipid bilayers quantitively, the fluorescent lifetime values of the probe were used to estimate the trend in microviscosity as the theory suggests that there is a linear relationship between lifetime and microviscosity.[207]

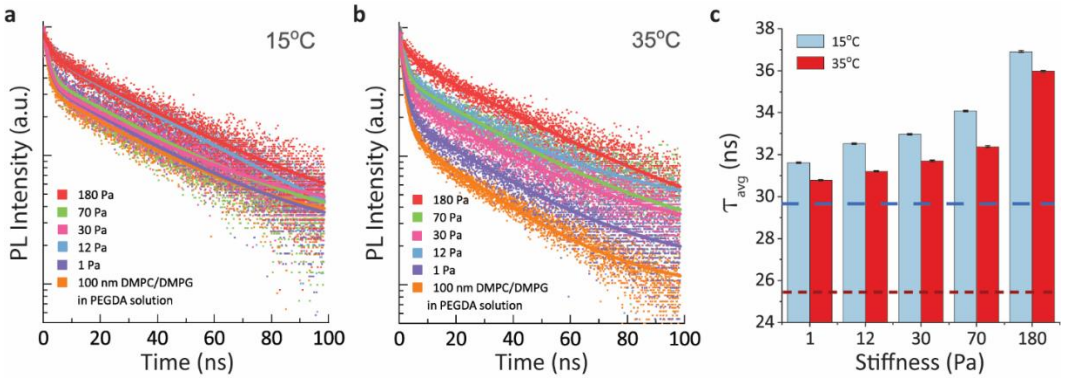

Figure 4.4 Time-resolved fluorescence decays of Oil-Red-O inside lipid bilayer in the uncrosslinked PEG solutions and PEG hydrogels a) 15℃ and b) 35℃ c) Comparison of the lifetime of Oil-Red-O inside the lipid bilayer in PEG hydrogels with different

stiffness values at 15℃ and 35℃. Long dashed lines and short dashed lines indicate the lifetime of Oil-Red-O inside the lipid bilayer in uncrosslinked PEG solution at 15℃ and 35℃, respectively.

We performed the measurements on liposomal hydrogels and compared the results with the uncrosslinked PEGDA solution before gelation at 15℃ and 35℃ (Figure 4.4.a and 4.4.b). The average lifetimes were calculated from the exponential decays and presented in Table 4.2. In the uncrosslinked PEG solution, the lifetime of the probe decreases from 29.8 ns in the gel phase to 25.32 ns in the fluid phase as the lipids were passed across the transition. Fluorescence intensity decreased fast at higher temperatures, and the fluorescence lifetime becomes longer which shows the high temperature-sensitivity of the lipid bilayer. In the hydrogel matrices, the bilayer microenvironment was strongly influenced by the elasticity of surrounding matrix as the fluorescence lifetime values increased as the gel stiffened suggesting an increase in microviscosity inside the bilayers, see Figure 4.4.c. As the stiffness and crosslinking density of the hydrogel increased, the crosslinked chains started applying an osmotic pressure through the membrane. This stress results in water outflow from the bilayer (dehydration), in turn, the membrane dynamics slows down. The dehydration level was higher in the fluid state of the membrane at 35℃ as the lifetime values increased as the polymer chains crosslinked. It was reported that water population surrounding the polar headgroup is greater in when the bilayer is in the fluid phase, which may facilitate a higher order of dehydration compared to solid state.[208]

Table 4.2 The lifetime of Oil-Red-O on 100 nm lipid bilayer in PEGDA solution and in PEGDA hydrogels at different stiffness. Error bars represents standard deviation, (n=3).

Stiffness (Pa)	τ_{avg}(ns) 15℃	τ_{avg}(ns) 35℃
Solution	29.8±0.029	25.32±0.039
1 Pa	31.61±0.033	30.78±0.033
12 Pa	32.52±0.032	31.20±0.037
30 Pa	32.97±0.041	31.71±0.039
70 Pa	34.09±0.038	32.38±0.043
180 Pa	36.91±0.044	35.97±0.041

4.3.2.2 Water Uptake Ratio of PEGDA Hydrogels and Liposomal Hydrogels

Next, we performed water uptake experiments to obtain the water uptake ratio of the neat PEG hydrogels and liposomal hydrogels to investigate the effect of liposomes and the rigidity of lipid bilayer at 15℃ and 35℃ as swelling behavior of hydrogels control the release patterns of drugs from the hydrogel networks.[62] Figure 4.5.a and 4.5.b shows the water uptake ratios of neat PEGDA hydrogels. It is clearly seen that the crosslinking density affects the equilibriums significantly. As expected, higher water uptake capacity (up to 350%) was observed as the crosslinking density decreased. Due to the enhanced swelling, the stiffer hydrogels showed lower uptake ratio (decreased to 50%) as a result of higher elastic response of the chains against swelling. Also, a remarkable change was not observed in the swelling behavior of PEG hydrogels with temperature. However, the swelling of the liposomal hydrogels was extremely sensitive to temperature as seen from Figure 4.5.c and 4.5.d. At 15℃, water uptake ratio decreased to 70% even for the softest hydrogel with the lowest crosslinking density.

As the liposomes acts as hard spheres with impermeable walls at below T_m, the rate of water permeation through the bilayer was restricted and decreased drastically[209] (as also suggested by FLS results, see Figure 4.4). In turn, the permeability of the membrane increased swelling capacity of the whole system. At 35℃ above the transition, the lipid bilayer transforms through the fluid phase where water diffusion was facilitated. Thus, a

similar swelling behavior and the degree of swelling equilibrium was obtained with the neat PEG hydrogels.

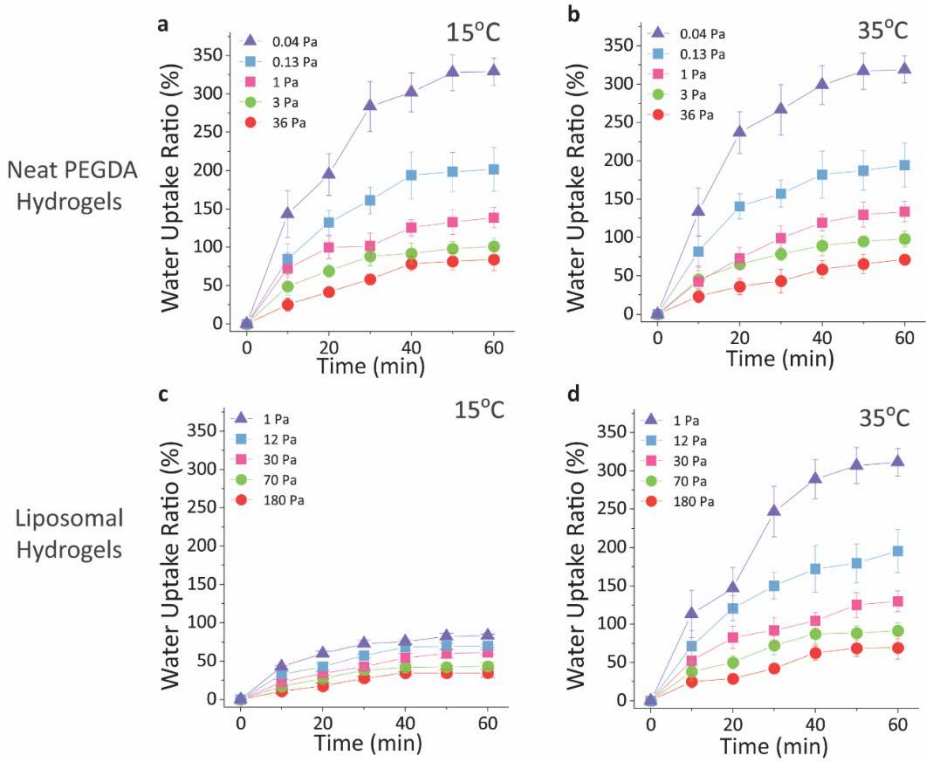

Figure 4.5 Water uptake ratio of neat PEG hydrogels a) at 15℃ b) at 35℃. Percentage swelling ratio of liposomal hydrogels c) at 15℃ d) at 35℃. Error bars represents standard deviation, (n=3).

4.4 Liposome Release from Hydrogels

As the diffusion properties of nanoparticles are known to affected by various parameters such as temperature, size of the particle, or external stimulus, we first investigate the liposome release from the liposomal hydrogels to examine the diffusion of liposomes under static conditions. Then, shear stimulus was applied by rheology to the stiffest hydrogel since it has the lowest time-dependent liposome release as the experimental setup and methodology are shown in Figure 4.6.a.

4.4.1 Time-Dependent Liposome Release Kinetics from Hydrogels

We evaluated time dependent liposome release from liposomal hydrogels through DI water with respect to rigidity of liposomes (Figure 4.6.b and 4.6.c). The release of the liposomes was monitored and reached at equilibrium at 7 hours. As expected, release

profiles changed according to the stiffness of the hydrogels. At 15℃, the fraction of released liposomes reached up to 12% for the softest hydrogel (1 Pa), whereas it remained 3% for the stiffest hydrogel, 180 Pa. At 35℃, a similar release behavior was obtained with a slight increase in the fraction of released liposomes which increased to 17% for the softest and 4% for the stiffest hydrogel as the membrane became deformable with its more fluid structure. Liposomes are widely used in drug release studies together with hydrogels, and they are expected to be immobilized in the hydrogel matrix due to the intact network bonds. In our case, the hydrogels were formed by chemical bonds restricting the mobility of liposomes inside. To investigate the release behavior, first the diffusion of liposomes should be elucidated as the vesicles which can diffuse fast could release from the hydrogel at higher fractions. The diffusion of liposomes was found to be temperature and rigidity dependent as the diffusion rate increased with the increasing temperature in PEO hydrogel as Stokes-Einstein equation suggested.[200] Liposomes with moderate rigidity can exhibit superior diffusivity since they can fluctuate around their initial radius and explore greater distances inside of the hydrogel. Besides, physical parameters such as mesh size, and adhesion property of the hydrogel affects the mobility of NPs in hydrogel.[201] As the crosslinking density changes, the mesh size of the hydrogel changes inversely accordingly. Thus, we calculated the mesh size of hydrogels to analyze the diffusion of liposomes from the hydrogels with different mesh sizes according to following equation: $\xi = \left(\frac{k_B T}{G_0} \right)^{\frac{1}{3}}$, where k_B is Boltzmann's constant, T is temperature and G_0 is the constant elastic modulus at low frequency. Table 4.3 shows the calculated mesh sizes of hydrogels at 15℃ and 35℃. We used G_0 values of neat PEG hydrogels obtained by rheology. The mesh size exceeded the size of the liposomes (~130 nm) for the three softest hydrogels. (1 Pa, 12 Pa, and 30 Pa) We observed a significant increase in the fraction of released liposomes after the mesh size became comparable or exceeded the size of the liposomes, especially beyond ~300 nm.

Table 4.3 Calculated mesh sizes of the hydrogels at 15℃, and 35℃.

Stiffness	Mesh Size at 35℃	Mesh Size at 15℃
1 Pa	42.36	41.43
12 Pa	111.35	108.89
30 Pa	157.9	154.41
70 Pa	319.81	312.74
180 Pa	473.7	463.23

To understand the governing mechanism of liposome release, we further analyzed the release curves by Weibull statistical distribution function which is applicable through whole release process with high accuracy and providing physical characteristics of release systems[210], and expressed as following: $M(t) = M_{\infty}(1 - e^{-\left(\frac{1}{\tau_K}\right)^{\beta}})$, where M_{∞} represents the maximum released drug amount, τ_K and β are the scale and shape factor, respectively. Fit lines of Weibull CDF were shown from the dash-dot gray lines in the release curves. The fit parameters were recorded in Table 4.4 for 15℃, and 35℃, respectively. All curves followed the fitted lines as R^2 was greater than 0.98 in all cases. A value of β <0.75 represents the Fickian diffusion, the release mechanism governed by the concentration or chemical potential difference. However, 0.75< β <1 is associated with a combined release mechanism (controlled by both Fickian diffusion and swelling dependent). If the β exceeds 1, it means that the release mechanism is more complex.

Table 4.4 Fit parameters of Weibull CDF for time-dependent liposome release from liposomal hydrogels at 15℃ and 35℃.

	15℃			35℃		
	R^2	τ_K	β	R^2	τ_K	β
1 Pa	0.99643	0.8427	0.68957	0.99438	1.27878	0.92658
12 Pa	0.99571	1.0743	0.70469	0.99642	0.72922	0.93457
30 Pa	0.99125	1.33386	0.74128	0.99162	1.00174	0.85643
70 Pa	0.98366	1.01779	0.79544	0.98448	2.87033	0.89321
180 Pa	0.99088	1.16804	0.77456	0.98592	1.88011	0.88277

At 15℃, β values were smaller than 0.75 and it exceeded 0.75 for the two stiffest hydrogels with mesh sizes of smaller than 130 nm. As suggested by swelling experiments, due to the high microviscosity of lipid bilayer, the swelling capacity of liposomal hydrogels decreased significantly compared to neat PEG hydrogels. Therefore, this effect was seen in the release data since β values are smaller or slightly close to 0.75 which means that the release mechanism was governed by diffusion. However, at 35℃, β values were higher than 0.75 due to the high swelling capacity of hydrogels with permeable liposomes. As the gel softens, the β values became higher which was a proof of increasing swelling ratio.

Liposome release from different hydrogels was shown by Thompson et al.[211] It was hypothesized that liposomes can release only if the bonds constructing the hydrogel environments are physical, no release was obtained in the case of chemically crosslinked hydrogels. Therefore, the gel can form temporary bonds enabling large pores for liposomes to squeeze out. The agarose and gelatin hydrogels used in the study were stiffer than our hydrogels (up to 30 kPa) and the mesh sizes changed between ~5 to 24 nm. In our system, hydrogels were formed by chemical bonds that cannot form temporary pores between crosslinked polymer chains. Also, we did not observe a sufficient release (~4%) for the stiffest hydrogel with a mesh size of ~42 nm. As the hydrogel became softer, a remarkable increase in the amount of released liposomes from the gel with a mesh size of up to ~460 nm which is sufficiently larger than the size of the liposomes. Thus, although the bonding type of the hydrogel is important, the mesh size is also an essential parameter controlling the release mechanism from hydrogels. However, this release was limited as we could obtain the maximum ~17% release from the softest hydrogel, where the liposomes could diffuse out faster, at 35℃, and the fluid state of the lipid bilayer. More importantly, we show in the next section that the oscillatory shearing of the liposomal hydrogels in the non-linear deformation regimes enhances the mobility of the entrapped liposomes in the gel matrix and increases the release rate of the particles.

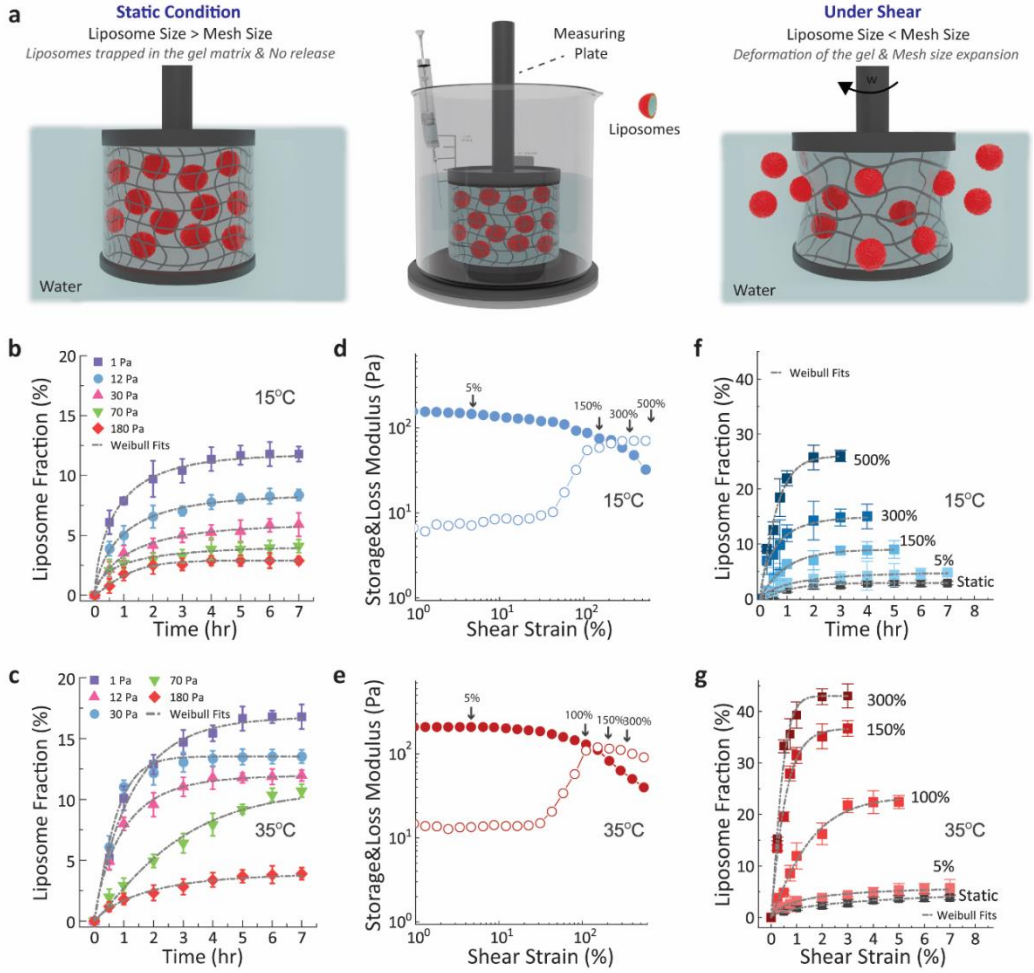

Figure 4.6 The fractional time-dependent and shear stimuli liposome release from liposomal hydrogels a) The illustrative image of the time dependent liposome release at static conditions(left), experimental setup (middle), and shear-stimuli liposome release (right). Time dependent fractional liposome release at b) 15 ℃ and c) 35℃. Amplitude sweeps of the stiffest liposomal hydrogel at d)15℃ and e) 35℃ with varying strains from 1 to 700%. 5%, 150%, 300%, and 500% were chosen for 15℃, and 5%, 100%, 150%, and 300% were chosen for 35℃ as marked with arrows on the figures. Shear-stimuli liposome release from liposomal hydrogel at f)15℃ and g) 35℃ with varying strains. Inset shows the released medium, the color of the solutions became whiteish as the strain values increased with increasing amount of released liposomes. Error bars represent standard deviation, (n=3)

4.4.2 Shear-Triggered Liposome Release Kinetics from Hydrogels

To stimulate the liposome release under shear, we chose the stiffest liposomal hydrogel (~180 Pa) having the lowest release amount with the smallest mesh size (~46 nm). We first performed the amplitude sweep tests (Figure 4.6.d and 4.6.e) on the liposomal hydrogels to determine the linear viscoelastic region (LVER) and to select the appropriate strain values for shear induced release at 15℃ and 35℃ (since temperature is

a significant parameter effecting the elasticity of hydrogels due to temperature sensitivity of liposomes, see Figure 4.2.e). We chose four strain values for both temperatures, two of which were in the LVER representing the quiescent state and the other two were beyond the LVER mimicking the mechanical response of several biological tissues are not linear.[212] 5%, 150%, 300%, and 500% were chosen for 15℃, and 5%, 100%, 150%, and 300% were chosen for 35℃ as marked on the graphs. The strain at the peak point of G'' is the deformation level at which the viscous dissipation reaches a maximum.

To realistically mimic the biological conditions (*i.e.,* continuous shear force in vessels), we applied the shear force on the hydrogels in a beaker filled with DI water so that the release of liposomes could be followed instantaneously in aqueous environment as the experimental setup was represented in Figure 4.6.a (see also Methods section for details). Figure 4.6.f shows shear stimuli liposome release from the hydrogels at 15℃. The release curve at static condition was added as the control experiment for comparison. At 5% strain value, a similar release behavior with a slight increase (~5% of liposomes were released) was obtained at 7 hours. As the strain value increased towards the nonlinear regime, the fraction of the released liposomes increased significantly at shorter times. The cumulative liposome release of 5%, 8%, 16%, and 26% were obtained for the 5%, 150%, 300% and 500% strains, respectively. We measured the hydrodynamic size and polydispersity of the released liposomes after applied shear using DLS as shown in Table 4.5. The size and polydispersity of the released liposomes increased only up to ~10 nm and ~0.15, respectively confirming that the liposomal structure is retained.

Similarly, at 35℃, the shear deformation increased the liposome release remarkably as the LVER region was passed after 150% strain (Figure 4.6.g). At 300%, the maximum liposome release was obtained as 43% over a short period of 3 hours. We collected the release medium after each experiment, the increased amount of released liposomes can be seen in the Figure 4.7 with increasing shear strain. Although the release times were comparable with the 15℃, the total amount of released liposomes increased around ~17% due to the increasing mobility of the lipid membrane which allowed the trapped liposomes to escape from the hydrogel mesh. Table 4.6 shows the DLS data of liposomes after the release experiments; the results were similar to those obtained for; thus, the liposomes mostly remain intact during escape from the hydrogels.

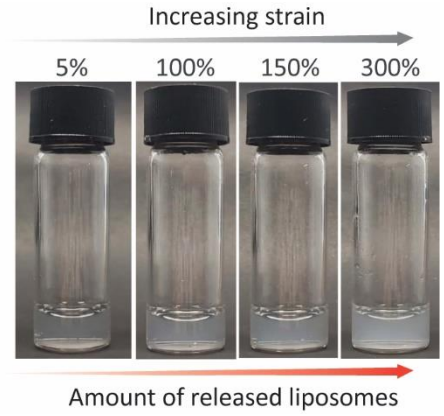

Figure 4.7 Representative images of the solution of released liposomes under shear at the end of each experiment at 35℃ with varying strains. The color of the medium became whiteish as the strain values increased with the increasing amount of released liposomes at 35℃.

Table 4.5 Hydrodynamic diameters of the released liposomes after applied strains at 15℃.

Applied Strain (%)	Hydrodynamic Size (nm)	PDI
No Strain	133.6±2.401	0.042±0.0041
5	134.0±1.682	0.098±0.058
100	138.7±1.361	0.135±0.012
150	144.8±5.950	0.141±0.012
300	147.7±0.9452	0.133±0.030

Table 4.6 Hydrodynamic diameters of the released liposomes after applied strains at 35℃.

Applied Strain (%)	Hydrodynamic Size (nm)	PDI
No Strain	133.6±2.401	0.042±0.0041
5	136.9±1.950	0.102±0.029
150	147.5±2.120	0.141±0.043
300	146.0±2.893	0.140±0.036
500	148.2±0.850	0.156±0.058

We then analyzed the release behavior with the Weibull CDF as the fit curves were shown on the data. Table 4.7 shows the model parameters for 15℃ and 35℃, respectively. At both temperatures, β values were similar to static case and at between 0.75 and 1 for 5% strain. As the strain values increased gradually from 0.77 to 1.11 at 15℃, and from

0.89 to 1.29 at 35℃ which means that release was governed by more complex mechanism which is shear stimuli for our system.

Table 4.7 Fit parameters of Weibull CDF for shear-triggered liposome release from liposomal hydrogels at 15℃ and 35℃.

	15℃				35℃		
	R^2	τ_K	β		R^2	τ_K	β
5%	0.98014	1.37574	0.77735	**5%**	0.98295	1.49435	0.8951
150%	0.98273	0.95992	0.98522	**100%**	0.99033	1.51005	1.11659
300%	0.98843	0.59097	1.04071	**150%**	0.99442	0.56647	1.06181
500%	0.99137	0.62252	1.11534	**300%**	0.98918	0.43323	1.27702

The enhanced release of liposomes from hydrogel environment was showed with different types of mechanical deformation such as tension and compression by destroying the structure of liposomes.[136, 137] In all studies, the liposomes were connected to the crosslinked matrix via chemical bonds causing the rupture of the vesicle membrane under mechanical stress and enabling the release of cargo of the liposomes. As the force is dissipated uniformly during compression and tension, vesicles could evade the stress applied to the hydrogel, and no release was obtained in the case of physical bonding of liposomes. However, in our system, we observed a remarkable liposome release under large shear force although they were physically entrapped (possibly due to hydrogen bonding between PEG and lipids in hydrogel matrix.[150]

During the oscillatory shear deformation, the hydrogel is deformed in a way that shear rate is zero at the center and maximum at the edges. By increasing the strain value beyond the LVER of the hydrogel, this deformation resulted in the expansion in mesh size of the hydrogel. (See right side of Figure 4.6.a) As a result, liposomes could diffuse out through the hydrogel under shear force.

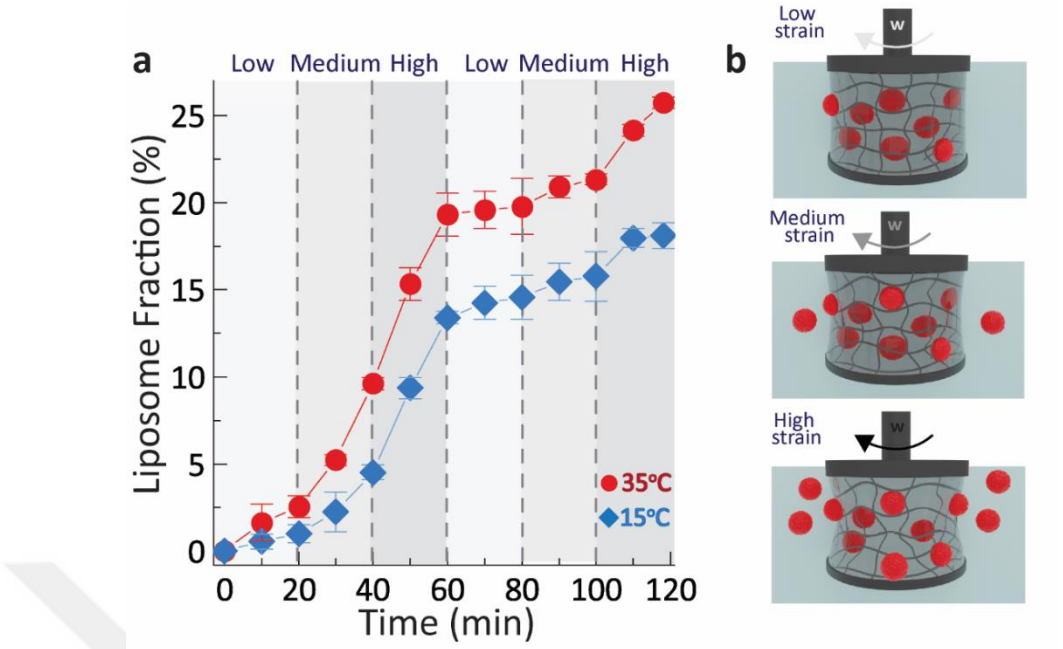

Figure 4.8 Modulation of liposome release by varying the strain values a) The fractional liposome release under low, medium, and high strain. The red lines represent 35°C, the blue line represents 15°C. Error bars represents standard deviation, (n=3) The strain was applied with the cycle of 20 min time periods. Strain values were categorized as low, medium, and high with respect to the distance from the LVER. 5%, 300%, and 500% were chosen for 15°C, and 5%, 100%, and 300% were chosen for 35°C release experiments b) Representative images of modulated liposome release under low, medium, and high shear.

We further investigated whether the amount of the released liposomes could be modulated by continuously changing the shear strain. The liposome release was monitored by applying low, medium, and high shear for 20 min periods. The applied strain values were chosen as 5%, 300%, and 500% for 15°C, and 5%, 100%, and 300% for 35°C release experiments. As shown in Figure 4.8.a, increasing the strains towards high values increased the liposome release rates as the slope of the release curve increased significantly for both temperatures. Then in the second cycle, the release rate slowed down to the low strain values. (See the representation in Figure 4.8.b) This indeed mimics the vessels in the body where different shear stresses are encountered as the size of the vessels change. Likewise, in the case of stenosis in arteries, or some medical treatments such as catheters or angioplasty, shear stress increases more than one order of magnitude compared to a healthy artery. [189, 190] This programmable release can adopt the dynamic shear profile of the blood flow as it enables dosage and time-controlled release by changing the shear strain.

Chapter 5:
CONCLUSIONS & OUTLOOK

Advancements of pharmaceuticals industry offer novel drug delivery approaches to increase the therapeutic efficacy. Dosage-controlled delivery through targeted locations with keeping the drug safe is a major drawbacks of drug delivery applications. Liposomes with their unique encapsulation properties are the most promising drug delivery platforms and cell membrane models as, they are biocompatible, biodegradable, low-toxic, able to entrap hydrophilic and hydrophobic drugs, and similar with the biological membranes. They are small artificial vesicles made up from self-assembling of phospholipids, and have tunable properties such as fluidity, rigidity, and permeability by changing surface charge, size, lamellarity, and the type of lipid. The combination of liposomes with polymers and hydrogels are widely utilized in all application areas of liposomes since polymer chains provide liposomes mechanical and thermodynamical stability, increased circulation-time, and responsive release properties. However, the effect of polymers on structural dynamics of lipid bilayer and elucidating the interactions between them are needed for rationale designs of liposome-polymer complexes.

In the first project named as “Multiscale Dynamics of Lipid Vesicles in Polymeric Microenvironment”, we used unilamellar DMPC/DMPG liposomes as artificial cell membrane models and investigated the effect of PEG chains, used as mimicking the viscoelastic surrounding medium of the cells, on the structure and dynamics of liposomes from bulk to nano scale. We observed that PEG chains formed an adsorbed polymer layer on liposome surface due to attractive interactions between them, although they did not cause a notable structural change as suggested by SAXS and DSC results. The mesoscale membrane undulations are affected by the polymer layer when the lipids are in fluid phase, since the viscous motion of the polymers and liposomes is coupled with comparable time scales. At the macroscopic level, liposomes act as reinforcing particles for polymer solutions with a remarkable increase in viscosity at the gel-to-fluid transition temperature and thermal thickening thereafter. The microviscosity of the lipid bilayers is directly affected by surrounding PEG chains and therefore by the relaxation of the whole chain, resulting an enhancement of the membrane dynamics in the case of short chains due to the fast relaxation time of the shorter chains, which enables dynamic coupling of

membrane and polymer motion. In summary, we showed that nanoscale membrane dynamics, diffusive motion, and rheological behavior of liposomes can be effectively tuned by changing the polymer chain length, concentration, and lamellarity.

In the second project named as “Shear Stimuli-Responsive Liposome Release from ECM-Mimetic Hydrogels”, we utilize liposomes as drug nanocarriers and PEG hydrogels as surrounding medium. We showed a shear-stimuli based liposome release from the hydrogels having different stiffness in the range of 1 to 180 Pa as matched with. To elucidate the underlying mechanism behind the enhanced diffusion and release properties at static and shear-applied conditions, we first investigated the structural and dynamical interaction between liposomes and hydrogels. Liposomes acted as reinforcing nanoparticles and improved the elasticity of hydrogels. The transition of the membrane also affected the swelling behavior since microviscosity, and permeability of the lipid bilayer is highly sensitive to temperature. We observed a mesh size-dependent liposome release as a remarkable increase of the liposome release was obtained while the mesh size is comparable to or larger than the liposome size with increasing temperature. Finally, we design an experimental setup to instantaneously follow the liposome release in aqueous environment. With a systematic application of shear force according the LVER of hydrogels, the controlled and increased liposome release up to ~2-fold was observed with deforming the hydrogel to expand the mesh sizes. In view of these results, we believe that understanding the mechanism of shear stimuli for liposome-hydrogel systems will be useful to design smarter and on-demand drug delivery systems being adaptable to dynamic and complex environments of biological systems.

BIBLIOGRAPHY

1. Gradisar, H.; Jerala, R., Self-assembled bionanostructures: proteins following the lead of DNA nanostructures. *Journal of Nanobiotechnology* **2014,** *12* (1), 4.
2. Daraee, H.; Etemadi, A.; Kouhi, M.; Alimirzalu, S.; Akbarzadeh, A., Application of liposomes in medicine and drug delivery. *Artificial Cells, Nanomedicine, and Biotechnology* **2016,** *44* (1), 381-391.
3. Li, M.; Du, C.; Guo, N.; Teng, Y.; Meng, X.; Sun, H.; Li, S.; Yu, P.; Galons, H., Composition design and medical application of liposomes. *Eur J Med Chem* **2019,** *164*, 640-653.
4. Ahmed, K. S.; Hussein, S. A.; Ali, A. H.; Korma, S. A.; Lipeng, Q.; Jinghua, C., Liposome: composition, characterisation, preparation, and recent innovation in clinical applications. *Journal of Drug Targeting* **2019,** *27* (7), 742-761.
5. Abdelkader, H.; Alani, A. W. G.; Alany, R. G., Recent advances in non-ionic surfactant vesicles (niosomes): self-assembly, fabrication, characterization, drug delivery applications and limitations. *Drug Delivery* **2014,** *21* (2), 87-100.
6. Khan, A. A.; Allemailem, K. S.; Almatroodi, S. A.; Almatroudi, A.; Rahmani, A. H., Recent strategies towards the surface modification of liposomes: an innovative approach for different clinical applications. *3 Biotech* **2020,** *10* (4), 163-163.
7. Milani, D.; Athiyah, U.; Hariyadi, D.; Pathak, Y., Surface Modifications of Liposomes for Drug Targeting. 2019; pp 207-220.
8. Dowhan, W., The role of phospholipids in cell function. In *Advances in Lipobiology*, Gross, R. W., Ed. JAI: 1997; Vol. 2, pp 79-107.
9. Tang, S.; Davoudi, Z.; Wang, G.; Xu, Z.; Rehman, T.; Prominski, A.; Tian, B.; Bratlie, K. M.; Peng, H.; Wang, Q., Soft materials as biological and artificial membranes. *Chemical Society Reviews* **2021,** *50* (22), 12679-12701.
10. Lorent, J. H.; Levental, K. R.; Ganesan, L.; Rivera-Longsworth, G.; Sezgin, E.; Doktorova, M.; Lyman, E.; Levental, I., Plasma membranes are asymmetric in lipid unsaturation, packing and protein shape. *Nature Chemical Biology* **2020,** *16* (6), 644-652.
11. Yeagle, P. L., Non-covalent binding of membrane lipids to membrane proteins. *Biochimica et Biophysica Acta (BBA) - Biomembranes* **2014,** *1838* (6), 1548-1559.
12. Dias, C.; Nylandsted, J., Plasma membrane integrity in health and disease: significance and therapeutic potential. *Cell Discovery* **2021,** *7* (1), 4.
13. Bangham, A. D.; Standish, M. M.; Watkins, J. C., Diffusion of univalent ions across the lamellae of swollen phospholipids. *Journal of Molecular Biology* **1965,** *13* (1), 238-IN27.
14. Allen, T. M.; Cullis, P. R., Liposomal drug delivery systems: From concept to clinical applications. *Advanced Drug Delivery Reviews* **2013,** *65* (1), 36-48.
15. Israelachvili, J. N.; Mitchell, D. J.; Ninham, B. W., Theory of self-assembly of lipid bilayers and vesicles. *Biochimica et Biophysica Acta (BBA) - Biomembranes* **1977,** *470* (2), 185-201.
16. van Meer, G.; Voelker, D. R.; Feigenson, G. W., Membrane lipids: where they are and how they behave. *Nature Reviews Molecular Cell Biology* **2008,** *9* (2), 112-124.
17. Collier, J. H.; Messersmith, P. B., Phospholipid Strategies in Biomineralization and Biomaterials Research. *Annual Review of Materials Research* **2001,** *31* (1), 237-263.

18. Vemuri, S.; Rhodes, C. T., Preparation and characterization of liposomes as therapeutic delivery systems: a review. *Pharmaceutica Acta Helvetiae* **1995,** *70* (2), 95-111.
19. Eibl, H. r., Phospholipids as Functional Constituents of Biomembranes. *Angewandte Chemie International Edition in English* **1984,** *23* (4), 257-271.
20. Antimisiaris, S. G.; Kallinteri, P.; Fatouros, D. G., Liposomes and Drug Delivery. In *Pharmaceutical Manufacturing Handbook*, 2008; pp 443-533.
21. Eibl, H. r.; Kaufmann-Kolle, P., Medical Application of Synthetic Phospholipids as Liposomes and Drugs. *Journal of Liposome Research* **1995,** *5* (1), 131-148.
22. Vemuri, S.; Rhodes, C. T., Preparation and characterization of liposomes as therapeutic delivery systems: a review. *Pharmaceutica acta Helvetiae* **1995,** *70 2*, 95-111.
23. Drummond, D. C.; Meyer, O.; Hong, K.; Kirpotin, D. B.; Papahadjopoulos, D., Optimizing Liposomes for Delivery of Chemotherapeutic Agents to Solid Tumors. *Pharmacological Reviews* **1999,** *51* (4), 691.
24. Papahadjopoulos, D.; Nir, S.; Ohki, S., Permeability properties of phospholipid membranes: Effect of cholesterol and temperature. *Biochimica et Biophysica Acta (BBA) - Biomembranes* **1972,** *266* (3), 561-583.
25. Tsukanova, V.; Salesse, C., On the Nature of Conformational Transition in Poly(ethylene glycol) Chains Grafted onto Phospholipid Monolayers. *The Journal of Physical Chemistry B* **2004,** *108* (30), 10754-10764.
26. Monteiro, N.; Martins, A.; Reis, R. L.; Neves, N. M., Liposomes in tissue engineering and regenerative medicine. *J R Soc Interface* **2014,** *11* (101), 20140459-20140459.
27. Sahoo, S. K.; Labhasetwar, V., Nanotech approaches to drug delivery and imaging. *Drug Discovery Today* **2003,** *8* (24), 1112-1120.
28. Shinoda, W., Permeability across lipid membranes. *Biochimica et Biophysica Acta (BBA) - Biomembranes* **2016,** *1858* (10), 2254-2265.
29. Eibl, H. r.; Kaufmann-Kolle, P., Medical Application of Synthetic Phospholipids as Liposomes and Drugs. *Journal of Liposome Research* **2008,** *5*, 131-148.
30. Jacquot, A.; Francius, G. g.; Razafitianamaharavo, A.; Dehghani, F.; Tamayol, A.; Linder, M.; Arab-Tehrany, E., Morphological and Physical Analysis of Natural Phospholipids-Based Biomembranes. *PLOS ONE* **2014,** *9* (9), e107435.
31. Kinnunen, P. K. J., On the principles of functional ordering in biological membranes. *Chemistry and Physics of Lipids* **1991,** *57* (2), 375-399.
32. Demetzos, C., Differential Scanning Calorimetry (DSC): a tool to study the thermal behavior of lipid bilayers and liposomal stability. *J Liposome Res* **2008,** *18* (3), 159-73.
33. Inoue, T.; Yanagihara, S.-i.; Misono, Y.; Suzuki, M., Effect of fatty acids on phase behavior of hydrated dipalmitoylphosphatidylcholine bilayer: saturated versus unsaturated fatty acids. *Chemistry and Physics of Lipids* **2001,** *109* (2), 117-133.
34. Gupta, S.; De Mel, J. U.; Schneider, G. J., Dynamics of liposomes in the fluid phase. *Current Opinion in Colloid & Interface Science* **2019,** *42*, 121-136.
35. Dufourc, E. J., Sterols and membrane dynamics. *Journal of Chemical Biology* **2008,** *1* (1), 63-77.
36. Falke, S.; Betzel, C., Dynamic Light Scattering (DLS): Principles, Perspectives, Applications to Biological Samples. *Radiation in Bioanalysis* **2019,** *8*, 173-193.

37. Woodka, A. C.; Butler, P. D.; Porcar, L.; Farago, B.; Nagao, M., Lipid Bilayers and Membrane Dynamics: Insight into Thickness Fluctuations. *Physical Review Letters* **2012,** *109* (5), 058102.
38. Bonifacino, J. S.; Glick, B. S., The Mechanisms of Vesicle Budding and Fusion. *Cell* **2004,** *116* (2), 153-166.
39. Monzel, C.; Sengupta, K., Measuring shape fluctuations in biological membranes. *Journal of Physics D: Applied Physics* **2016,** *49* (24), 243002.
40. Lipowsky, R.; Sackmann, E.; Hoff, A. J., Structure and Dynamics of Membranes I. from Cells to Vesicles. *Handbook of Biological Physics* **1995,** *1*.
41. Faucon, J.; Mitov, M.; Meleard, P.; Bivas, I.; Bothorel, P., Bending elasticity and thermal fluctuations of lipid membranes. Theoretical and experimental requirements. *Journal De Physique* **1989,** *50*, 2389-2414.
42. Helfrich, W., Elastic Properties of Lipid Bilayers: Theory and Possible Experiments. *Z. Naturforsch. C* **1973,** *28*.
43. Mader, M.; Vitkova, V.; Abkarian, M.; Viallat, A.; Podgorski, T., Dynamics of viscous vesicles in shear flow. *The European physical journal. E, Soft matter* **2006,** *19*, 389-97.
44. Miller, I. R., Energetics of fluctuation in lipid bilayer thickness. *Biophysical Journal* **1984,** *45* (3), 643-644.
45. Gao, L.; Lipowsky, R.; Shillcock, J., Tension-induced vesicle fusion: pathways and pore dynamics. *Soft Matter* **2008,** *4* (6), 1208-1214.
46. Guedeau-Boudeville, M.-A.; Jullien, L.; Meglio, J., Drug delivery: Piercing vesicles by their adsorption onto a porous medium. *Proc Natl Acad Sci U S A* **1995,** *92*, 9590-2.
47. Bernard, A. L.; Guedeau-Boudeville, M. A.; Sandre, O.; Palacin, S.; di Meglio, J. M.; Jullien, L., Permeation through Lipid Bilayers by Adhesion of Giant Vesicles on Decorated Surfaces. *Langmuir* **2000,** *16* (17), 6801-6808.
48. Brochard-Wyart, F.; Gennes, P.-G.; Sandre, O., Transient pores in stretched vesicles: role of leak-out. *Physica A: Statistical Mechanics and its Applications* **2000,** *278*, 32-51.
49. McConnell, H. M.; Kornberg, R. D., Inside-outside transitions of phospholipids in vesicle membranes. *Biochemistry* **1971,** *10* (7), 1111-1120.
50. Flynn, A.; Ducey, M.; Yethiraj, A.; Morrow, M. R., Dynamic properties of bicellar lipid mixtures observed by rheometry and quadrupole echo decay. *Langmuir* **2012,** *28* (5), 2782-90.
51. Nakazawa, K.; Kawata, Y.; Hishida, M.; Yamamura, Y.; Saito, K., Reduction of Shear Viscosity in Phospholipid Vesicle Dispersions by Self-organized Ripple Structures of Vesicle Surfaces. *Chemistry Letters* **2017,** *47* (2), 240-242.
52. Seto, H.; Yamada, N. L.; Nagao, M.; Hishida, M.; Takeda, T., Bending modulus of lipid bilayers in a liquid-crystalline phase including an anomalous swelling regime estimated by neutron spin echo experiments. *The European Physical Journal E* **2008,** *26* (1), 217.
53. Feldman, D., Principles of polymer engineering, by N. G. McCrum, C. P. Buckley and C. B. Bucknall, Oxford University Press, New York, 1988, 391 pp. Price: $44.95. *Journal of Polymer Science Part C: Polymer Letters* **1989,** *27* (8), 280-280.
54. Painter, P. C.; Coleman, M. M., *Fundamentals of polymer science : an introductory text*. 2nd ed. ed.; Lancaster (Pa.) : Technomic Pub. Co.: 1997.
55. Dilute Solution Thermodynamics, Molecular Weights, and Sizes. In *Introduction to Physical Polymer Science*, 2005; pp 71-143.

56. Concentrated Solutions, Phase Separation Behavior, and Diffusion. In *Introduction to Physical Polymer Science*, 2005; pp 145-195.
57. Ahmed, E. M., Hydrogel: Preparation, characterization, and applications: A review. *Journal of Advanced Research* **2015,** *6* (2), 105-121.
58. Li, J.; Mooney, D. J., Designing hydrogels for controlled drug delivery. *Nature Reviews Materials* **2016,** *1* (12), 16071.
59. Peppas, N. A.; Bures, P.; Leobandung, W.; Ichikawa, H., Hydrogels in pharmaceutical formulations. *European Journal of Pharmaceutics and Biopharmaceutics* **2000,** *50* (1), 27-46.
60. Crosslinked Polymers and Rubber Elasticity. In *Introduction to Physical Polymer Science*, 2005; pp 427-505.
61. Polymer Viscoelasticity and Rheology. In *Introduction to Physical Polymer Science*, 2005; pp 507-556.
62. Ganji, F.; Vasheghani Farahani, S.; Vasheghani-Farahani, E., Theoretical Description of Hydrogel Swelling: A Review. *Iranian Polymer Journal* **2010,** *19*, 375-398.
63. Singer, S. J.; Nicolson, G. L., The Fluid Mosaic Model of the Structure of Cell Membranes. *Science* **1972,** *175* (4023), 720-731.
64. Xing, H.; Lee, H.; Luo, L.; Kyriakides, T. R., Extracellular matrix-derived biomaterials in engineering cell function. *Biotechnol Adv* **2020,** *42*, 107421-107421.
65. Frantz, C.; Stewart, K. M.; Weaver, V. M., The extracellular matrix at a glance. *J Cell Sci* **2010,** *123* (Pt 24), 4195-4200.
66. TГjrker, E.; Yildiz, U.; Arslan Yildiz, A., *Polymer based extracellular matrix mimetics for 3D cell culture*. 2016; p 1-3.
67. Zhang, S.; Gao, H.; Bao, G., Physical Principles of Nanoparticle Cellular Endocytosis. *ACS Nano* **2015,** *9* (9), 8655-8671.
68. Fujiwara, T.; Ritchie, K.; Murakoshi, H.; Jacobson, K.; Kusumi, A., Phospholipids undergo hop diffusion in compartmentalized cell membrane. *Journal of Cell Biology* **2002,** *157* (6), 1071-1082.
69. WILLIAMS, E. E., Membrane Lipids: What Membrane Physical Properties are Conserve during Physiochemically-Induced Membrane Restructuring?1. *American Zoologist* **2015,** *38* (2), 280-290.
70. Escribá, P. V.; Busquets, X.; Inokuchi, J.-i.; Balogh, G.; Török, Z.; Horváth, I.; Harwood, J. L.; Vígh, L., Membrane lipid therapy: Modulation of the cell membrane composition and structure as a molecular base for drug discovery and new disease treatment. *Progress in Lipid Research* **2015,** *59*, 38-53.
71. Batta, G.; Soltész, L.; Kovács, T.; Bozó, T.; Mészár, Z.; Kellermayer, M.; Szöllősi, J.; Nagy, P., Alterations in the properties of the cell membrane due to glycosphingolipid accumulation in a model of Gaucher disease. *Scientific Reports* **2018,** *8* (1), 157.
72. Mohanty, J. G.; Shukla, H. D.; Williamson, J. D.; Launer, L. J.; Saxena, S.; Rifkind, J. M., Alterations in the red blood cell membrane proteome in alzheimer's subjects reflect disease-related changes and provide insight into altered cell morphology. *Proteome Science* **2010,** *8* (1), 11.
73. Stok, R.; Ashkenazi, A., Lipids as the key to understanding α-synuclein behaviour in Parkinson disease. *Nature Reviews Molecular Cell Biology* **2020,** *21* (7), 357-358.
74. Zalba, S.; ten Hagen, T. L. M., Cell membrane modulation as adjuvant in cancer therapy. *Cancer Treatment Reviews* **2017,** *52*, 48-57.

75. Gonda, K.; Watanabe, T. M.; Ohuchi, N.; Higuchi, H., In vivo nano-imaging of membrane dynamics in metastatic tumor cells using quantum dots. *Journal of Biological Chemistry* **2010,** *285* (4), 2750-2757.
76. EscribГЎ, P. V., Membrane-lipid therapy: a new approach in molecular medicine. *Trends in Molecular Medicine* **2006,** *12* (1), 34-43.
77. Liu, P.; Chen, G.; Zhang, J., A Review of Liposomes as a Drug Delivery System: Current Status of Approved Products, Regulatory Environments, and Future Perspectives. *Molecules (Basel, Switzerland)* **2022,** *27* (4), 1372.
78. Barenholz, Y., Chapter 13 DoxilВ® вЂ“ the First FDA-approved Nano-drug: from Basics via CMC, Cell Culture and Animal Studies to Clinical Use. In *Nanomedicines: Design, Delivery and Detection*, The Royal Society of Chemistry: 2016; pp 315-345.
79. Liu, X.; Peng, H.-S.; Wang, Q., Surface Engineering of Liposomal Formulations for Targeted Drug Delivery. *Chemical Engineering & Process Techniques* **2014,** *2*, 1024.
80. Akbarzadeh, A.; Rezaei-Sadabady, R.; Davaran, S.; Joo, S. W.; Zarghami, N.; Hanifehpour, Y.; Samiei, M.; Kouhi, M.; Nejati-Koshki, K., Liposome: classification, preparation, and applications. *Nanoscale Research Letters* **2013,** *8* (1), 102.
81. Maestrelli, F.; GonzГЎlez-RodrГ-guez, M. L.; Rabasco, A. M.; Mura, P., Effect of preparation technique on the properties of liposomes encapsulating ketoprofenвЂ“cyclodextrin complexes aimed for transdermal delivery. *International Journal of Pharmaceutics* **2006,** *312* (1), 53-60.
82. Sakai, H.; Gotoh, T.; Imura, T.; Sakai, K.; Otake, K.; Abe, M., Preparation and Properties of Liposomes Composed of Various Phospholipids with Different Hydrophobic Chains Using a Supercritical Reverse Phase Evaporation Method. *Journal of Oleo Science* **2008,** *57* (11), 613-621.
83. Bakker-Woudenberg, I. A. J. M., Long-circulating sterically stabilized liposomes as carriers of agents for treatment of infection or for imaging infectious foci. *International Journal of Antimicrobial Agents* **2002,** *19* (4), 299-311.
84. Torchilin, V. P., Recent advances with liposomes as pharmaceutical carriers. *Nature Reviews Drug Discovery* **2005,** *4* (2), 145-160.
85. Antonietti, M.; Förster, S., Vesicles and Liposomes: A Self-Assembly Principle Beyond Lipids. *Advanced Materials* **2003,** *15* (16), 1323-1333.
86. Needham, D.; McIntosh, T. J.; Lasic, D. D., Repulsive interactions and mechanical stability of polymer-grafted lipid membranes. *Biochimica et Biophysica Acta (BBA) - Biomembranes* **1992,** *1108* (1), 40-48.
87. Mititelu Tartau, L.; Bogdan, M.; Buca, B. R.; Pauna, A. M.; Tartau, C. G.; Dijmarescu, L. A.; Popa, E. G., Evaluation of Antinociceptive Effects of Chitosan-Coated Liposomes Entrapping the Selective Kappa Opioid Receptor Agonist U50,488 in Mice. *Medicina* **2021,** *57* (2).
88. Hui, C.; Huang, H., A study on chitosan-coated liposomes as a carrier of bovine serum albumin as oral protein drug. *Journal of Dispersion Science and Technology* **2021**, 1-10.
89. Liu, D.; Zhang, Q.; Wang, J.; Guan, S.; Cai, D.; Liu, J., Inhibition of growth and metastasis of breast cancer by targeted delivery of 17-hydroxy-jolkinolide B via hyaluronic acid-coated liposomes. *Carbohydrate Polymers* **2021,** *257*, 117572.
90. Gao, X.; Zhang, J.; Huang, Z.; Zuo, T.; Lu, Q.; Wu, G.; Shen, Q., Reducing Interstitial Fluid Pressure and Inhibiting Pulmonary Metastasis of Breast Cancer by

Gelatin Modified Cationic Lipid Nanoparticles. *ACS Applied Materials & Interfaces* **2017,** *9* (35), 29457-29468.
91. Haidar, Z. S.; Hamdy, R. C.; Tabrizian, M., Protein release kinetics for core–shell hybrid nanoparticles based on the layer-by-layer assembly of alginate and chitosan on liposomes. *Biomaterials* **2008,** *29* (9), 1207-1215.
92. Takeuchi, H.; Kojima, H.; Yamamoto, H.; Kawashima, Y., Polymer coating of liposomes with a modified polyvinyl alcohol and their systemic circulation and RES uptake in rats. *Journal of Controlled Release* **2000,** *68* (2), 195-205.
93. Trucillo, P.; Reverchon, E., Production of PEG-coated liposomes using a continuous supercritical assisted process. *The Journal of Supercritical Fluids* **2021,** *167*, 105048.
94. Chen, E.; Chen, B.-M.; Su, Y.-C.; Chang, Y.-C.; Cheng, T.-L.; Barenholz, Y.; Roffler, S. R., Premature Drug Release from Polyethylene Glycol (PEG)-Coated Liposomal Doxorubicin via Formation of the Membrane Attack Complex. *ACS Nano* **2020,** *14* (7), 7808-7822.
95. Bakker-Woudenberg, I. A. J. M.; Schiffelers, R. M.; Storm, G.; Becker, M. J.; Guo, L., Long-Circulating Sterically Stabilized Liposomes in the Treatment of Infections. In *Methods in Enzymology*, Academic Press: 2005; Vol. 391, pp 228-260.
96. Suktham, K.; Koobkokkruad, T.; Saesoo, S.; Saengkrit, N.; Surassmo, S., Physical and biological characterization of sericin-loaded copolymer liposomes stabilized by polyvinyl alcohol. *Colloids and Surfaces B: Biointerfaces* **2016,** *148*, 487-495.
97. Immordino, M.; Dosio, F.; Cattel, L., Stealth liposomes: review of the basic science, rationale, and clinical applications, existing and potential. *International Journal of Nanomedicine* **2006,** *1*, 297 - 315.
98. Sushma, D.; Surabhi, K.; Ritesh, B.; Bhawna, K., CLINICAL PHARMACOKINETIC ASPECTS OF STEALTH LIPOSOMES: AREVIEW. *International Journal of Drug Development and Research* **2010,** *2*.
99. Woodle, M. C., Surface-modified liposomes: assessment and characterization for increased stability and prolonged blood circulation. *Chemistry and Physics of Lipids* **1993,** *64* (1), 249-262.
100. Torchilin, V. P.; Omelyanenko, V. G.; Papisov, M. I.; Bogdanov, A. A.; Trubetskoy, V. S.; Herron, J. N.; Gentry, C. A., Poly(ethylene glycol) on the liposome surface: on the mechanism of polymer-coated liposome longevity. *Biochimica et Biophysica Acta (BBA) - Biomembranes* **1994,** *1195* (1), 11-20.
101. Hoffman, A. S., Hydrogels for biomedical applications. *Advanced Drug Delivery Reviews* **2002,** *54* (1), 3-12.
102. Chen, M. H.; Wang, L. L.; Chung, J. J.; Kim, Y.-H.; Atluri, P.; Burdick, J. A., Methods To Assess Shear-Thinning Hydrogels for Application As Injectable Biomaterials. *ACS Biomater Sci Eng* **2017,** *3* (12), 3146-3160.
103. Bandara, S. R.; Molley, T. G.; Kim, H.; Bharath, P. A.; Kilian, K. A.; Leal, C., The structural fate of lipid nanoparticles in the extracellular matrix. *Materials Horizons* **2020,** *7* (1), 125-134.
104. Mourtas, S.; Haikou, M.; Theodoropoulou, M.; Tsakiroglou, C.; Antimisiaris, S. G., The effect of added liposomes on the rheological properties of a hydrogel: A systematic study. *Journal of Colloid and Interface Science* **2008,** *317* (2), 611-619.
105. Hurler, J.; ESakelj, S.; Mravljak, J.; Pajk, S.; Kristl, A.; Schubert, R.; E kalko-Basnet, N., The effect of lipid composition and liposome size on the release

properties of liposomes-in-hydrogel. *International Journal of Pharmaceutics* **2013,** *456* (1), 49-57.
106. Stojkov, G. N. Z. P. F. B. R. K. T. I. R. b. S.; Rheology of Hydrogels for Various, A.*Gels* [Online], 2021.
107. El Kechai, N.; Bochot, A. l.; Huang, N.; Nguyen, Y.; Ferrary, E.; Agnely, F., Effect of liposomes on rheological and syringeability properties of hyaluronic acid hydrogels intended for local injection of drugs. *International Journal of Pharmaceutics* **2015,** *487* (1), 187-196.
108. Correa, S.; Grosskopf, A. K.; Klich, J. H.; Lopez Hernandez, H.; Appel, E. A., Injectable liposome-based supramolecular hydrogels for the programmable release of multiple protein drugs. *Matter* **2022,** *5* (6), 1816-1838.
109. Mellati, A.; Akhtari, J., Injectable Hydrogels: A Review of Injectability Mechanisms and Biomedical Applications. *Research in Molecular Medicine* **2019,** *2017*.
110. Guvendiren, M.; Lu, H. D.; Burdick, J. A., Shear-thinning hydrogels for biomedical applications. *Soft Matter* **2012,** *8* (2), 260-272.
111. De Leo, V.; Milano, F.; Agostiano, A.; Catucci, L., Recent Advancements in Polymer/Liposome Assembly for Drug Delivery: From Surface Modifications to Hybrid Vesicles. *Polymers (Basel)* **2021,** *13* (7), 1027.
112. Lee, J.-H.; Oh, H.; Baxa, U.; Raghavan, S. R.; Blumenthal, R., Biopolymer-Connected Liposome Networks as Injectable Biomaterials Capable of Sustained Local Drug Delivery. *Biomacromolecules* **2012,** *13* (10), 3388-3394.
113. Rao, Z.; Inoue, M.; Matsuda, M.; Taguchi, T., Quick self-healing and thermo-reversible liposome gel. *Colloids and Surfaces B: Biointerfaces* **2011,** *82* (1), 196-202.
114. Shanmugam, V.; Selvakumar, S.; Yeh, C.-S., Near-infrared light-responsive nanomaterials in cancer therapeutics. *Chemical Society Reviews* **2014,** *43* (17), 6254-6287.
115. Dunne, M.; Epp-Ducharme, B.; Sofias, A. M.; Regenold, M.; Dubins, D. N.; Allen, C., Heat-activated drug delivery increases tumor accumulation of synergistic chemotherapies. *Journal of Controlled Release* **2019,** *308*, 197-208.
116. Sirsi, S. R.; Borden, M. A., State-of-the-art materials for ultrasound-triggered drug delivery. *Advanced Drug Delivery Reviews* **2014,** *72*, 3-14.
117. Wang, J.; Kaplan, J. A.; Colson, Y. L.; Grinstaff, M. W., Mechanoresponsive materials for drug delivery: Harnessing forces for controlled release. *Advanced Drug Delivery Reviews* **2017,** *108*, 68-82.
118. Gu, M.; Wang, X.; Toh, T. B.; Chow, E. K.-H., Applications of stimuli-responsive nanoscale drug delivery systems in translational research. *Drug Discovery Today* **2018,** *23* (5), 1043-1052.
119. Ma, L.; Tu, C.; Le, P.; Chitoor, S.; Lim, S. J.; Zahid, M. U.; Teng, K. W.; Ge, P.; Selvin, P. R.; Smith, A. M., Multidentate Polymer Coatings for Compact and Homogeneous Quantum Dots with Efficient Bioconjugation. *Journal of the American Chemical Society* **2016,** *138* (10), 3382-3394.
120. Hu, X.; Zhang, Y.; Xie, Z.; Jing, X.; Bellotti, A.; Gu, Z., Stimuli-Responsive Polymersomes for Biomedical Applications. *Biomacromolecules* **2017,** *18* (3), 649-673.
121. Mu, Y.; Gong, L.; Peng, T.; Yao, J.; Lin, Z., Advances in pH-responsive drug delivery systems. *OpenNano* **2021,** *5*, 100031.
122. Shibata, T.; Giaccia, A. J.; Brown, J. M., Development of a hypoxia-responsive vector for tumor-specific gene therapy. *Gene Therapy* **2000,** *7* (6), 493-498.

123. de la Rica, R.; Aili, D.; Stevens, M. M., Enzyme-responsive nanoparticles for drug release and diagnostics. *Advanced Drug Delivery Reviews* **2012,** *64* (11), 967-978.
124. Karimi, M.; Sahandi Zangabad, P.; Ghasemi, A.; Amiri, M.; Bahrami, M.; Malekzad, H.; Ghahramanzadeh Asl, H.; Mahdieh, Z.; Bozorgomid, M.; Ghasemi, A.; Rahmani Taji Boyuk, M. R.; Hamblin, M. R., Temperature-Responsive Smart Nanocarriers for Delivery Of Therapeutic Agents: Applications and Recent Advances. *ACS applied materials & interfaces* **2016,** *8* (33), 21107-21133.
125. Sommerfeld, SvenB D.; Elisseeff, JenniferB H., Time to Relax: Mechanical Stress Release Guides Stem Cell Responses. *Cell Stem Cell* **2016,** *18* (2), 166-167.
126. Feng, Y.; Fuentes, D., Model-based planning and real-time predictive control for laser-induced thermal therapy. *International Journal of Hyperthermia* **2011,** *27* (8), 751-761.
127. Chen, K.-J.; Chaung, E.-Y.; Wey, S.-P.; Lin, K.-J.; Cheng, F.; Lin, C.-C.; Liu, H.-L.; Tseng, H.-W.; Liu, C.-P.; Wei, M.-C.; Liu, C.-M.; Sung, H.-W., Hyperthermia-Mediated Local Drug Delivery by a Bubble-Generating Liposomal System for Tumor-Specific Chemotherapy. *ACS Nano* **2014,** *8* (5), 5105-5115.
128. Karimi, M.; Sahandi Zangabad, P.; Baghaee-Ravari, S.; Ghazadeh, M.; Mirshekari, H.; Hamblin, M. R., Smart Nanostructures for Cargo Delivery: Uncaging and Activating by Light. *Journal of the American Chemical Society* **2017,** *139* (13), 4584-4610.
129. McCoy, C. P.; Rooney, C.; Edwards, C. R.; Jones, D. S.; Gorman, S. P., Light-Triggered Molecule-Scale Drug Dosing Devices. *Journal of the American Chemical Society* **2007,** *129* (31), 9572-9573.
130. Nayar, R.; Schroit, A. J., Generation of pH-sensitive liposomes: use of large unilamellar vesicles containing N-succinyldioleoylphosphatidylethanolamine. *Biochemistry* **1985,** *24* (21), 5967-5971.
131. Shi, G.; Guo, W.; Stephenson, S.; Lee, R., Efficient intracellular drug gene delivery using folate receptor-targeted pH-sensitive liposomes composed of cationic/anionic lipid combinations. *Journal of controlled release : official journal of the Controlled Release Society* **2002,** *80*, 309-19.
132. Kauscher, U.; Holme, M. N.; BjΓ¶rnmalm, M.; Stevens, M. M., Physical stimuli-responsive vesicles in drug delivery: Beyond liposomes and polymersomes. *Advanced Drug Delivery Reviews* **2019,** *138*, 259-275.
133. Zhang, Y.; Yu, J.; Bomba, H.; Zhu, Y.; Gu, Z., Mechanical Force-Triggered Drug Delivery. *Chemical reviews* **2016,** *116*.
134. Cipolla, D.; Wu, H.; Gonda, I.; Eastman, S.; Redelmeier, T.; Chan, H.-K., Modifying the Release Properties of Liposomes Toward Personalized Medicine. *Journal of Pharmaceutical Sciences* **2014,** *103* (6), 1851-1862.
135. Sercombe, L.; Veerati, T.; Moheimani, F.; Wu, S. Y.; Sood, A. K.; Hua, S., Advances and Challenges of Liposome Assisted Drug Delivery. *Frontiers in pharmacology* **2015,** *6*, 286-286.
136. Stalder, E.; Zumbuehl, A., Liposome-Containing Mechanoresponsive Hydrogels. *Macromolecular Materials and Engineering* **2017,** *302* (5), 1600549.
137. Ming, Z.; Pang, Y.; Liu, J., Mechanical Deformation Mediated Transmembrane Transport. *Macromolecular Rapid Communications* **2020,** *41* (2), 1900518.
138. Natsume, T.; Yoshimoto, M., Membrane Permeability and Stability of Liposomes Suspended in Shear Flow. *Journal of Dispersion Science and Technology* **2013,** *34* (11), 1557-1562.

139. Yoshimoto, M.; Tamura, R.; Natsume, T., Liposome clusters with shear stress-induced membrane permeability. *Chemistry and Physics of Lipids* **2013,** *174*, 8-16.
140. Kogan, M.; Feng, B.; NordΓ©n, B.; Rocha, S.; Beke-Somfai, T., Shear-Induced Membrane Fusion in Viscous Solutions. *Langmuir* **2014,** *30* (17), 4875-4878.
141. Turecek, P. L.; Siekmann, J., 4 - PEG–protein conjugates: nonclinical and clinical toxicity considerations. In *Polymer-Protein Conjugates*, Pasut, G.; Zalipsky, S., Eds. Elsevier: 2020; pp 61-101.
142. Jesorka, A.; Orwar, O., Liposomes: Technologies and Analytical Applications. *Annual Review of Analytical Chemistry* **2008,** *1* (1), 801-832.
143. Kazakov, S., Liposome-Nanogel Structures for Future Pharmaceutical Applications: An Updated Review. *Curr Pharm Des* **2016,** *22* (10), 1391-413.
144. Birgul Akolpoglu, M.; Inceoglu, Y.; Kizilel, S., An all-aqueous approach for physical immobilization of PEG-lipid microgels on organoid surfaces. *Colloids and Surfaces B: Biointerfaces* **2020,** *186*, 110708.
145. Nanomedicine and the COVID-19 vaccines. *Nature Nanotechnology* **2020,** *15* (12), 963-963.
146. Bigini, P.; Gobbi, M.; Bonati, M.; Clavenna, A.; Zucchetti, M.; Garattini, S.; Pasut, G., The role and impact of polyethylene glycol on anaphylactic reactions to COVID-19 nano-vaccines. *Nature Nanotechnology* **2021,** *16* (11), 1169-1171.
147. Sellaturay, P.; Nasser, S.; Islam, S.; Gurugama, P.; Ewan, P. W., Polyethylene glycol (PEG) is a cause of anaphylaxis to the Pfizer/BioNTech mRNA COVID-19 vaccine. *Clinical & Experimental Allergy* **2021,** *51* (6), 861-863.
148. Granek, R.; Diamant, H., Membrane undulations in a structured fluid: Universal dynamics at intermediate length and time scales. *The European Physical Journal E* **2018,** *41* (1), 1.
149. Elmore, D. E., Molecular dynamics simulation of a phosphatidylglycerol membrane. *FEBS Letters* **2006,** *580* (1), 144-148.
150. Zhang, W.; Metzger, J. M.; Hackel, B. J.; Bates, F. S.; Lodge, T. P., Influence of the Headgroup on the Interaction of Poly(ethylene oxide)-Poly(propylene oxide) Block Copolymers with Lipid Bilayers. *The Journal of Physical Chemistry B* **2020,** *124* (12), 2417-2424.
151. Lentz, B. R.; Lee, J. K., Poly(ethylene glycol) (PEG)-mediated fusion between pure lipid bilayers: a mechanism in common with viral fusion and secretory vesicle release. *Molecular Membrane Biology* **1999,** (16), 279-296.
152. Pal, S.; Milano, G.; Roccatano, D., Synthetic Polymers and Biomembranes. How Do They Interact?: Atomistic Molecular Dynamics Simulation Study of PEO in Contact with a DMPC Lipid Bilayer. *The Journal of Physical Chemistry B* **2006,** *110* (51), 26170-26179.
153. Kalyanram, P.; Puri, A.; Gupta, A., Thermotropic effects of PEGylated lipids on the stability of HPPH-encapsulated lipid nanoparticles (LNP). *Journal of Thermal Analysis and Calorimetry* **2021**.
154. Wang, J.; Yang, L.-J.; Zhu, T.-T.; Wang, S.-Z.; Chen, Z.-X., Phase Transition of Phospholipid Vesicles Induced by Fatty Acids in Macromolecular Crowding: a Differential Scanning Calorimetry Study. *ACTA PHYSICO-CHIMICA SINICA* **2016,** *32*, 2027-2038.
155. Yamazaki, M.; Ohshika, M.; Kashiwagi, N.; Asano, T., Phase transitions of phospholipid vesicles under osmotic stress and in the presence of ethylene glycol. *Biophysical Chemistry* **1992,** *43* (1), 29-37.

156. Sahu, S.; Talele, P.; Patra, B.; Verma, R. S.; Mishra, A. K., A Multiparametric Fluorescence Probe to Understand the Physicochemical Properties of Small Unilamellar Lipid Vesicles in Poly(ethylene glycol)-Water Medium. *Langmuir* **2020,** *36* (17), 4842-4852.
157. Zakim, D.; Kavecansky, J.; Scarlata, S., Are membrane enzymes regulated by the viscosity of the membrane environment? *Biochemistry* **1992,** *31* (46), 11589-94.
158. Ma, Y.; Benda, A.; Kwiatek, J.; Owen, D. M.; Gaus, K., Time-Resolved Laurdan Fluorescence Reveals Insights into Membrane Viscosity and Hydration Levels. *Biophys J* **2018,** *115* (8), 1498-1508.
159. Nojima, Y.; Iwata, K., Viscosity Heterogeneity inside Lipid Bilayers of Single-Component Phosphatidylcholine Liposomes Observed with Picosecond Time-Resolved Fluorescence Spectroscopy. *The Journal of Physical Chemistry B* **2014,** *118* (29), 8631-8641.
160. Bozuyuk, U.; Dogan, N. O.; Kizilel, S., Deep Insight into PEGylation of Bioadhesive Chitosan Nanoparticles: Sensitivity Study for the Key Parameters Through Artificial Neural Network Model. *ACS Applied Materials & Interfaces* **2018,** *10* (40), 33945-33955.
161. Bozuyuk, U.; Gokulu, I. S.; Dogan, N. O.; Kizilel, S., A novel method for PEGylation of chitosan nanoparticles through photopolymerization. *RSC Advances* **2019,** *9* (25), 14011-14015.
162. Macdonald, P. M.; Leisen, J.; Marassi, F. M., Response of phosphatidylcholine in the gel and liquid-crystalline states to membrane surface charges. *Biochemistry* **1991,** *30* (14), 3558-3566.
163. Drazenovic, J.; Wang, H.; Roth, K.; Zhang, J.; Ahmed, S.; Chen, Y.; Bothun, G.; Wunder, S. L., Effect of lamellarity and size on calorimetric phase transitions in single component phosphatidylcholine vesicles. *Biochimica et Biophysica Acta (BBA) - Biomembranes* **2015,** *1848* (2), 532-543.
164. Lichtenberg, D.; Menashe, M.; Donaldson, S.; Biltonen, R. L., Thermodynamic characterization of the pretrasition of unilamellar dipalmitoyl-phosphatidylcholine vesicles. *Lipids* **1984,** *19* (6), 395-400.
165. Konarev, P. V.; Gruzinov, A. Y.; Mertens, H. D. T.; Svergun, D. I., Restoring structural parameters of lipid mixtures from small-angle X-ray scattering data. *J Appl Crystallogr* **2021,** *54* (Pt 1), 169-179.
166. Takeuchi, H.; Kojima H Fau - Yamamoto, H.; Yamamoto H Fau - Kawashima, Y.; Kawashima, Y., Evaluation of circulation profiles of liposomes coated with hydrophilic polymers having different molecular weights in rats. (0168-3659 (Print)).
167. Fetters, L. J.; Lohse, D. J.; Richter, D.; Witten, T. A.; Zirkel, A., Connection between Polymer Molecular Weight, Density, Chain Dimensions, and Melt Viscoelastic Properties. *Macromolecules* **1994,** *27* (17), 4639-4647.
168. De Mel, J. U.; Gupta, S.; Willner, L.; Allgaier, J.; Stingaciu, L. R.; Bleuel, M.; Schneider, G. J., Manipulating Phospholipid Vesicles at the Nanoscale: A Transformation from Unilamellar to Multilamellar by an n-Alkyl-poly(ethylene oxide). *Langmuir* **2021,** *37* (7), 2362-2375.
169. Devanand, K.; Selser, J. C., Asymptotic behavior and long-range interactions in aqueous solutions of poly(ethylene oxide). *Macromolecules* **1991,** *24* (22), 5943-5947.
170. Jouault, N.; Moll, J. F.; Meng, D.; Windsor, K.; Ramcharan, S.; Kearney, C.; Kumar, S. K., Bound Polymer Layer in Nanocomposites. *ACS Macro Letters* **2013,** *2* (5), 371-374.

171. Money, N. P., Osmotic Pressure of Aqueous Polyethylene Glycols 1: Relationship between Molecular Weight and Vapor Pressure Deficit. *Plant Physiology* **1989,** *91* (2), 766-769.
172. Enoki, T. A.; Henriques, V. B.; Lamy, M. T., Light scattering on the structural characterization of DMPG vesicles along the bilayer anomalous phase transition. *Chemistry and Physics of Lipids* **2012,** *165* (8), 826-837.
173. Krieger, I. M.; Dougherty, T. J. In *A Mechanism for Non Newtonian Flow in Suspensions of Rigid Spheres*, 1959.
174. Transport phenomena, R. B. Bird, W. E. Stewart, and E. N. Lightfoot, John Wiley and Sons, Inc., New York (1960). 780 pages. $11.50. *AIChE Journal* **1961,** *7* (2), 5J-6J.
175. Shewan, H. M.; Stokes, J. R., Viscosity of soft spherical micro-hydrogel suspensions. *Journal of Colloid and Interface Science* **2015,** *442*, 75-81.
176. Steinmark, I. E.; James, A. L.; Chung, P.-H.; Morton, P. E.; Parsons, M.; Dreiss, C. c. A.; Lorenz, C. D.; Yahioglu, G.; Suhling, K., Targeted fluorescence lifetime probes reveal responsive organelle viscosity and membrane fluidity. *PLOS ONE* **2019,** *14* (2), e0211165.
177. Raut, S. L.; Kimball, J. D.; Fudala, R.; Bora, I.; Chib, R.; Jaafari, H.; Castillo, M. K.; Smith, N. W.; Gryczynski, I.; Dzyuba, S. V.; Gryczynski, Z., A triazine-based BODIPY trimer as a molecular viscometer. *Physical Chemistry Chemical Physics* **2016,** *18* (6), 4535-4540.
178. Kuimova, M. K.; Yahioglu, G.; Levitt, J. A.; Suhling, K., Molecular Rotor Measures Viscosity of Live Cells via Fluorescence Lifetime Imaging. *Journal of the American Chemical Society* **2008,** *130* (21), 6672-6673.
179. Mehlem, A.; Hagberg, C. E.; Muhl, L.; Eriksson, U.; Falkevall, A., Imaging of neutral lipids by oil red O for analyzing the metabolic status in health and disease. *Nature Protocols* **2013,** *8* (6), 1149-1154.
180. Hoffmann, T. F. a. G., Die Viskositätsabhängigkeit der Fluoreszenzquantenausbeuten einiger Farbstoffsysteme. *Zeitschrift fГjr Physikalische Chemie* **1971,** *75* (1_2), 63-76.
181. Wu, Y.; E tefl, M.; OlzyE„ska, A.; Hof, M.; Yahioglu, G.; Yip, P.; Casey, D. R.; Ces, O.; HumpolГ-ДЌkovГЎ, J.; Kuimova, M. K., Molecular rheometry: direct determination of viscosity in Lo and Ld lipid phases via fluorescence lifetime imaging. *Physical Chemistry Chemical Physics* **2013,** *15* (36), 14986-14993.
182. Mohapatra, M.; Mishra, A. K., Excited state proton transfer based fluorescent molecular probes and their application in studying lipid bilayer membranes. *Photochemical & Photobiological Sciences* **2019,** *18* (12), 2830-2848.
183. Merkel, R.; Sackmann, E.; Evans, E., Molecular friction and epitactic coupling between monolayers in supported bilayers. *Journal De Physique* **1989,** *50*, 1535-1555.
184. Wang, Y.; Pisapati, A. V.; Zhang, X. F.; Cheng, X., Recent Developments in Nanomaterial-Based Shear-Sensitive Drug Delivery Systems. *Advanced Healthcare Materials* **2021,** *10* (13), 2002196.
185. Yetisgin, A. A.; Cetinel, S.; Zuvin, M.; Kosar, A.; Kutlu, O., Therapeutic Nanoparticles and Their Targeted Delivery Applications. *Molecules* **2020,** *25* (9).
186. Saxer, T.; Zumbuehl, A.; MГjller, B., The use of shear stress for targeted drug delivery. *Cardiovascular Research* **2013,** *99* (2), 328-333.
187. Li, Y.-S. J.; Haga, J. H.; Chien, S., Molecular basis of the effects of shear stress on vascular endothelial cells. *Journal of Biomechanics* **2005,** *38* (10), 1949-1971.

188. Holme, P. A.; Γ˜ rvim, U.; Hamers, M. J. A. G.; Solum, N. O.; Brosstad, F. R.; Barstad, R. M.; Sakariassen, K. S., Shear-Induced Platelet Activation and Platelet Microparticle Formation at Blood Flow Conditions as in Arteries With a Severe Stenosis. *Arteriosclerosis, Thrombosis, and Vascular Biology* **1997,** *17* (4), 646-653.
189. Dardik, A.; Chen, L.; Frattini, J.; Asada, H.; Aziz, F.; Kudo, F. A.; Sumpio, B. E., Differential effects of orbital and laminar shear stress on endothelial cells. *Journal of Vascular Surgery* **2005,** *41* (5), 869-880.
190. Davies, P. F., Hemodynamic shear stress and the endothelium in cardiovascular pathophysiology. *Nat Clin Pract Cardiovasc Med* **2009,** *6* (1), 16-26.
191. Blanco, E.; Shen, H.; Ferrari, M., Principles of nanoparticle design for overcoming biological barriers to drug delivery. *Nature Biotechnology* **2015,** *33* (9), 941-951.
192. Teo, B. M.; van der Westen, R.; Hosta-Rigau, L.; StΓ¤dler, B., Cell response to PEGylated poly(dopamine) coated liposomes considering shear stress. *Biochimica et Biophysica Acta (BBA) - General Subjects* **2013,** *1830* (10), 4838-4847.
193. Hosta-Rigau, L.; StΓ¤dler, B., Shear Stress and Its Effect on the Interaction of Myoblast Cells with Nanosized Drug Delivery Vehicles. *Molecular Pharmaceutics* **2013,** *10* (7), 2707-2712.
194. Chakravarthy, S. R.; Giorgio, T. D., Shear stress-facilitated calcium ion transport across lipid bilayers. *Biochimica et Biophysica Acta (BBA) - Biomembranes* **1992,** *1112* (2), 197-204.
195. Bernard, A.-L.; Guedeau-Boudeville, M.-A.; Marchi-Artzner, V. r.; Gulik-Krzywicki, T.; Meglio, J.-M.; Jullien, L., Shear-induced permeation and fusion of lipid vesicles. *Journal of Colloid and Interface Science* **2005,** *287*, 298-306.
196. Trevisan, J.; Cavalcanti, L.; Oliveira, C.; Torre, L.; Santana, M. H., Technological Aspects of Scalable Processes for the Production of Functional Liposomes for Gene Therapy. 2011.
197. Natsume, T.; Yoshimoto, M., Mechanosensitive Liposomes as Artificial Chaperones for Shear-Driven Acceleration of Enzyme-Catalyzed Reaction. *ACS Applied Materials & Interfaces* **2014,** *6* (5), 3671-3679.
198. Grijalvo, S.; Mayr, J.; Eritja, R.; DΓ-az, D. D. a., Biodegradable liposome-encapsulated hydrogels for biomedical applications: a marriage of convenience. *Biomaterials Science* **2016,** *4* (4), 555-574.
199. GonzΓŸlez-DΓ-az, E. C.; Varghese, S., Hydrogels as Extracellular Matrix Analogs. *Gels (Basel, Switzerland)* **2016,** *2* (3), 20.
200. Yu, M.; Song, W.; Tian, F.; Dai, Z.; Zhu, Q.; Ahmad, E.; Guo, S.; Zhu, C.; Zhong, H.; Yuan, Y.; Zhang, T.; Yi, X.; Shi, X.; Gan, Y.; Gao, H., Temperature- and rigidity-mediated rapid transport of lipid nanovesicles in hydrogels. *Proceedings of the National Academy of Sciences* **2019,** *116* (12), 5362-5369.
201. Yu, S.; Tian, F.; Shi, X., Diffusion of deformable nanoparticles in adhesive polymeric gels. *Journal of the Mechanics and Physics of Solids* **2022,** *167*, 105002.
202. Karaz, S.; Han, M.; Akay, G.; Onal, A.; Nizamoglu, S.; Kizilel, S.; Senses, E., Multiscale Dynamics of Lipid Vesicles in Polymeric Microenvironment. *Membranes (Basel)* **2022,** *12* (7).
203. Hammouda, B.; Ho, D. L.; Kline, S., Insight into Clustering in Poly(ethylene oxide) Solutions. *Macromolecules* **2004,** *37* (18), 6932-6937.
204. Hill, D.; Vasquez, P.; Mellnik, J.; McKinley, S.; Vose, A.; Mu, F.; Henderson, A.; Donaldson, S.; Alexis, N.; Boucher, R.; Forest, M., A Biophysical

Basis for Mucus Solids Concentration as a Candidate Biomarker for Airways Disease. *PloS one* **2014,** *9*, e87681.
205. Mehlem, A.; Hagberg, C.; Muhl, L.; Eriksson, U.; Falkevall, A., Imaging of neutral lipids by oil red O for analyzing the metabolic status in health and disease. *Nature protocols* **2013,** *8*, 1149-1154.
206. Douglas, J. F. T. I. W.; Strong, G.; the Emergence of the Amorphous Solid, S.*Gels* [Online], 2018.
207. Wu, Y.; Štefl, M.; Olzyńska, A.; Hof, M.; Yahioglu, G.; Yip, P.; Casey, D. R.; Ces, O.; Humpolíčková, J.; Kuimova, M. K., Molecular rheometry: direct determination of viscosity in Lo and Ld lipid phases via fluorescence lifetime imaging. *Physical Chemistry Chemical Physics* **2013,** *15* (36), 14986-14993.
208. Watanabe, N.; Suga, K.; Slotte, J. P.; Nyholm, T. K. M.; Umakoshi, H., Lipid-Surrounding Water Molecules Probed by Time-Resolved Emission Spectra of Laurdan. *Langmuir* **2019,** *35* (20), 6762-6770.
209. Blok, M. C.; van Deenen, L. L. M.; de Gier, J., Effect of the gel to liquid crystalline phase transition on the osmotic behaviour of phosphatidycholine liposomes. *Biochimica et Biophysica Acta (BBA) - Biomembranes* **1976,** *433* (1), 1-12.
210. Kolar-Anić, L.; Veljković, S.; Kapor, S.; Dubljević, B., Weibull distribution and kinetics of heterogeneous processes. *The Journal of Chemical Physics* **1975,** *63* (2), 663-668.
211. Thompson, B. R.; Zarket, B. C.; Lauten, E. H.; Amin, S.; Muthukrishnan, S.; Raghavan, S. R., Liposomes Entrapped in Biopolymer Hydrogels Can Spontaneously Release into the External Solution. *Langmuir* **2020,** *36* (26), 7268-7276.
212. GuimarГJes, C. F.; Gasperini, L.; Marques, A. P.; Reis, R. L., The stiffness of living tissues and its implications for tissue engineering. *Nature Reviews Materials* **2020,** *5* (5), 351-370.
213. KuДЌerka, N.; Nieh, M.-P.; Katsaras, J., Fluid phase lipid areas and bilayer thicknesses of commonly used phosphatidylcholines as a function of temperature. *Biochimica et Biophysica Acta (BBA) - Biomembranes* **2011,** *1808* (11), 2761-2771.
214. Drabik, D.; Chodaczek, G.; Kraszewski, S.; Langner, M., Mechanical Properties Determination of DMPC, DPPC, DSPC, and HSPC Solid-Ordered Bilayers. *Langmuir* **2020,** *36* (14), 3826-3835.

APPENDIX A: CALCULATION OF THE VOLUME FRACTION OF LIPOSOMES

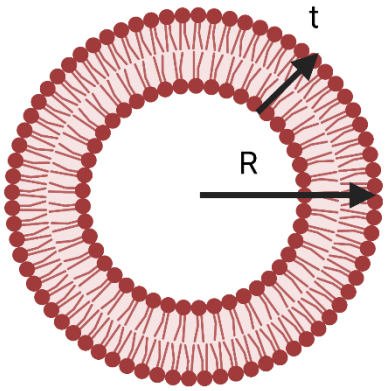

For 100 nm liposomes at 35°C and 2% concentration:

Hydrodynamic radius, R= $\frac{119.9nm}{2}$

$\frac{119.9nm}{2}$ = 59.95 nm,

Total surface area = $4\pi[R^2+(R-t)^2]$ where t is the bilayer thickness obtained from SAXS/WAXS.

Total number of lipid molecules per liposome,

$N_{Total}= \frac{4\pi[R^2+(R-t)^2]}{a}=\frac{4\pi[(59.59nm)^2+(59.95nm\ -6.28nm)^2]}{0.6nm^2}=135601$,

where *a* is area per lipid. (*a* is equal to 0.6 nm^2 [213]for fluid phase, and 0.605nm^2 for gel phase[214].)

Total number of liposomes in solution:

$N_{Liposomes}=\frac{M_{lipid}\times N_A}{N_{Total}}=\frac{0.027M\times 6.02\times 10^{23}/mol}{13560\times 1000}=1.19\times 10^{14} liposomes/mL$

Volume of a single liposome:

$V_{single\ Liposome}=\frac{4}{3}\pi R^3=\frac{4}{3}\pi(59.95)^3=902518.633nm^3$

Total volume of liposomes:

$V_{TotalLiposomes} = N_{Liposomes} \times V_{single\ Liposome} = 1.08 \times 10^{20}\ nm^3$

Volume Fraction= $\frac{Vliposomes}{Vtotal}=\frac{1.39\times 10^{20}nm^3}{1mL}\times\frac{1mL}{10^{21}nm^3}=0.108$

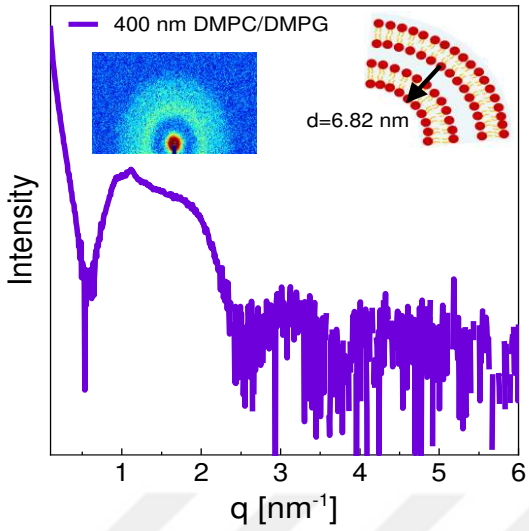

Figure A 1 SAXS data of 400 nm DMPC/DMPG liposomes at 15oC, inset is raw detector data. Bilayer thickness is obtained as 6.82 nm for the q*=0.92 nm^{-1}.

Table A 1 Calculated Volume Fractions of 100-nm Liposomes and 100-nm Liposomes in PEG 100kDa solutions

	100nm Liposomes $\phi_{Liposomes}$		100nm Liposomes in PEG100kDa $\phi_{Liposomes}$	
Concentrations	35°C	15°C	35°C	15°C
0.08%	0.136	0.119	0.159	0.119
1.2%	0.108	0.095	0.136	0.103
1.7%	0.080	0.070	0.092	0.073
2.0%	0.052	0.046	0.064	0.048